Title
Temporal dynamics of neural coding in rat SI

Author
Garabedian, Catherine

Publication Date
2004

Peer reviewed|Thesis/dissertation

Temporal Dynamics of Neural Coding in Rat SI

by

Catherine E. Garabedian

DISSERTATION

Submitted in partial satisfaction of the requirements for the degree of

DOCTOR OF PHILOSOPHY

in

Neuroscience

in the

GRADUATE DIVISION

of the

UNIVERSITY OF CALIFORNIA, SAN FRANCISCO

ACKNOWLEDGEMENTS

I would like to thank my advisor, Mike Merzenich, for inspiring me to think outside the box and reminding me that science can have an important impact outside the laboratory. Mike has always been kind and patient during my most challenging moments and supported my decisions, even when they were not what he would advise.

I owe immeasurable gratitude to Chris Moore for his mentorship on all aspects of this thesis project. Chris has supported me through nights spent eating half feta/half eggplant pizzas with a half dead rat, through bugs in data analysis, through broken vibrissa wigglers, and through papers written somewhere between San Francisco and Boston. His boundless enthusiasm has inspired and challenged my scientific pursuits and I have learned from each of our discussions. I am grateful to him for welcoming me as an unofficial member of his lab at MIT and for continuing to encourage me through the completion of this thesis. I am lucky to have him as a mentor and a friend.

I have had the privilege of collaborating with two talented scientists during the course of this project. The network model described in Chapter II is the work of Stephanie Jones. Mark Andermann shared preliminary data with me that resulted in the second set of studies described in Chapter III. I have learned a tremendous amount from both Mark and Stephanie through our scientific conversations.

Thanks to my thesis committee, Steve Lisberger, Christoph Schreiner, and Allison Doupe for their helpful and insightful guidance. I am particularly grateful to Allison for her kindness and encouragement during some of my most frustrating hurdles, and for many helpful discussions during the completion of this project.

Many thanks are owed to the current and former members of the Merzenich lab. Ted Moallem gave me my first introduction to the electrophysiology rig and rat surgery, and I have valued his friendship ever since our first year at UCSF. Dave Blake has provided guidance in my studies of the somatosensory system and helped with several obstacles I encountered both with programming and statistical analysis. John Houde was extremely patient and kind when he taught me the basics of Matlab during the early part of my graduate work. Dan Polley has been an outstanding rig czar for the past two years and has provided several stimulating conversations about barrel cortex. Thanks to Tal Kenet and Jen Linden for feedback on my data analysis and for encouragement with my research. I am also grateful to Henry Markram for the patient and expert training he gave me during my second year in graduate school.

Many members of the Keck Center and the neuroscience community have given me support over the past several years. Ram Ramachandran has been particularly helpful and patient in helping with statistical analyses and programming hurdles, and has offered much sound scientific advice as well. Greg Hjelmstad and Charlotte Boettiger guided me through my qualifying exams and helped with many slice physiology experiments. David Wolfgang-Kimball has gone out of his way to save me from numerous computer catastrophes and is cheerful and respectful during every interaction. Laszlo Bocskai built the very awesome stimulator that was used in the experiments in Chapter II. Thanks to the Basbaum lab for the use of their lab equipment, and to the Jonathan Horton and Lawrence Sincich for teaching me how to perform cytochrome oxidase reactions. Thanks to Pat Veitch, Deb Rosenberg, and Cindy Kelly for always offering help with a smile on their faces.

My experience at UCSF would not have been the same without the support and companionship of my friends and classmates. Megan Carey has been a close friend for the past six years and has given me valuable scientific and personal advise as well as great empathy, often over red wine and pizza. Robin LeWinter was a true friend and excellent roommate during some of the most trying moments in graduate school, and has kept me in shape through her enthusiasm for biking and jogging around Golden Gate Park. I cannot imagine having survived graduate school without the companionship of these two friends.

Many thanks to all of my friends who have supported me over the years. Liz has been the most loyal of friends since we first met over ten years ago. Thanks to Melissa for putting me up in Boston for a summer so I could work at MIT on my thesis, and to Laura, Heather, Rachel, Erica, Nick, Tom, and Chris for their friendship and for sharing their homes with me during my many visits to Boston. Thank you Dirk, for six months of support and for many laughs.

Finally, I owe the greatest thanks to family. My parents, Lynnel and Paul, have encouraged me throughout my life my pursuits and have always believed I could succeed in anything I put my mind to. My sister Emily has always been a role model for me and had grown to be one of my closest and trusted friends during the past few years. And finally, thank you to Hazel for all the fuzzy hugs.

PREFACE

The material presented as Chapter II in this thesis is published. 'Band-pass response properties of rat SI neurons', was published in *The Journal of Neurophysiology* (2003), 20(3-4): 297-303. The computational modeling described in this chapter is the work of Stephanie Jones.

ABSTRACT

Rats use their vibrissae to explore features such as the texture and shape of objects in their environment. During exploration, they "whisk" their vibrissae in repetitive elliptical movements at frequencies that are typically centered at 5-12 Hz. Despite the importance of sensory sampling at these characteristic rates, most studies of sensory processing in the vibrissa sensory pathway have employed single vibrissa deflections to assess neural response properties. In this thesis, I characterized tuning properties of neurons in primary somatosensory cortex (SI) of anesthetized rats in response to repetitive vibrissa deflections at stimulus rates up to 40 Hz.

In the experiments presented in **Chapter II**, four second-long trains of deflections at 0.3-40 Hz were presented to the primary vibrissa while recording multi-unit responses from the corresponding barrel column in middle layers of SI. As previously reported by many groups, responses to the first deflection in the train were typically robust, but showed dynamic adaptation that reached a steady state after ~1 second. Both the total spike rate and the temporal precision of responses, measured as vector strength, were assessed during this steady state period from 1-4 seconds after the onset of the stimulus train. Both of these measurements, which reflect pure spike rate and pure temporal neural codes, showed band-pass peaks in responsiveness at 5-12 Hz, the typical whisking frequency range. A cortical network model was developed to investigate putative mechanisms underlying these band-pass response properties. Results showed that the peak in spike rate was largely dependent on short-term adaptation, while the peak in vector strength resulted from slow post-stimulus suppression that may be a result of $GABA_B$- mediated synaptic currents.

In **Chapter III**, direction selectivity of single and multi-unit barrel responses was assessed using four-second-long trains of vibrissa deflections at 4-16 Hz. In response to the first deflection in a train, multi-unit responses were weakly direction tuned, while single unit responses showed more direction selectivity. Responses typically showed robust adaptation to all directions of stimulation. Improvements in direction tuning were observed in response to single deflections in the middle of stimulus trains. This frequency-specific sharpening of direction tuning may function to facilitate tactile discrimination of objects during whisking. In a second experiment, the direction of vibrissa deflection was changed in the middle of stimulus trains. Neural response amplitudes dramatically increased when the novel stimulus direction was presented, demonstrating direction-specific adaptation of barrel cortex responses. In the context of repetitive whisking patterns, increased neural responses to changes in direction may alert animals to novel features in their environment.

Together, the experiments in this thesis demonstrate that temporal dynamics of thalamocortical and cortical networks may optimize neural responses for the perception of specific stimulus features during whisking behavior.

Stephen G. Lisberger

TABLE OF CONTENTS

CHAPTER I:

INTRODUCTION

OVERVIEW

I begin this thesis with a brief history of the somatosensory system as a model for understanding human perception. I then introduce the rat vibrissa sensory system by summarizing the research that has been performed on the system through both behavioral and physiological studies. I follow with a discussion of a novel direction of research in this field, the study of temporal dynamics in sensory processing. I conclude the Introduction with a description of the experiments that form the core of this thesis and how they extend our understanding of sensory processing in the rat vibrissa system.

I. HISTORY OF SENSORY SCIENCE

For hundreds of years, philosophers and scientists have struggled to understand the biological foundations of human perception. In the 5th century B.C., the Greek philosopher Alcamaeon proposed that the brain was the central organ of sensation and thought (Finger 1994). However, this view was not well accepted for hundreds of years. Aristotle argued against this philosophy, suggesting that the heart was the seat of perceptual function, an opinion that is echoed both in ancient Indian medical texts and by the Chinese doctrine of Zhang Fu. In the 17th century Decartes originated a new theory, identifying the pineal gland as the center of consciousness within a reflexive brain and nervous system (Finger 1994). Although modern neuroscientists agree that sensory experience occurs in the brain, they continue to battle over the specific neural pathways and mechanisms that underlie our wide range of sensory capabilities.

Neurophsyiologists typically study the sensory systems by exploring how the brain organizes, represents, and codes sensory information. Several seminal principles of sensory processing were originally discovered in the somatosensory system. In the early 1900's, Henry Head observed that epileptic seizures typically spread systematically across the body, and proposed that this progression reflected a topographic motor map in the brain (Finger 1994). The neurosurgeon Wilder Penfield provided the first detailed description of the topographic organization of sensory maps while testing responses of epileptic patients to cortical electrical stimulation (Penfield and Rasmussen 1950). Later investigations of the somatosensory system were the first to demonstrate the existence of multiple distinct cortical areas representing the same modality (Marshal et al. 1941). Studies of tactile sensory processing were also the first to reveal that sensory maps are organized in cortical columns with similar receptive field properties (Marshal et al. 1941; Mountcastle 1957). In the 1980's the somatosensory cortex was exploited in the first demonstration of adult cortical map plasticity following manipulations of peripheral sensory input (Merzenich et al. 1984). Initial demonstrations of the similarity between psychometric functions and neurometric functions were also performed using the somatosensory system; Mountcastle showed that activity of both primary sensory afferents and cortical somatosensory neurons could account for human perceptual thresholds for cutaneous stimuli (Talbot et al. 1968; Mountcastle et al. 1969). Each of these discoveries has since been replicated in other sensory systems and each has contributed an important element to our understanding of sensory processing in the brain.

II. Sensory Processing in the Vibrissa System: An Overview

The rat vibrissa sensory system began to evolve as a preferred model of tactile processing in the early 20th century. In 1920 Lorente De Noe observed discrete clusters of cells arranged in rows across layer IV of the rat cortex (Woolsey 1970). It was not until years later that Tom Woolsey discovered a functional correlate of these columns; evoked potential studies demonstrated that these neural clusters served as a functional correlate of the prominent vibrissae, or "whiskers" on the rodent's face (Woolsey 1970). Woolsey gave the neural clusters the name "barrels" because their shape and order was reminiscent of barrels of beer stored in breweries.

A brief observation of an exploring mouse or rat easily illustrates the significance of the vibrissa system. The vibrissae, or "whiskers" on a rodent's face form a prominent array of 30-35 sensors arranged topographically across each side of the face in a precise grid of rows and columns (Figure 1A). The caudal macrovibrissae protrude in long arcs from the side of the whisker pad, while the rostral microvibrissae from a short dense patch near the rat's mouth. A rodent exploring the furnishings of its cage, or, in a more natural context, the dark tunnels of the earth or crannies of a subway track, will "whisk" the vibrissa against objects in its environment. Nocturnal rodents have poor visual acuity and limited binocular vision, and consequently rely on their vibrissae during typical exploratory activity (Prusky et. al. 2000). The relevance of this system for rodents is demonstrated by the disproportionately large cortical representation of the vibrissae, which occupies over 20% of the area of primary somatosensory cortex (SI) (Welker 1971).

Why Study the Vibrissa Sensory System?

Several features of the vibrissa-sensory system make it a useful model for studies of sensory processing. The discrete vibrissae on the rodent's face are easily manipulated with spatial and temporal precision for sensory stimulation. The one to one correspondence between the vibrissae on the whisker pad and the layer IV barrels in SI provide a simple way to anatomically identify topographic representations of each vibrissa. This organizational feature is ideal for plasticity studies in which specific vibrissae are plucked or trimmed to assess the extent of reorganization of topographic cortical maps (see Wallace and Fox 1999 for review of plasticity studies).

As the methods available to study the biological basis of sensation have advanced to include sophisticated genetic, cellular and synaptic manipulations, the demand for a good rodent model of sensory processing has increased. The vibrissa sensory system may be the best model of a sensory system with which to utilize these techniques. The discrete barrels can be anatomically identified in cortical slices and targeted for intracellular or patch recordings or for slice imaging with voltage sensitive dyes. Genetic manipulations of sensory systems are limited by current technology to a selection of small animal models, and of these the mouse is the only mammal.

Whisking behavior

The characteristic "whisking" behavior of rodents has been analyzed in numerous studies (Welker 1964; Carvell and Simons 1990). At rest, the vibrissae on a rodent's face are stationary. However, during exploration, the vibrissae are actively used to palpate objects in the rodent's environment. Each of the vibrissae is held by a sling

muscle which is used to actively protract the vibrissa forward during whisking, while retraction is largely passive (Dorfl 1982; Carvell and Simons 1990; Berg and Kleinfeld 2003). The vibrissae follow an elliptical path, moving synchronously along a rostro-caudal axis (Carvell and Simons 1990). A single bout of whisking may last for over 100 msecs and is repeated often as a rat explores (Carvell and Simons 1990). During this time, multiple vibrissae come into contact with each object of interest at various point along the hair shaft. The rodent's repetitive sampling behavior with the vibrissa array bears similarity to exploratory tactile behavior of primates and humans; when human subjects are required to explore the shape or texture of an object, they scan the surface of the relevant object with active repetitive movements that are fundamentally similar to whisking (Gamzu and Ahissar 2001).

The temporal patterns of whisking behavior are typically quite stereotyped, but may be modulated by behavioral state of the animal. Classical studies described a range of whisking frequencies in rats occurring between 1-20 Hz, with a dominant frequency of 8 Hz (Welker 1964; Carvell and Simons 1990). Numerous studies have replicated this result, reporting dominant whisking patterns from 4-12 Hz (Fanselow and Nicolelis 1999; Carvell and Simons 1995; Gao et al. 2001; Harvey et al. 2001). Additional whisking behaviors have also been described. Whisking twitching occurs at 7-12 Hz, while a second, high frequency motion between 12-25 Hz has also been reported (Nicolelis et al. 1995; Nicolelis and Fanselow 2002; Berg and Kleinfeld 2003). Although a variety of animals have facial vibrissae, true whisking occurs only in rodents such as mice, rats, and guinea pigs. In addition, the whisking frequency range differs amongst these species; mice whisk at higher frequencies than rats (~10-15 Hz vs ~4-12 Hz), and guinea pigs

whisk only rarely, at low frequencies around 5 Hz (Woolsey et al. 1981; Jin et. al. 2004). The effect of whisking behavior and whisking rates on sensory processing is a key motivation for the experiments reported in this thesis.

Perceptual Abilities of Rats

Rodents are capable of performing a variety of complex psychophysical tasks using their vibrissa. The ability of rats to discriminate fine textures with perceptual acuity similar to that of primates has been documented in multiple studies. Traditionally, blindfolded rats have been trained with gap crossing tasks to palpate two textured gratings in order to correctly cross a gap to a platform containing a food reward (Carvell and Simons 1990, 1995; Guic-Robles 1989; 1992). Behavioral experiments have shown that rats can discriminate between gratings with groove widths that differ by only tens of microns (Carvell and Simons 1990, 1995). When the vibrissae on a rat's face are trimmed, rats can perform texture discriminations with only two vibrissae, while sparing of a single vibrissa results in dramatic disruption of discriminative perceptual performance (Carvell and Simons 1995).

The ability of rats to discriminate between different shapes has also been investigated by numerous groups. Brecht et al. (1997) trained rats to discriminate small sweet and bitter cookies based on their shapes. Harvey et al. (2001) trained head-posted rats to whisk against either a cubic or spherical object and to discriminate between these shapes for a food reward. In a more recent study, the ability of rats to discriminate between bars with different angular orientations was documented as well, providing the

first evidence that rats may use the direction of vibrissa movement as a cue for object recognition (Polley et. al. 2004).

During the course of both texture and shape discrimination studies with rodents, researchers have observed that whisking behavior and temporal dynamics modulate task performance. Carvell and Simons (1995) observed that during performance of a texture discrimination task, low whisking frequencies were correlated with correct responses. Brecht et al. (1997) noted that rats seemed to whisk more "intensely" during discriminative portions of a task, in contrast with slower vibrissa movements observed while animals searched for objects in their path. Finally, Harvey et al (2001) quantified the whisking frequencies of rats that were trained to either detect or discriminate between different shapes. When rats were in a detection mode, whisking rates were centered around ~2-5 Hz. However, when rats were required to perform an active discrimination task, whisking rates increased to ~7-10 Hz. Each of these results suggests that the repetitive sensory sampling that occurs during whisking behavior may increase the salience of specific tactile features. I will return to this proposal in the discussion of my thesis experiments.

Use of the vibrissae and whisking behavior are central to the perceptual abilities of rats. Rats may even actively modulate whisking frequencies to match the perceptual demands of a specific task. However, certain tasks, such as the detection of gap widths assessed across both whisker pads, have typically been performed in the absence of whisking, and may rely on signals that are not modulated by the frequency of sensory input (Krupa et. al. 2001). The diversity of difficult tasks that can be performed by rats using their vibrissae and the range of whisking or non-whisking strategies that are used

during task performance demonstrate the importance of the vibrissa system for a rodent and the complexity with which sensory information in this system must be processed in the central nervous system.

The Sensory Pathway: From Vibrissa to Cortex

Sensory responses to vibrissa stimulation ascend to the cortex through a well-documented sensory pathway. Movement of the vibrissae activates a set of mechanoreceptors that surround each hair follicle (Rice et. al.1986). First order neurons, whose cell bodies are located in the trigeminal ganglion (NV), each innervate the follicle of only a single vibrissa (Pubols et. al. 1973). These neurons send signals through an ascending pathway to the nucleus principalis (PrV) of the brainstem trigeminal complex, and subsequently across the midline to the ventral posterior medial nucleus (VPm) and posterior medial nucleus (POm) of the thalamus, (Figure 1B, Ref). The main cortical targets of VPm inputs are the layer IV barrels of the primary somatosensory cortex (SI), while POm neurons terminate primarily in the cell sparse area between barrels, known as the septa. Both thalamic nuclei also send smaller projections to supra and infra-granular layers. Barrel and septal neurons in layer IV send partially segregated inputs to the infra- and supra-granular layers of SI cortex (for review of the vibrissa-to-barrel system see *Cerebral Cortex*, eds Jones EG and Diamonds IT. New York: Plenum Press, 1995).

Sensory Physiology: Receptive Field Sizes in the Vibrissa Sensory System

Receptive field sizes change as they ascend through the vibrissa sensory system. Primary afferents are highly selective for single vibrissae, although multi-vibrissa

receptive fields have been reported even at this level (Nord et. al. 1968). As signals ascend to the PrV and the thalamus, the convergence of information from multiple whiskers generates larger receptive fields. Action potential responses in layer IV barrels show selectivity for one vibrissa, which is typically called the "primary vibrissa" (PV), though multiple vibrissae can evoke weaker responses. Septal neurons respond to several vibrissae with less robust responses (Armstrong-James and Fox 1987). Excitation of a single vibrissa results in hierarchal flow of information from the barrel to supragranular layers, and then to infragranular layers (Simons 1978; Armstrong-James et al 1992; Laaris and Keller 2002; Contreras et al. 2001). Neurons in non-granular layers respond with longer latencies than barrel neurons and exhibit broad multi-vibrissa receptive fields (Simons 1978; Armstrong James et al. 1992).

Within SI, excitatory and inhibitory neurons have different response properties that interactively modulate responses of the barrel network. Two main subtypes of neurons are found in layer IV of SI; regular spiking units (RSUs), which are believed to be predominantly excitatory cells, and fast spiking units (FSUs) which are thought to be mainly inhibitory (Agmon and Connors 1992). FSUs can be identified by their non-selective response properties; both direction tuning and spatial tuning are notably sharper in RSUs than in FSUs (for review see Simons 1995). The broad spatial tuning of FSUs suppresses responses of RSUs to input from non-preferred vibrissae. In experimental studies, when the cortex was dis-inhibited with a GABA receptor antagonist, responses to the neighboring vibrissae increased substantially more than responses to the preferred vibrissa (Kyriazi et al 1996). Similarly, stimulation of multiple vibrissae within a short interval resulted in substantial suppression of non-preferred vibrissa responses (Simons

1985; Simons and Carvell 1989). The complexity of interactions between RSUs and FSUs will be considered again during the discussion of my thesis experiments.

Sensory Physiology: Neural Tuning to Specific Features of Vibrissa Deflections

Throughout the vibrissa sensory pathway, neurons show considerable selectivity for a variety of sensory features including the amplitude, velocity, and direction of vibrissa movements. NV neurons show the greatest relative selectivity for the direction of vibrissa movement; they are also amplitude and velocity sensitive (Nord 1968; Shipley 1974; Waite 1973; Lichtenstein et. al. 1990; Minnery 2003a). PrV and VPm neurons are similar to NV neurons in that they are amplitude, velocity, and direction selective, although they have less precise direction tuning, on average, than NV neurons (Ito 1988; Minnery et al. 2003a; 2003b). Cortical neurons maintain velocity sensitivity, but show little selectivity for the amplitude of vibrissa movements; neurons in the cortex are particularly sensitive to the timing and synchrony of thalamic inputs, which is dependent on the velocity of vibrissa movement (Pinto et al. 2000). In addition, direction selectivity appears to be slightly weaker in the cortex than the thalamus, and is present in fewer neurons (Simons and Carvell 1989). The weak direction tuning of cortical neurons will be addressed in relation to my experiments in Chapter III of this thesis.

Recent studies have shown that the velocity sensitivity of neurons in the vibrissa sensory system, in conjunction with biomechanical properties of the vibrissae, provide a mechanism for rats to decode information about high frequency (>100 Hz) vibrations. When vibrissae are stimulated at specific "resonance frequencies", they show an increase in both the amplitude and velocity of movements (Neimark et. al. 2003; Hartmann et al.

2003). The distribution of vibrissa lengths across the face create a topographic organization of these resonance frequencies; the longer caudal vibrissae have low frequency tuning, while the shorter rostral vibrissae have higher frequency tuning, up to 800 Hz (Neimark et al 2003). Single- and multi-unit recordings show that increased velocity of vibrissa movement at specific frequencies translates into higher spike rates and increased temporal precision in both trigeminal ganglion and cortical neurons (Andermann et. al. 2004, Moore and Andermann 2004). Consequently, the map of frequency across the rat face translates into a map of isofrequency columns across SI, similar to the map of frequencies in the primary auditory cortices. Because the vibrissae within an arc have similar resonance properties, high frequencies are represented topographically in columns of barrels reflecting these arcs. This organization is important because it suggests a possible system for rats to decode high frequency information that may be important for performing texture discriminations using their vibrissae. (Guic-Robles et al. 1989; 1992; Carvell and Simons 1995; Neimark et al. 2003; Andermann 2004, Moore and Andermann 2004).

III. Temporal Dynamics in the Vibrissa Sensory System: Sensory Processing in the Whisking Frequency Range.

Classic studies of the vibrissa system have focused on sensory processing of single deflections of individual vibrissae. These experiments have provided a foundation for understanding the system by exposing key filtering properties of different building blocks within the ascending sensory pathway. However, the simple stimuli used in many studies differ significantly from the spatially and temporally complex stimuli encountered

by an exploring rat. In the past decade, investigations of sensory processing in the rat vibrissa system have evolved to include investigations of the role of temporal dynamics in sensory coding. The distinct temporal structure of whisking behavior has inspired studies of neural coding in the whisking frequency range. It has been proposed that through active whisking, cortical temporal dynamics may optimize responses for discrimination of tactile stimuli (for reviews see Moore et al. 1999; Moore 2004).

Temporal Effects on Spatial Cortical Representations

The specificity of barrel responses to single vibrissae supports a common presumption that the role of layer IV is to segregate information from different vibrissae into distinct units (see discussion of A. Keller in Garabedian 2003). However, two recent studies complicated this theory by demonstrating that sub-threshold receptive fields of layer IV neurons may extend to as many as ≥ 10 vibrissae (Moore et al. 1998; Zhu and Connors 1999). Another complication for understanding spatial processing in barrel cortex is the modulation of receptive field sizes by temporal cortical dynamics. Optical imaging and electrophysiology in anesthetized animals has shown that when a single vibrissa is deflected at low frequencies (1 Hz), broad cortical activation is observed. However, during repetitive vibrissa stimulation at rates of 5-10 Hz, the cortical extent of the vibrissa representation is restricted (Sheth et. al. 1998). Recordings from SI in awake animals implanted with electrode arrays have shown similar results. The probability of recording neural activity in response to stimulation of the infraorbital sensory nerve was lower during whisking than during quiet, non-whisking states (Fanselow et. al. 2001). This shrinking effect may be modulated by strong lateral inhibition from FSUs, which

follow repetitive stimuli at higher rates than RSUs. The sharpening of spatial receptive fields in the whisking frequency range may serve to optimize discrimination of spatial stimuli during exploratory behavior (Moore et. al. 1999).

Temporal Dynamics in the Non-Behaving Animal

Temporal responses to low frequency (0-40 Hz) repetitive vibrissa movements are progressively transformed as signals are transmitted through the ascending sensory pathway. Neurons in the trigeminal ganglion and trigeminal brainstem complex respond to fast, repetitive vibrissa deflections without significant adaptation, preserving the precise temporal structure of tactile inputs (Sosnik et al. 2001; Castro-Alamancos 2001; Deschenes 2003; Hartings et al. 2003; Jones et al. 2004). In contrast, responses of thalamic VPm neurons show significant adaptation to repetitive vibrissa stimulation, decreasing in amplitude at repetition rates as low as 2-5 Hz (Sosnik et al. 2001; Castro-Alamancos 2002a; Diamond et al. 1992; Hartings et al. 2003). Thalamic adaptation is controlled by an array of complex factors, including modulation through an inhibitory feedback loop. The VPm projects to the reticular nucleus of the thalamus (NRt), which in turn sends inhibitory feedback projections to the thalamus (Figure 1) (Lee et al. 1994). Both VPm and RT neurons undergo synaptic depression in response to vibrissa stimulation, causing an interaction in the temporal dynamics of these two nuclei that is not completely understood (Castro-Alamancos 2002a,b).

One recent study investigated various potential codes for temporal stimulus rate through a serious of electrophysiological recordings in the VPm (Hartings et al. 2003).

Results of this study confirmed previous reports that VPm responses show adaptation of response amplitudes in response to repetitive vibrissa stimuli at rates greater than ~ 5-10 Hz. Despite the decrease in response amplitudes to individual stimuli, however, both the total spike rate during extended trains of vibrissa stimulation and the phase locking precision of thalamic neurons to these stimuli showed high pass filtering characteristics. Thus, the studies demonstrated that the thalamus is capable of relaying precise neural signals to the cortex at whisking frequencies. In Chapter II of my thesis, I report studies of frequency-dependent representations of total firing rate and temporal fidelity in rat SI neurons.

Cortical processing of temporal signals is likely to be more complex than VPm processing due to the diversity of cell types and synaptic connections in the cortical network. Barrel neurons, which receive VPm inputs, respond to repetitive stimuli with consistently short latencies, while septal neurons, which receive POm inputs, show latency shifts of up to 45 msec to successive stimuli (Ahissar 2001a). These latency shifts are hypothesized to underlie coding of object location (for review see Ahissar 2001b). In the barrel, RSUs display relatively robust adaptation to repetitive stimuli at low frequencies (5-10 Hz), while FSUs show consistently robust responses to higher stimulus rates (30-40 Hz, Simons 1978). More detailed investigations of cortical codes for stimulus rate have not been investigated in the cortex.

Temporal Dynamics and Behavioral State

One complication in studies of temporal coding in rat SI is the modulation of temporal dynamics by the behavioral state of the animal. This behavioral modulation

originates, at least in part, in the thalamus; the thalamus receives modulatory inputs from the reticular formation in the brainstem (Figure 1). During states of arousal, cholinergic synapses from the reticular formation (RF) strongly depolarize thalamic neurons, causing them to fire at higher rates that lead to synaptic depression at the thalamocortical synapse (Castro-Alamancos 2002a-c; Deschenes 2003). This depression has a paradoxical effect on cortical responses; evoked cortical responses are smaller during aroused states than during quiescent states because thalamic inputs are chronically depressed (Castro-Alamancos 2002a-c). Fanselow and Nicolelis (1999) demonstrated this effect by electrically stimulating the infraorbital nerve in freely moving animals. When animals were quiescent and immobile, cortical responses to stimulation were robust, but when animals whisked, responses were dramatically smaller. These behavioral influences on cortical responses must be considered when interpreting studies performed in anesthetized animals.

IV. Contributions of this Thesis to Our Understanding of the Vibrissa Sensory System

In this thesis, I have extended the classical studies of responses to single vibrissa deflections to include a investigation of SI barrel responses to several key stimulus features during repetitive vibrissa deflections in the whisking frequency range. Although repetitive sampling of the environment normally occurs in awake, whisking animals, I have chosen to perform these initial experiments in anesthetized animals because immobile animals offer the advantage of allowing precise stimulus control over long periods of time. The specific aims addressed in these experiments are:

1) **To characterize how the spike rate of rat SI neurons is modulated by the rate of vibrissa deflections.**

2) **To characterize how phase locking of rat SI neurons is modulated by the rate of vibrissa deflections.**

3) **To characterize how direction tuning of rat SI neurons is modulated by the rate of vibrissa deflections.**

4) **To investigate how rat SI neurons encode the presence of novel directional stimuli in the context of repetitive vibrissa stimulation.**

In **Chapter II** I investigated the response properties of rat SI neurons to repetitive stimulation of a single primary vibrissa at rates from 0.3 to 40 Hz. Using mulit-unit recordings, I confirmed previous reports of robust cortical adaptation to stimuli above ~5 Hz. In addition, I presented the first evidence that both spike rate and vector strength show band-pass peaks in response to stimulus train from 5-12 Hz. The frequency-specific effects suggest that using either a rate code or a temporal code, cortical temporal dynamics optimize sensory coding in the whisking frequency range. Modeling studies exploring the potential mechanisms responsible for these temporal characteristics suggested that short-term adaptation causes a peak in spike rate, while slow post-stimulus

inhibition, perhaps mediated by $GABA_B$ currents, results in a band-pass peak in vector strength.

In **Chapter III** I characterized changes in an important tuning property, direction selectivity, in response to repetitive vibrissa deflections at 4-16 Hz. I demonstrated that both multi-unit and single unit responses become more selectively tuned to the direction of vibrissa deflections during repetitive stimulation at 8-12 Hz. I also demonstrated that adaptation of cortical responses is direction specific; when the direction of a repetitive stimulus is changed after 2 seconds, responses to the novel direction increase to pre-adaptation amplitudes. Frequency-dependent improvements in direction tuning may serve to facilitate tactile discrimination during whisking, while direction-specific adaptation may function to alert rats to novel stimuli.

In total, the results of this thesis show that cortical temporal dynamics modulate representations of several stimulus features during repetitive stimulation in the whisking frequency range. These experiments represent an important step in a progression from classical sensory coding studies that employ single vibrissa deflections, to investigations of complex, behaviorally relevant stimuli. Some ideas for futures experiments that would contribute significantly to understanding sensory processing in the vibrissa-sensory system can be found in the **Future Directions** at the end of this thesis.

Figure 1. An overview of the vibrissa-sensory system. A. The arrangement of vibrissa in rows and columns on the rodent face, and the corresponding topography of barrels across the surface of SI cortex. Rows are indicated by letter and columns by number. B. An overview of the main projections of the vibrissa sensory cortex, from first order sensory neurons to SI cortex. Black arrows indicate excitatory projections, grey arrow show inhibitory projections, and dashed lines show descending projections. NV, trigeminal ganglion, PrV, principal nucleus of the trigeminal brainstem complex, VPm, ventral posterior medial nucleus of the thalamus, POm, posterior medial nucleus of the thalamus, RF, reticular formation, NRt, reticular nucleus of the thalamus, B, barrel, S, septa.

A.

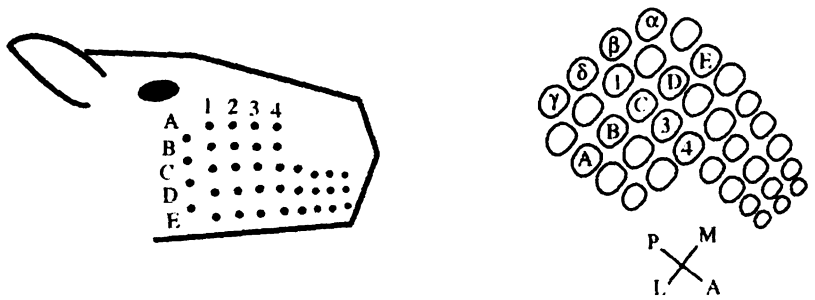
1 2 3 4
A
B
C
D
E
α
β
γ
δ
1
2
3
4
A
B
C
D
E
P
M
L
A

B.

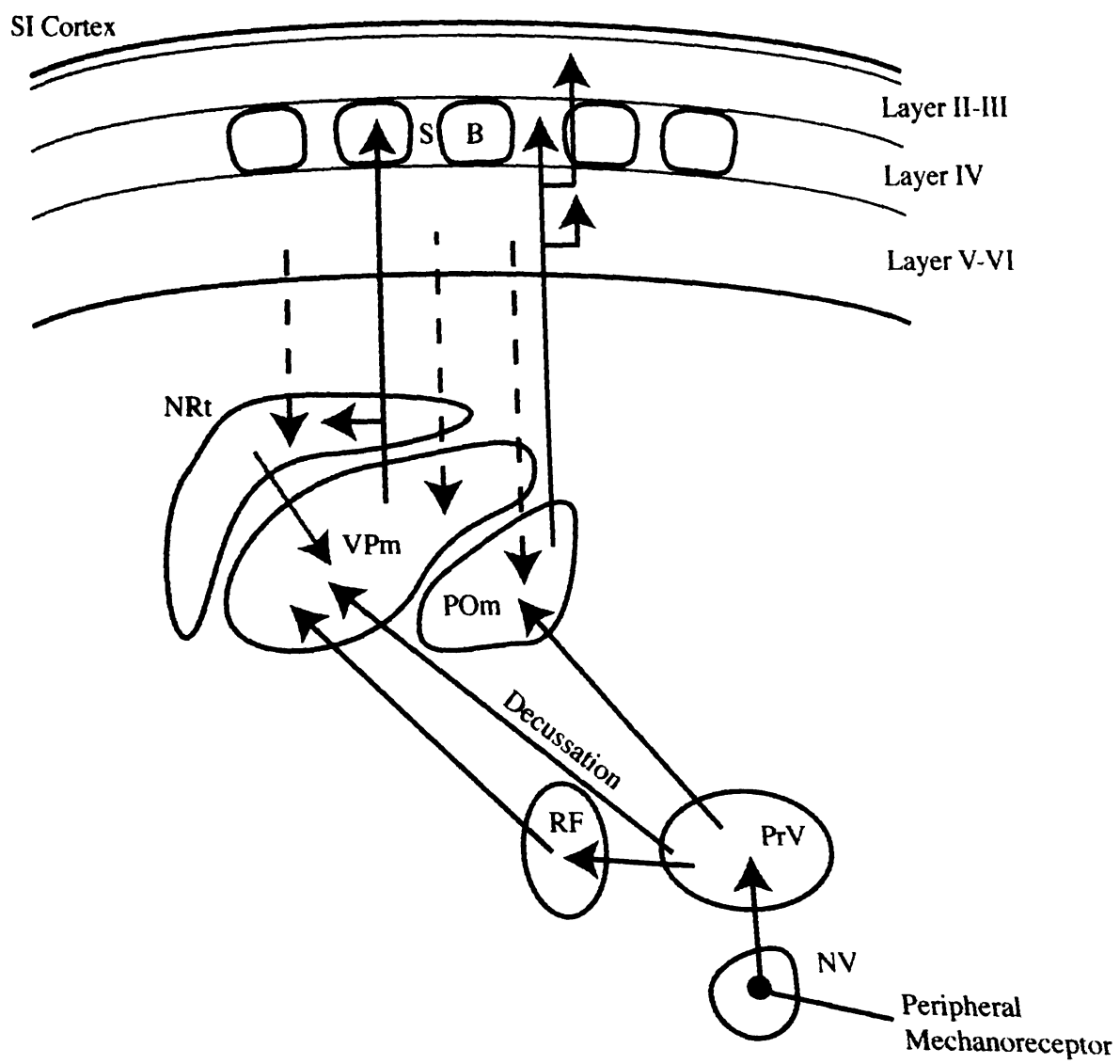
SI Cortex
Layer II-III
Layer IV
Layer V-VI
S
B
NRt
VPm
POm
Decussation
RF
PrV
NV
Peripheral
Mechanoreceptor

REFERENCES

Agmon, A. and Connors, B.W. Correlation between intrinsic firing patterns and thalamocortical synaptic responses of neurons in mouse barrel cortex. *J. Neurosci.* 12(1): 319-329, 1992.

Ahissar, E., Sosnik, R., Bagdasarian, K., and Haidarliu, S. Temporal frequency of whisker movement. II. Laminar organization of cortical representation. *J.Neurophysiol.* 86(1): 354-367, 2001a.

Ahissar, E., and Arieli, A. Figuring space by time. *Neuron* 32: 185-201, 2001b.

Andermann, M.L., Ritt, J.R., Neimark, M.A., and Moore, C.I. Neural correlates of vibrissa resonance: Band-pass and somatotopic representation of high-frequency stimuli. *Neuron* 42: 451-463, 2004.

Armstrong-James, M, and Fox, K. Spatiotemporal convergence and divergence in the rat S1 "barrel" cortex. *J. Comp. Neurol.* 263(2): 265-81, 1987.

Armstrong-James M., Fox, K., and Das-Gupta, A. Flow of excitation within rat barrel cortex on striking a single vibrissa. *J. Neurophysiol.* 68: 1345-1358, 1992.

Berg, R.N. and Kleinfeld, D. Rhythmic whisking by rat: Retraction as well as protraction of the vibrissae is under active muscular control. *J. Neurphysiol.* 89: 104-117, 2003.

Brecht, M., Preilowski, B., and Merzenich, M.M, Functional architecture of the mysacial vibrissae. *Behav. Brain Research.* 84: 81-97, 1997.

Carvell, G.E. and Simons, D.J. Biometric analyses of vibrissal tactile discrimination in the rat. *J. Neurosci.* 10: 2638-2648, 1990.

Carvell, G.E. and Simons, D.J. Task- and subject-related differences in sensorimotor behavior during active touch. *Somatosens. Mot. Res.* 12: 1-9, 1995.

Castro-Alamancos, M.A. Properties of primary sensory (lemniscal) synapses in the ventrobasal thalamus and the relay of high-frequency sensory inputs. J. Neurophysiol. 87: 946-953, 2001.

Castro-Alamancos, M.A. Different temporal processing of sensory inputs in the rat thalamus during quiescent and information processing states in vivo. *J. Physiol.* 539: 567-578, 2002a.

Castro-Alamancos, M.A. and Oldford, E. Cortical sensory suppression during arousal is due to the activity-dependent depression of thalamocortical synapses. *J. Physiol.* 541: 319-331, 2002b.

Castro-Alamancos, M.A. Role of thalamocortical sensory suppression during arousal: focusing sensory inputs in neocortex. J. Neurophysiol. 22(22): 9651-9655, 2002c.

Contreras, D. and Llinas, R. Voltage-sensitive dye imaging of neocortical spatiotemporal dynamics to afferent activation frequency. *J. Neurosci.* 21(23): 9403-9413, 2001.

Deschenes, M., Timofeeva, E., and Lavallee, P. The relay of high-frequency sensory signals in the whisker-to-barreloid pathway. *J. Neurosci.* 23(17): 6778-1787, 2003.

Diamond, M.E., Armstrong-James, M., and Ebner, F.F. Somatic sensory responses in the rostral sector of the posterior group (POm) and in the ventral posterior medial nucleus (VPM) of the rat thalamus. *J. Comp. Neurol.* 318: 462-76, 1992.

Dorfl, J. The musculature of the mystacial vibrissae of the white mouse. *J. Anat.* 135:147-154, 1982

Fanselow, E.E. and Nicolelis, M.A. Behavioral modulation of tactile responses in the rat somatosensory system. *J. Neurosci.* 19: 7603-7616, 1999.

Fanselow, E.E., Sameshima, K., Baccala, L.A., and Nicolelis, M.A. Thalamic bursting in rats during different awake behavioral states. *PNAS* 98(26): 15330-15335, 2001

Finger, S. Origins of Neuroscience: A History of Explorations into Brain Function. New York: Oxford University Press, 1994.

Gamzu, E. and Ahissar, E. Importance of temporal cues for tactile spatial-frequency discrimination. *J. Neurosci.* 21(18): 7416-7427, 2001.

Gao, P., Bermejo, R., and Zeigler, H.P. Whisker deafferentation and rodent whisking patterns: behavioral evidence for a central pattern generator. *J. Neurosci.* 21(14): 5374-5380, 2001.

Garabedian, C.E. Proceedings of the barrels II workshop: Cortical circuits. *Somatosens. Mot. Res.* 20(3-4): 297-301, 2003.

Guic-Robles, E., Valdivieso, C., and Guajardo, G. Rats can learn a roughness discrimination using only their vibrissal system. *Behav. Brain Res.* 31: 285-189, 1989.

Guic-Robles, E., Jenkins, W.M., and Bravo, H. Vibrissal roughness discrimination is barrel-cortex dependent. *Behav.Brain Res.* 48: 145-152, 1992.

Hartings, J.A., Temereanca, S., and Simons, D.J. Processing of periodic whisker deflections by neurons in the ventroposterior medial and thalamic reticular nuclei. *J. Neurophysiol. 90*: 3087-3094, 2003.

Hartmann, M.J., Johnson, N.J., Towal, R.B., and Assad, C. Mechanical characteristics of rat vibrissae: Resonant frequencies and damping in isolated whiskers and in the awake behaving animal. *J. Neurosci.* 23(16): 6510-6519, 2003.

Harvey, M.A., Bermejo, R., and Zeigler, H.P. Discriminative whisking in the head-fixed rat: optoelectronic monitoring during tactile detection and discrimination tasks. *Somatosensory Mot. Res.* 18(3): 211-222, 2001.

Ito, M. Response properties and topography of vibrissa-sensitive VPM neurons in the rat. *J. Neurophysiol.* 60(4): 1181-1197.

Jin, T., Witzemann, V., and Brecht, M. Fiber types of the intrinsic whisker muscle and whisking behavior. *J. Neurosci.* 24(31): 3386-3393, 2004.

Jones, L.M., Depireux, D.A., Simons, D.J., and Keller, A. Robust temporal coding in the trigeminal system. *Science* 304(5679): 1986-1989, 2004.

Kyriazi, H.T., Carvell, G.E., Brumberg, J.C., and Simons, D.J. Effects of baclofen and phaclofen on receptive fields properties of rat whisker barrel neurons. *Brain Res.* 712: 325-328, 1996.

Krupa, D.J., Matell, M.S., Brisben, A.J., Oliveira, I.M., and Nicolelis, M.A. Behavioral properties of the trigeminal somatosensory system in rats performing whisker-dependent tactile discriminations. *J. Neurosci.* 21(15): 5752-5763, 2001.

Laaris, N. and Keller, A. (2002) Functional independence of layer IV barrels. J. *Neurophysiol.* 87: 1028-1034.

Lee, S.M., Friedberg, M.H., and Ebner, F.F. The role of GABA-mediated inhibition in the rat ventral posterior medial thalamus. I. Assessment of receptive field changes following thalamic reticular nucleus lesions. *J. Neurophysiol.* 71(5): 1702-1715, 1994.

Lichtenstein, S.H., Carvell, G.E., and Simons, D.J. Responses of rat trigeminal ganglion neurons to movements of vibrissae in different directions. *Somatosens. Mot. Res.* 7(1): 47-65, 1990.

Marshal, W.H., Woolsey, C.N., and Bard, P. Observations of cortical somatic sensory mechanisms of cat and monkey. *J.Neurophysiol.* 4: 1-24, 1941.

Merzenich, M.M., Kaas, J.H., Wall, J., Nelson, R.J., Sur, M., and Felleman, D. Topgraphic reorganization of somatosensory cortical areas 3b and 1 in adult monkeys following restricted deafferentation. *Neuroscience*, 8(1): 33-55, 1984

Minnery, B.S. and Simons, D.J. Response properties of wisker-associated trigemino-thalamic neurons in rat nucleus principalis. *J. Neurophysiol.* 89: 40-56, 2003a.

Minnery, B.S., Bruno, R.M., and Simons, D.J. Response transformation and receptive-field synthesis in the lemniscal trigeminothalamic circuit. *J. Neurophysiol.* 90: 1556-1570, 2003b.

Moore, C.I. and Nelson, S.B. Spatio-temporal subthreshold receptive fields in the vibrissa representation of rat primary somatosensory cortex. *J. Neurophysiol.* 80: 2882-2892, 1998.

Moore, C.I., Nelson, S.B., and Sur, M. Dynamics of neuronal processing in rat somatosensory cortex. *TINS* 22(11): 513-520, 1999.

Moore, C.I. Frequency-dependents processing in the vibrissa sensory system. *J. Neurophysiol.* 91: 2390-2399, 2004.

Moore, C. I. & Andermann, M. L. (2004) The Vibrissa Resonance Hypothesis. Chapter in *Somatosensory Plasticity*, Ford Ebner, Editor. *In Press*.

Mountcastle, V.,B. Modality and topographic properties of single neurons of cat's somatic sensory cortex. *J. Neurophysiol.* 20: 408-434, 1957.

Mountcastle, V.B., Talbot, W.H., Sakata, H., Hyvarinen, J. Cortical neuronal mechanisms in flutter-vibration studied in unanesthetized monkeys. Neuronal periodicity and frequency discrimination. *J. Neurophysiol.* 32: 452-84, 1969.

Nicolelis, M.A., Bacala, L.A., Lin, R.C., and Chapin, J.K. Sensorimotor encoding by synchronous neural ensemble activity at multiple levels of the somatosensory system. *Science* 268: 1353-1358, 1995.

Nicolelis, M.A. and Fanselow, E.E. Thalamocortical optimization of tactile processing according to behavioral state. *Nat. Neurosci.* 5: 517-523, 2002.

Neimark, M.A., Andermann, M.L., Hopfield, J.J., and Moore, C.I. Vibrissa resonance as a transduction mechanism for tactile encoding. *J. Neurosci.* 23(16): 6499-6509, 2003.

Nord, S.G. Receptor field characteristics of single cells in the rat spinal trigeminal complex. *Exp. Neurol.* 21: 236-243, 1968.

Penfield, W. and Rasmussen, T. (1950) The Cerebral Cortex of Man: A Clinical Study of Localization of Function. New York: Macmillan.

Pinto, D.J., Brumberg, J.C., and Simons, D.J. Circuit dynamics and coding strategies in rodent somatosensory cortex. *J. Neurophysiol.* 83: 1158-1166, 2000.

Polley, D., Rickert, J.L., and Frostig, R.D. Whisker-based discrimination of object orientation determined with a rapid training paradigm. *Neurobiol. of Learning and Memory*, submitted.

Prusky, G.T., West, P.W., and Douglas, R.M. Behavioral assessment of visual acuity in mice and rats. *Vision Res.* 40(16): 2201-2209, 2000.

Pubols, B.H., Donovick, P.J., and Pubols, L.M. Opossum trigeminal afferents associated with vibrissa and rhinarial mechanoreceptors. *Brain, Behav. Evol.* 7: 360-381, 1973.

Rice, F.L., Mance, A., and Munger, B.L. A comparative light microscopic analysis of the sensory innervation of the mystacial pad. I. Innervation of vibrissal follicle-sinus complexes. *J. Comp. Neurol.* 252: 154-174, 1986.

Sheth, B.R., Moore, C.I., and Sur, M. Temporal modulation of spatial borders in rat barrel cortex. *J. Neurophysiol.* 79: 464-470, 1998.

Shipley, M.T. Response characteristics of single units in the rat's trigeminal nuclei to vibrissa displacements. *J. Neurophysiol.* 37(1): 73-90, 1974.

Simons, D.J. Response properties of vibrissa units in rat SI somatosensory neocortex. *J. Neurophysiol.* 41: 798-820, 1978.

Simons, D.J. Temporal and spatial integration in the rat SI vibrissa cortex. *J.Neurophysiol.* 54(3): 615-635, 1985.

Simons, D.J. Neuronal integration in the somatosensory whisker/barrel cortex. In: *Cerebral Cortex*, edited by Jones EG and Diamonds IT. New York: Plenum Press, 1995, p. 263-298.

Simons, D.J. and Carvell, G.E. Thalamocortical response transformation in the rat vibrissa/barrel system. *J. Neurophysiol.* 61: 311-330, 1989.

Sosnik, R., Haiderliu, S., and Ahissar, E. Temporal frequency of whisker movement. I. Representations in the brain stem and thalamus. *J. Neurophysiol.* 86: 339-353, 2001.

Talbot, W.H., Darian-Smith, I., Kornhuber, H.H., and Mountcastle, V.B. The sense of flutter-vibration: comparison of the human capacity response patterns or mechanoreceptive afferents from the monkey hand. *J. Neurophysiol.* 31: 301-34, 1968.

Waite, P.M.E. The responses of cells in the rat thalamus to mechanical movements of the whiskers. *J. Physiol.* 228: 541-561, 1973.

Wallace, H. and Fox, K. Local cortical interactions determine the form of cortical plasticity. *J. Neurobiol.* 41(1): 58-63, 1999.

Welker, W.I. Analysis of sniffing of the albino rat. *Behavior* 12: 223-244, 1964.

Welker, C. Microelectric delineation of fine grain somatotopic organization of SmI cerebral neocortex in albino rat. *Brain Res.* 26: 259-275, 2971.

Woolsey, T.A. and Van Der Loos, H. The structural organization of layer IV in the somatosensory region (S 1) of mouse cerebral cortex. *Brain Res.* 17: 205-242, 1970.

Woolsey, T.A. et al. (1981) Somatosensory development. In: *The development of perception: psychobiological perspectives*, edited by R.N. Aslin and D.B. Pisani, pp. 259-292.

Zhu, J.J. and Connors, B.W. Intrinsic firing patterns and whisker-evoked synaptic responses of neurons in the rat barrel cortex. *J. Neurophysiol.* 81: 1171-1183, 1999.

CHAPTER II:

BAND-PASS RESPONSE PROPERTIES OF RAT SI NEURONS

ABSTRACT

Rats typically employ 4-12 Hz "whisking" movements of their vibrissae during tactile exploration. The intentional sampling of signals in this frequency range suggests that neural processing of tactile information may be differentially engaged in this bandwidth. We examined action potential responses in rat primary somatosensory cortex (SI) to a range of frequencies of vibrissa motion. Single vibrissae were mechanically deflected with 5 second pulse trains at rates up to 40 Hz. As previously reported, vibrissa deflection evoked robust neural responses that consistently adapted to stimulus rates $\geq$ 3 Hz. In contrast with this low-pass feature of the response, several other characteristics of the response revealed band-pass response properties. While average evoked response amplitudes measured 0-35 msec after stimulus onset typically decreased with increasing frequency, the later components of the response (>15 msec post stimulus) were augmented at frequencies between 3-10 Hz. Further, during the steady state, both rate and temporal measures of neural activity, measured as total spike rate or vector strength (a measure of temporal fidelity of spike timing across cycles) showed peak signal values at 5-10 Hz. A minimal biophysical network model of SI layer IV, consisting of an excitatory and inhibitory neuron and thalamocortical input, captured the spike rate and vector strength band-pass characteristics. Further analyses in which specific elements were selectively removed from the model suggest that slow inhibitory influences give rise to the band-pass peak in temporal precision, while thalamocortical adaptation can account for the band-pass peak in spike rate. The presence of these band-pass characteristics may be a general property of thalamocortical circuits that lead rodents to target this frequency range with their whisking behavior.

INTRODUCTION

The rat primary somatosensory cortex (SI) is a popular model for studies of spatial cortical representation because of the discrete one to one topographic correspondence of vibrissae to cortical layer IV "barrels" (Woolsey and Van der Loos 1970). The rat vibrissa system also engages a range of temporally specific information-sampling behaviors. During rest or inactivity, the facial vibrissae are stationary. Following an alerting contact or during active exploration, vibrissae are "whisked" in rhythmic ellipsoid movements through the air and over objects being discriminated (Carvell and Simons 1990; Harvey et al. 2001; Welker 1964). Measurements of whisking reveal a frequency power spectrum with a peak between 4 and 12 Hz, and a relatively narrow band-width (typically less than 3 Hz; Carvell and Simons 1990, 1995; Fanselow and Nicolelis 1999; Gao et al. 2001; Harvey et al. 2001; Nicolelis and Fanselow 2002; Welker 1964). Whisking frequency can vary during sampling epochs and can be modified as the result of learning (Harvey et al. 2001). In addition to the predominant whisking behavior, two other frequency-specific vibrissa motion patterns have been observed: Vibrissa twitching, a brief period of low-amplitude vibrissa motion between 7-12 Hz (Berg and Kleinfeld 2003; Nicolelis et al. 1995; Nicolelis and Fanselow 2002), and a second, higher frequency motion of protracted vibrissae, peaking in a range from 15 to 25 Hz (Berg and Kleinfeld 2003; see also Carvell and Simons 1990; Harvey et al. 2001).

Electrophysiological studies of temporal processing in rat SI have reported robust adaptation of layer IV responses to repetitive stimulation of vibrissae above 3 Hz (Chung et al. 2002; Simons 1978; Ahissar 2000, 2001b; Castro-Alamancos and Oldford 2002b).

In layer IV, differential adaptation patterns have been observed in distinct neuron populations. Regular spiking units, which are putative excitatory neurons, show action potential and EPSP adaptation at frequencies as low as 4 Hz (Simons, 1978: Chung et al., 2002). In contrast, fast spiking units, which are putative inhibitory neurons, emulate ventral posterior thalamic neurons by responding robustly to stimulus rates as high as 40 Hz (Simons 1978). Robust adaptation is observed in the barrels and septa of layer IV, although the mechanistic underpinning of adaptation in these regions may be different (Ahissar et al. 2000, 2001b).

The frequencies of vibrissa motion displayed during rest (<1 Hz) and whisking (4-12 Hz) may optimize the vibrissa processing system for the detection or discrimination of stimulus features, respectively (Moore et al. 1999; Nicolelis and Fanselow 2002). During rest, general alertness to incoming stimuli is crucial, while during whisking, the ability to make fine and rapid discriminations between stimuli is potentially more important. Consistent with this hypothesis, the cortical representation of a single vibrissa is more spatially focused during high frequency (5-10 Hz) vibrissa stimulation than low frequency (1 Hz) stimulation (Sheth et al. 1998). Further, inter-vibrissa lateral inhibition is robust within rat SI, suggesting that multi-vibrissa contact enhances the functional isolation of each vibrissa (Brumberg et al. 1996). These findings suggest that in the context of low frequencies of vibrissa motion (e.g., during rest), contact on any vibrissa may be more easily detected by the broader recruitment of cortical neurons, while during whisking, the somatotopic identity of a specific vibrissa may be better discriminated (Moore et al. 1999). Behavioral studies further support this framework. When rats were trained to whisk an object to obtain a reward, whisking frequency peaked from 2-5 Hz.

However, when the same animals learned to discriminate between these objects for reward, a second peak emerged at 7-10 Hz. The power of this peak correlated with task performance level, demonstrating that higher frequency whisking may be used as a strategy to increase perceptual selectivity (Harvey et al. 2001).

In this paper, we present physiological evidence that several temporal response properties are amplified by vibrissa stimulation in the whisking frequency range, supporting the idea that information processing at these sampling rates is differentially represented in SI. We characterized responses of 64 SI recording sites to stimulation of individual vibrissae at rates up to 40 Hz. In agreement with previous studies (Ahissar et al. 2001b; Castro-Alamancos and Oldford 2002b; Chung et al. 2002; Simons 1978), steady state responses showed adaptation at high stimulation rates. Several other features of the evoked neural responses showed band-pass effects. Between 5-10 Hz, late components of the steady state response were facilitated, total spike count over the steady-state period of the train increased, and vector strength (VS), a measure of temporal fidelity, was maximal. Results from a model of the layer IV 'barrel' cortical network with feedforward thalamic input replicated these band-pass effects, suggesting that input layer cortical circuitry can account for these phenomena. These results, taken with previous findings, suggest that cortical representations of sensory stimuli are selectively optimized for this behaviorally relevant range of processing frequencies.

METHODS

Preparation

Adult Sprague-Dawley rats (275-325 grams) were anesthetized with sodium pentobarbitol (50 mg/kg ip) and a craniotomy and durotomy were performed to expose the left primary somatosensory cortex (SI). A tracheotomy and a cisternum magnum drain were performed. Animals were maintained at a constant level of anesthesia with supplemental doses of pentobarbitol as needed (10% of the induction dose) so that they remained unresponsive to hindpaw pinch, with a stable breathing rate (30-60 breaths/min) and heart rate (4-7 beats/sec). At the end of each experiment, animals were euthanized with an overdose of sodium pentobarbital (150mg/kg) and a bilateral thoracotomy was performed.

Stimulation and Electrophysiology

We recorded multiunit activity from 64 recording sites in the primary somatosensory cortex of 12 rats. Recordings were made with tungsten microelectrodes (FHC # UEWMCJSE2P4G, 2-4 MΩ) from the middle layers (500-750 μm), depths that typically correspond to layer IV in rat SI (Diamond et al., 1994). The time resolution for data collection was 25 kHz. Activity was band-pass filtered between 300 Hz and 10 kHz; spike times and shapes were recorded using a window discriminator, which was set well above noise level to isolate only action potential responses. Before each recording, the tip of the electrode was placed at the surface of the cortex and lowered down incrementally while monitoring the depth with microdrive readings. The primary vibrissa corresponding to each recording site was identified by hand mapping. Sites that

responded robustly to a single vibrissa were identified as being putative barrel sites, while signals that showed weak responses to vibrissa stimulation or that responded equally well to more than one vibrissa were rejected as putative septal or non-layer IV sites, and were not used in this study. Responses were collected from the vibrissae in columns 1-3, rows C, D, and E, and from the gamma and delta vibrissae. A piezoelectric stimulator with a three cm extension attached to a wire loop was positioned so that the ventral surface of the vibrissa just contacted the loop one cm from the face. Mechanical dorsal deflections of the vibrissa were presented in trains of half-sinusoidal symmetric pulses (from trough to trough; 14 msec duration, ~100 μm maximal amplitude), for a vibrissa velocity of 20 mm/sec at the point of simulator contact. Five-second-long pulse trains were presented at each frequency 10 times each in random order, with 3 second intervals between trains. At each recording site, we presented ≥ 9 frequencies, including 1, 2, 3, 5, 8, 10, 12, 15, 20, 25, 30, 35, and 40 Hz (1, 3, 20, 30 and 40 Hz: N=59; 5, 8 , 10, 15 Hz: N=64). Because significantly fewer responses were collected across recordings at 2, 12, 25, and 35 Hz, those frequencies were not included in the present analysis.

Analysis

We applied several different analyses to the cumulative data set. For each of the analyses described below (repetition rate transfer function, vector strength, spike rate, and latency), the analysis of responses to frequency trains from 1-40 Hz were performed on the *steady state* response, defined as the period 1-5 seconds after the onset of the stimulus train. This time period was chosen for analysis to eliminate confounding effects of the dynamic changes in response latency or amplitude that characterized the first second (*the*

dynamic period) of the response to each stimulus train. Unless otherwise stated, all analyses were performed with a resolution of 1 msec time bins.

Repetition Rate Transfer Function (RRTF): The number of spikes evoked by each vibrissa deflection during the steady state (1-5 seconds post-stimulus) period of the stimulus train was averaged for a given recording and normalized by the average number of spikes evoked by the first deflection of the stimulus train. The period over which individual response amplitudes were integrated for the RRTF calculation was defined in two ways. In the first analysis, spikes 0-35 msec post-pulse onset were included, which was sufficient time to include all evoked spikes. This analysis was performed separately for each individual recording site. An RRTF value of 1 indicates no adaptation, a value above 1 indicates increased spike rate in the steady state, and a value below 1 indicates a decrease in response rate. In the second analysis, 5 msec time windows (5-10, 10-15, 15-20, 20-25, 25-30, and 30-35 msec post stimulus) after each vibrissa deflection were analyzed. Because the numbers of evoked responses in these short time windows were small and variable, this analysis was conducted only on the averaged PSTH over all recording sites. Because each 5 msec time window included only a subset of the evoked spikes at each frequency, the resulting RRTF values quantifies the relative response amplitude during a particular time epoch, and is meant to capture changes in the latency, as well as the amplitude of responses at different frequencies. For both RRTF analyses, the same time window was used to quantify responses to the first deflection and deflections during the steady state period.

Total Spike Rate (SR): In this analysis, the average spike rate during the entire steady state period of each stimulus train was calculated. All spikes, regardless of their post-stimulus latency, were included in this analysis.

Vector Strength (VS): The temporal consistency of spike timing across stimulus cycles during the steady state period was quantified using vector strength (VS). The VS was calculated as per Goldberg and Brown (1969):

$$VS = \sqrt{\Sigma(\cos\theta)^2 + \Sigma(\sin\theta)^2} \,/\, N$$
$$\theta = 2\pi(t/T)$$

Where N is the total number of spikes evoked during the stimulus train, t is the time between the most recent previous vibrissa deflection and the evoked spike, and T is the period of the stimulus frequency. For each recording site and stimulus frequency, an average cycle histogram with 1 msec bins was constructed for the steady state response to all repetitions of a stimulus train, and the VS was calculated from this histogram. The VS quantifies the precision with which spikes are locked to the same phase of a stimulus period during each repetitive cycle of stimulation. The VS measure is proportional to the amplitude of the Fourier component of the driving frequency of the period histogram normalized by the total number of spikes during this period. A value of 1 signifies perfect phase locking; a value of 0 signifies random spike timing. Latency shifts presumably did not affect this statistic because only steady state responses were analyzed.

Latency: The response latency for each frequency at each recording site was evaluated from the average cycle histogram at steady state. For the first deflection, the ten repetitions of the first response to all stimulus trains were used to calculate latency. The

latency was defined as the post-stimulus time at which the response amplitude reached 50% of its peak value. In separate analyses, histograms were convolved with a right triangle as in Ahissar et al. (2001b), yielding similar results. Similarly, the latency to the declining slope of the PSTH was defined as the post-stimulus time after the peak response at which the response amplitude fell below 50% of its peak value. We chose to use averaged steady state histograms to calculate latency rather than averaging latencies for individual deflections because there were often insufficient spike responses to single deflections to make reliable latency estimations, particularly at high frequencies. To make statistical comparisons of onset and decay latencies at different frequencies, we chose 55 recording sites at which the VS was ≥ 0.3 for frequencies between 3 and 15 Hz, to eliminate recordings in which there were no significant periodic responses (see Figure 3C). For these sites, the response width was defined as the difference in time between the latency onset and decline at each frequency.

In analyses of latency, a sign test was applied to assess whether a significant subset of recordings demonstrated a given trend ($p < 0.05$), for example, a higher probability of longer-latencies to response onset with increasing frequency.

Depth comparisons: Recording sites were divided into five groups based upon recording depth as measured on a microdrive (500-550, 551-600, 601-650, 651-700, and 701-750 μms). The mean RRTF, SR, and VS, as well as onset and decay latencies were calculated for each group independently. For each analysis, a one way ANOVA was performed to test for any significant differences between the five groups. For RRTF, SR, and VS analyses, N=20 for 500-550 μms, N=18 for 551-600 μms, N=9 for 601-650 and

651-700 μms, and N=8 for 701-750 μms. For latency analyses, N=12 for 500-550 and 551-600 μms and N=5 for 601-650, 651-700, and 701-750 μms. Only sites at which VS $\geq$ 0.3 for 3-15 Hz were included in the latency analyses.

Minimal Cortical Model

The numerical simulations were performed on a model representing a layer IV vibrissa barrel circuit. The circuit consisted of two cells – an excitatory cell (E cell) and an inhibitory cell (I cell). Both cells were modeled with Hodgkin-Huxley-based current-balance equations as follows:

$$C\frac{dV_E}{dt} = I_L + I_{NA} + I_K + I_{appe} + I_{GABA_A} + I_{GABA_B} + I_{Thal} + noise$$

$$C\frac{dV_I}{dt} = I_L + I_{NA} + I_K + + I_{appi} + I_{AMPA} + I_{GABA_A} + I_{GABA_B} + I_{Thal} + noise$$

$$I_{ion} = g_{ion} m^p h^q (V_{ion} - V)$$

Here, C is the membrane capacitance, V_j is the membrane potential of cell j, I_{ion} is an ionic current, g_{ion}, m and h are, respectively, the maximal conductance, and the dynamic activation and inactivation variables for that current, V_{ion} is the associated reversal potential, and p and q are integers.

The sodium (I_{NA}), potassium (I_K) and leak (I_L) currents represent voltage dependent currents of regular spiking cells (Simons, 1978) and cause each cell to display a typical spike pattern of a suprathreshold spike followed by a brief refractory period. The applied currents (I_{appe} and I_{appi}) represent constant tonic drive to each cell. Thalamic input was also captured by an applied current (I_{thal}) and was modeled as a 30ms square-wave pulse delivered to each cell at various frequencies (1-20 and 30 Hz). The thalamic

input was stronger for inhibitory than excitatory cells (Simons 1995). The intrinsic currents were modeled as follows:

$$I_L = g_L(E_L - V)$$
$$I_{NA} = g_{NA} m^3 h(E_{NA} - V)$$
$$\alpha_m(v) = 0.32*(54+v)/(1-\exp(-(v+54)/4))$$
$$\beta_m(v) = 0.28*(v+27)/(\exp((v+27)/5)-1)$$
$$\alpha_h(v) = 0.128*\exp(-(50+v)/18)$$
$$\beta_h(v) = 4/(1+\exp(-(v+27)/5))$$
$$I_K = g_{NA} n^4 (E_K - V)$$
$$\alpha_n(v) = 0.032*(v+52)/(1-\exp(-(v+52)/5))$$
$$\beta_n(v) = 0.5*\exp(-(57+v)/40)$$

The functions α_y and β_y capture the forward and backward rates of the activation and inactivation variables (y) of each of the currents, as in standard Hodgkin-Huxley notation, where $\frac{dy}{dt} = \alpha_y(1-y) - \beta_y y$. Time is in milliseconds. The local two-cell circuit was established by synaptically coupling the cells using a model fast excitatory synapse (AMPA), and model fast and slow inhibitory synapses ($GABA_A$ and $GABA_B$, respectively).

The synapses are given by the following equations (Koch and Segev, 1998):

$$I_{AMPA} = g_{AMPA} AMPA(E_{AMPA} - V)$$
$$I_{GABA_A} = g_{GABA_A} GABA_A(E_{GABA_A} - V)$$
$$I_{GABA_B} = g_{GABA_B}(GABA_B^4/(GABA_B^4 + 5))(E_{GABA_B} - V)$$
$$\frac{dAMPA}{dt} = ke(V_E)(1 - AMPA) - AMPA/\tau_{EI}$$
$$\frac{dGABA_A}{dt} = ki(V_I)(1 - GABA_A) - GABA_A/\tau_I$$

$$ke(V) = 5*(1+\tanh(V/4))$$
$$ki(V) = 2*(1+\tanh(V/4))$$
$$\frac{dGABA_B}{dt} = 1.8(r_B)\text{-}0.34GABA_B$$
$$\frac{dr_B}{dt} = 0.9trans(1\text{-}r_B)\text{-}0.012r_B$$

where *trans* is set to one for 1ms when V_I crosses zero.

To capture thalamocortical input on each cycle of the square-wave thalamic input (I_{thal}) the height, *h*, of the square-wave pulse changed according to

$$h \rightarrow d*f\ ,$$

where *d* is a depression term that resets to $d*C_d$ during each cycle of the thalamic input. Between cycles of the thalamic input *d* changes according to $d' = (1\text{-}d)/\tau_d$. Similarly, *f* is a facilitation term that resets to $f*C_f$ during each cycle of the thalamic input, and between cycles changes according to $f' = (fsat - f)/\tau_f$. (Varela et al., 1997). The time constants *d* and *f* were chosen so that the RRTF curve resulting from data generated by the model matched the RRTF curve generated experimentally. The input activity is shown in Figure 7B to demonstrate the interaction between depression and facilitation at each frequency. The additional noise current (*noise*) in each cell was modeled as a noisy excitatory (AMPA) synapse that comes from a presynaptic cell outside of the two-cell circuit. The presynaptic cell fires randomly with a uniform distribution in time.

The values of the parameters employed were derived from the experimental data and from other models of the rat somatosensory system (Jones et. al. 2000; Kyriazi and Simons 1993; Pinto et. al. 1996) and are as follows: Iappe=0.5, Iappi=0.5, E_K=100, E_{NA}=50, E_L=-67, , E_{GABAA}=-80, E_{GABAB}=-80, E_{AMPA}=0, g_L=.1, g_K=80, g_{NA}=100, g_{AMPA}=0.1, g_{GABAA}=0.2, g_{GABAB}=0.2, τ_{ei}=2,τ_i=10, τ_d=80, τ_f=1000, C_d=0.5, C_f=0.6, f_{sat}=2.

All simulations were performed using G.B. Ermentrout's package for solving ordinary differential equations, XPPAUT. This package is available from ftp://ftp.math.pitt.edu/-pub/bardware. The usual method of integration was a fourth-order Runge-Kutta method with a time step of dt=0.02.

RESULTS

Adaptation to repetitive stimuli

The average post stimulus time histogram (PSTH) for all 64 recordings is shown in Figure 1A. At 1 Hz, each repetition of the stimulus elicited a robust response. At higher frequencies, responses changed dynamically over the first ~1000 milliseconds of stimulation, typically decreasing in amplitude, and then stabilized to a *steady state* response, defined as the last 4 seconds of the 5 second stimulus period. After each initial excitatory response, activity was suppressed below spontaneous rates for ~130 msec after stimulus onset (Figure 1B). At high stimulus rates, deflections during this time resulted in few, if any, evoked spikes. At lower frequencies with periods > 130 msec (1-5 Hz), a 'rebound' back to or above spontaneous activity levels was observed after this suppression (Figure 1B). At most recording sites, a frequency was reached above which no systematic or periodic spiking was evoked after the first ~1 second of stimulation. At this frequency, sites often responded to every other repetition of a stimulus, firing at half the stimulus frequency presented to the vibrissa. This type of response is reflected in the average PSTH at 15 Hz (Figures 1A, B), where responses to every other stimulus during the first second of the train are enhanced.

To quantify a commonly measured feature of adaptation, we calculated a repetition rate transfer function (RRTF) for the responses in our sample. For each site, the average amplitude of the response to vibrissae deflections (0-35 msec post-stimulus) at steady state was normalized to the amplitude of the first response to the train. At low frequencies, a high amplitude response was maintained during the course of the train, which is reflected in high RRTF values (Figure 2A, 2B). Although facilitation was not uncommon at low frequencies (42/64 sites showed facilitation at some frequency, 20 of these at 1 Hz), an inspection of the individual RRTF curves shows that all responses had predominantly low pass RRTF characteristics that saturated by 20 Hz (Figure 2B). The slope of the mean RRTF curve was steepest between 5-10 Hz. These results confirm previous reports of low pass response adaptation of cortical neurons to repetitive vibrissa stimulation (Ahissar et al. 2001b; Castro-Alamancos and Oldford 2002b; Chung et al. 2002; Simons 1978).

Band-pass properties of adaptation

Although the net evoked response to a given stimulus within a train decreased with frequency, this adaptation was dependent on the time window in which responses were calculated. The steady state responses at different frequencies of stimulation exhibited a small but consistent (0-5 msec) latency shift compared to the average first deflection in a train (Figure 3). This effect was found to be significant for all frequencies evaluated ($p < 0.01$ for rates from 3-15 Hz, $p=0.073$ for 1 Hz, sign test for incidence of longer latencies at each recording site for each frequency vs. first pulse latency). Increased latency was paralleled by a later response decline that is demonstrated by the

normalized and averaged cycle histograms at each frequency (Figure 3B, $p < 0.01$ for rates up to 15 Hz, sign test). Even at rates as low as 1 Hz, the average steady state response began later than the response to the first deflection, and there was a systematic increase in both onset and decline time with increasing frequency and a trend towards longer lasting responses at higher frequencies ($p < 0.05$ for 8, 10, and 15 Hz, sign test). This latency shift suggests that although average response amplitudes decreased with increasing repetition rates, within specific longer-latency time windows, responses were facilitated relative to onset amplitude. To characterize this phenomenon, we calculated an RRTF of the averaged PSTH in 5 msec post-stimulation time windows (Figure 3D). During the 5-10 and 10-15 msec post-stimulus time windows, steady state responses were smaller than responses to the first deflection, as suggested by the overall RRTF value from 0-35 msec. However, for time windows beginning $\geq$ 15 msec after vibrissa deflection, responses showed band-pass facilitation at intermediate frequencies due to fast decline of first pulse responses and increased latency of steady state responses. At 15-35 msec post-stimulus, facilitation of later time window responses peaked at rates between 3-10 Hz, with a systematic increase in facilitation in later time windows.

Band-pass temporal and spike rate responses

Additional analyses assessed overall spike rate (SR) and spike timing (VS) as a function of the frequency of vibrissa movement. The SR at each recording site was plotted as a function of stimulus frequency. In the majority of individual examples (70%, N = 45/64) and in the grand average, neurons displayed a peak in mean SR between 5-10

Hz (Figures 4A, B). Above 15 Hz, firing rate at individual recording sites and in the average response were consistently lower.

The temporal fidelity of each response to the stimulus rate was quantified by calculating the VS for each frequency. The VS reflects the precision with which a response locks its firing to the same phase of the stimulus period across deflections, with higher values signifying more consistent spike timing between cycles. Figure 5 shows the average VS (Figure 5A) and the VS for each recording (Figure 5B). Like the overall SR measure, VS peaked at 5-10 Hz in the grand average, and in almost all individual cases (89%, N = 57/64).

Comparison of responses by recording depth

We divided recording sites into five groups based on electrode depth to determine whether any of the observed temporal responses might vary with recording position. The RRTF, VS, and SR measures as well as onset and decay latency, were independently quantified for sites between 500-550, 551-600, 601-650, 651-700, and 701-750 μms depths (Figure 6). For each group, RRTF values decreased with increasing frequency, while VS and SR responses showed band pass peaks between 5-10 Hz, as in the cumulative data set. For each characteristic, a one way ANOVA at each frequency showed no statistical difference between responses at each recording depth ($p > 0.1$ for RRTF, VS, SR and onset latency at all frequencies, $p > 0.08$ for decay latency at all frequencies).

Modeling of cortical transformations

We employed a minimal cortical model including basic features of layer IV circuitry to provide insight into the mechanistic bases of the observed temporal phenomena. The model consisted of a spiking inhibitory and excitatory cell that were synaptically coupled via fast excitation (AMPA) and fast and slow inhibition ($GABA_A$ and $GABA_B$) (Figure 7A). Each cell also received adapting depolarizing thalamic input and additional noisy excitatory drive. Calculations of RRTF, VS, and SR from simulations of the model produced results similar to our physiological data (Figure 7).

The experimentally observed facilitation at the lowest sampled frequencies, and low pass adaptation at higher frequencies were built into the model via thalamocortical input (Figure 7B). Adaptation and facilitation parameters where chosen while holding all other variables constant, so that the RRTF curve generated from numerical simulations (Figure 7D, black curve) matched those generated from the physiological data (compare to Figure 2A). Thus, the origin of the adaptation in the model is non-explicit and may capture either the adaptation at the thalamocortical synapse or a reduction in thalamic or pre-thalamic firing. The relative amplitude of the input activity during the stimulus train is shown for each frequency in Figure 7B. At 1 Hz, facilitation dominates over depression during the steady state, while at frequencies > 3Hz, the input activity shows varying degrees of depression. When the adaptation is removed from the model, the height of the square-wave impulse train remains 1 (data not shown).

When thalamocortical adaptation alone was removed from the model, the low pass phenomenon disappears (Figure 7D, mid-gray curve). Slow suppressive intra-cortical mechanisms also influence the shape of the RRTF curve in the model. When the

$GABA_B$ synapse alone is removed from the model (Figure 7D, light gray curve), less intra-cortical inhibition is evoked overall on subsequent cycles of stimulation, leading to an increase in the normalized RRTF value. Interestingly, the contribution of modeled $GABA_B$ was not observed in the absence of thalamocortical adaptation (Figure 7D, light gray curve), suggesting a non-linear addition of these suppressive influences. The requirement that other concomitant inhibitory factors are present for the expression of $GABA_B$ affects has recently been observed in other sensory cortices (Wang et al., 2002).

Although no further manipulations were made in the model to capture the band-pass temporal features observed experimentally, SR and VS curves qualitatively similar to those generated from the physiological data emerged (compare black curves in Figures 7E and 7F to Figures 4A and 5A). Removal of thalamocortical adaptation evoked a linear rise in SR with stimulus frequency (Figure 7E, mid-gray curve). Slow intra-cortical inhibitory mechanisms also affected SR values. When the $GABA_B$ synapse alone was removed from the model (Figure 7E, light gray curve), SR values were higher and the band-pass character of this feature was diminished (compare black and light gray curves in Figure 7E). Unlike the SR response, the band-pass character of the VS was not influenced by thalamocortical adaptation (Figure 7F, mid-gray curve). However, slow intra-cortical inhibition played a dominant role in defining this band-pass peak, as verified by the lower degree of band-pass VS modulation in the light gray curve in Figure 7F, generated with $GABA_B$ removed from the model. The inhibitory influence of $GABA_B$ on the observed band pass phenomena was specific to the dynamics of this current, and not a general effect of inhibition. When $GABA_A$ was removed from the

model, higher spike rates were observed but there was little influence on the shape of the VS and RRTF curves (data not shown).

DISCUSSION

In this study, we replicated previous reports that described low pass adaptation of the evoked responses of layer IV cortical neurons to vibrissa deflection. In agreement with earlier studies (Ahissar et al. 2001b; Castro-Alamancos and Oldford 2002b; Chung et al. 2002; Simons 1978), almost all individual recording sites and the grand average of responses adapted to repetitive stimulation, and this adaptation was more robust with increasing frequency. Further analyses revealed several band-pass characteristics of the evoked responses. The relative response amplitude in late periods of the evoked response, and the average SR, and VS during the steady state peaked with repetitive stimulation between 5-10 Hz. These band-pass characteristics of SI neurons overlap closely with the reported range of whisking sampling frequencies of the vibrissae, suggesting that whisking frequencies reflect the optimal range for sensory information processing in the vibrissa to cortex pathway. The replication of the key features of these findings by a reduced computational model of layer IV circuitry suggests that, while many levels of information processing may contribute to the existence of these band-pass phenomena, basic features of layer IV cortical circuitry can account for their generation.

Implications for whisking behavior and sensory coding

We have previously proposed that cortical dynamics transform sensory representations to optimize perceptual performance in the whisking frequency range.

Specifically, low frequency input facilitates detection of tactile stimuli through spatially extensive recruitment of a greater number of cortical neurons by a given vibrissa, while stimulation at higher rates, initiated by whisking, facilitates spatial discrimination of distinct vibrissae through the restriction of activation extent (Moore et al. 1999). The current findings are consistent with the proposal that rat SI processing is differentially transformed in the whisking frequency range, and appear to extend the applicability of this framework to the temporal processing domain.

Each of the observed band-pass properties, the precise timing of spiking activity, the mean spike rate over an extended period, and response latency, have been central features of proposed somatosensory neural codes for frequency discrimination and spatial localization (Hernandez et al. 2000; Mountcastle et al. 1967, 1969, 1990; Recanzone et al. 1992; Salinas et al. 2000). Analyses of neural responses in monkeys discriminating the frequency of tactile stimuli on their fingers suggest that either the mean spike rate and/or temporal pattern of responses optimally predict perceptual performance (Hernandez et al. 2000; Mountcastle et al. 1967, 1969, 1990; Recanzone et al. 1992; Salinas et al. 2000). While parallel electrophysiological studies have not, to our knowledge, been conducted in the vibrissa to barrel system, the observed increase in spike count at 5-10 Hz may optimize the confidence of spike-rate based discriminations made in this frequency range. Similarly, the peak in the fidelity of spike timing (VS) at the whisking sampling rate, particularly in the context of a robust number of total spikes, might reflect enhanced ability of rats to discriminate frequencies in this range. Recently, Kleinfeld et al. (2002) found that spiking activity of awake rat primary motor cortex neurons selectively extracted the fundamental frequency of repetitive vibrissae

stimulation at rates from 5-15 Hz. This band-pass phenomenon parallels and may be related to those reported here, and underscores the importance of processing in this frequency range in the awake behaving animal.

We also observed band-pass enhancement of responses that resulted from small, frequency specific latency shifts with increasing frequency. Previous studies have reported latency shifts in the septa and in layers Va and II/III (Ahissar et al. 1997, 2000, 2001b). In these layers, onset latency shifts could be as great as 45 msec and increased with higher stimulus rates, while decline latencies remained constant. This combination of phenomena resulted in a rate code for stimulus frequency that is hypothesized to be important for coding object localization. In contrast, layer IV responses were hypothesized to be important for coding temporal information because latencies were stable (Ahissar et al. 2000, 2001a). Our data showed small onset latency shifts that were significantly shorter than latency shifts reported in other cortical layers but were not inconsistent with previously reported data showing slight latency shifts on the scale of a few milliseconds in layer IV (e.g., Figure 2B in Ahissar 2001b). We also observed small decline-latency shifts and a trend towards longer response widths, which differ from the non-granular pattern of responses. Although the latency shifts we observed are small in comparison with shifts in other layers, temporal processing on the millisecond time scale may be important for a variety of tasks, including texture discrimination (Carvell and Simons, 1995).

In addition to the possible utility of band-pass responses at whisking frequencies, several characteristics of low pass adaptation could improve information coding over these frequencies. The slope of the RRTF adaptation function was greatest from 5-10 Hz,

and the highest frequency at which cortical responses had not completely adapted occurred at approximately 8 Hz, where the RRTF slope is greatest. Sampling tactile information at this frequency could mediate a compromise between having an ample number of spikes per stimulus (highest statistical power observation), and collecting information at an optimal rate. A further possible advantage of the rapid change in response amplitude in the whisking frequency range is that rapid or long-term plasticity of responses would be expected to optimally effect sensory processing in this frequency range. Auditory plasticity studies in rodents have shown experience dependent changes in temporal properties of cortical neurons around the frequency range where RRTF curves were steepest (Kilgard and Merzenich 1998).

Possible Mechanisms for the Observed Phenomena

Previous biological studies as well as findings from our minimal cortical model suggest the following mechanisms for our results. With regards to the RRTF adaptation phenomenon observed in layer IV, several studies have demonstrated that the magnitude of adaptation within the VPm is significantly smaller than that observed in the cortex (Chung et al., 2002; Diamond et al. 1992; Hartings and Simons 1998; Sosnik et al. 2001; Hartings and Simons, personal communication). Data from whole cell recordings in barrel cortex have demonstrated that repetitive vibrissa stimulation depressed EPSPs evoked at the thalamocortical synapse, and that depression at this synapse can account for the consistently observed cortical adaptation in spiking activity (Chung et al. 2002). Thalamocortical adaptation was also crucial, in our model, to the emergence of the other spike count phenomenon observed, the band-pass characteristic of the SR. Because the

SR was calculated from the entire steady state period, the initial increase in SR at low frequencies reflects the increased number of vibrissa stimuli per second at increasing stimulus rates. At higher frequencies above 5-10 Hz, adaptation overcame this increase in SR even though the number of stimuli continued to increase. Thus, the band pass peak in SR reflects a trade off between an increase in the number of stimuli per second at higher rates and the adaptation resulting from high frequency vibrissa stimulation.

In contrast to these spike count measures, VS appears to depend largely on long-lasting inhibitory influences. Post-stimulus suppression commonly has been observed in intracellular and extracellular studies of somatosensory cortex (Carvell and Simons 1988; Hellweg et al. 1977; Kyriazi et al. 1996; Moore and Nelson 1998; Simons 1985; Zhu and Connors 1999). Application of $GABA_B$ antagonists to the cortex eliminates the slow component of this suppression, which lasts for hundreds of milliseconds (Kyriazi et al. 1996). We observed suppression of spontaneous activity after initial vibrissa deflections that lasted ~130 msec (Figure 1B). Recovery from this suppression coincided exactly with subsequent excitation by a second deflection at 8 Hz. A parsimonious explanation for the observed band-pass characteristic in VS is that at low frequencies, inhibition does not suppress the 'noisy' spikes that occur between longer inter-stimulus intervals (i.e., >130 msec). These spikes degrade the measured phase locking of the response to subsequent deflections. At higher frequencies (e.g., >10 Hz), interactions between the slow inhibition and thalamocortical depression effectively diminish the response and undermine the consistency of a greater number of spikes from cycle to cycle (e.g., see the response to the second pulse of stimulation at 15 Hz, Figure 1B). These suppressive interactions effectively impose an inherent periodicity on processing in this system. In

agreement with this prediction, removal of slow suppression from the model by removal of $GABA_B$ largely eliminated the band-pass VS characteristics.

Although we have shown that a cortical circuit model can account for the temporal response properties observed, other cellular or network mechanisms likely also contribute to these phenomena. The sustained inhibition in our model was constructed to represent $GABA_B$ synaptic currents derived from *in vitro* studies (Connors et al. 1988) and implicitly demonstrated by pharmacological blockade in the cortex *in vivo* (Kyriazi et al. 1996). However, these currents have been found to be less prominent *in vivo* than *in vitro* (Steriade 2001). A variety of other mechanisms may contribute to the increased band-pass temporal fidelity observed. Studies of cellular subthreshold oscillations have shown that the temporal reliability of cortical pyramidal neurons peaks at rates between 5-20 Hz when these cells are injected with sinusoidal current (Fellous 2001). Further, the time course of the sustained slow inhibitory period and rebound burst observed here follows the activation kinetics of intrinsic low threshold calcium currents (It) and hyperpolarization activated currents (Ih) observed in thalamic and cortical neurons (Destexhe et al. 1993; Foehring and Waters 1991; Monteggia et al. 2000). Several intrinsic currents in cells within the cortex and thalamus also influence adaptation (ie. Ca^{2+} or Na^+ dependent K^+ currents, and persistent Na^+ currents) and may hence contribute to the observed phenomena (Fuhrmann et al. 2002; Fleidervish and Gutnick 1996; Sanchez-Vives et. al. 2000a, 2000b). Corticothalamic loops have been hypothesized to help increase the sensitivity of thalamic and cortical responses during brief thalamic bursting modes that correspond to vibrissa twitching states, but not to play this role during tonic thalamic firing (Nicolelis and Fanselow 2002). Periodicity imposed

by the time constants of corticothalamic connectivity could also contribute to enhancing this band-pass fidelity of neuronal firing (Destexhe et al. 1998). While any of these response components may contribute to the observed phenomenae, we have shown that a minimal spike generating cortical circuit with adaptation arising at the level of the thalamocortical synapse is sufficient to produce the observed results.

Limitations of the experimental preparation

We recorded responses from depths of 500-750 μms in rat SI, as determined from microdrive readings. A limitation of the present study is that we did not reconstruct the position of the electrode tip in each case, preventing the conclusive identification of the layer of recording. Several lines of evidence suggest that our recordings were located either within a barrel, or within cell populations immediately superficial to the barrel that demonstrate overlapping response profiles. Physiologically, each site we recorded from showed strong single vibrissa responses that are typical of barrel responses (e.g., Armstrong-James et al., 1992; Simons and Carvell, 1989). The location of these recordings was addressed in a separate experiment (5 sites in 3 rats: Garabedian and Moore, unpublished observations), and in all cases the position of the lesion overlapped both layer IV and layer III directly above a cytochrome oxidase-defined barrel. This lesion study also suggested that the more superficial depth recordings from our microdrive readings (500-550 μm) corresponded to layer III or IV of the barrel cortex, and deeper recordings (700-750 μm) to layer IV. Comparison of the response measures at different depths showed that each trend (low pass RRTF, consistent response onset shifting with increasing frequency and band pass VS and SR curves) was replicated in a

smaller range of recording depths. Further, no significant difference was observed in these properties as a function of depth, nor were any trends in response profile observed to correlate with relative depth. Specifically, previous studies (Ahissar et al., 2001) suggest that, were our more superficial recordings in layer III, a significantly greater onset latency shift should have been observed with increasing frequency at these depths.

In the present study, we recorded multi-unit responses: As such, these data contribute to the understanding of the net activity of the population of neurons sampled. Because our recordings focused on multi-unit responses, however, certain aspects of these findings have multiple possible interpretations. For example, intermediate levels of adaptation, where some but not all of the response was diminished with increasing frequency, can be interpreted either as the cumulative adaptation of single neurons at a given rate or as the complete adaptation of a subset of neurons that contributed incompletely to the response while other neurons maintained activity in an un-adapted state. The latter scenario is unlikely based on previous reports showing that isolated single units and intracellular recordings also show temporal adaptation in the frequency ranges reported here (Chung et al. 2002; Simons 1978). In addition, although temporal properties of single units and clusters may vary, recent studies have emphasized the similarity in temporal features of both types of recordings, in somatosensory and auditory cortex (Ahissar et al. 2001b, Eggermont and Smith 1995).

There are obvious concerns when extrapolating data from the anesthetized preparation, employed in the current study, to the awake animal. While anesthesia allows greater control of stimulus presentation, a clear advantage when conducting precise temporal studies, it can modify barrel cortex response properties (Armstrong-James and

George 1988; Friedberg et al. 1999; Simons et al. 1992). In anesthetized, sleeping, or unaroused animals, single vibrissa deflections result in large cortical responses, while responses to repetitive stimuli show depression (Castro-Alamancos and Oldford 2002b; Fanselow and Nicolelis 1999; Moore et al. 1999; Sheth et al. 1998). During arousal, thalamic firing rates are high, likely in part due to ongoing whisking (Fee et al., 1997) and in part due to depolarizing cholinergic input from the reticular formation: These high thalamic firing rates are hypothesized to maximize thalamocortical depression, resulting in smaller cortical responses (Castro-Alamancos et al. 2002a, 2002b). Cortical responses to repetitive electrical stimulation of the fifth nerve have been characterized as showing little adaptation in awake, whisking animals (Fanselow and Nicolelis 1999), a response pattern that can be attributed to the already depressed/adapted state of the sensory pathway engaged by simultaneous whisking. As other authors have recently suggested, the steady state induced by repetitive stimuli in the anesthetized preparation is perhaps an appropriate model of the condition in the aroused animal during whisking (Castro-Alamancos and Oldford 2002b). Whether the band-pass properties described here are also observed in the awake state and, more importantly, during repeated contact with an object during whisking, remains an open question.

Implications of Band-pass Phenomena for Whisking Behavior

The coincidence between the frequency range of whisking behavior and the neural response properties we have identified as band-pass suggests the rat may modulate its whisking rate to take advantage of the inherent time constants of cortical dynamics and thalamocortical circuitry. Our findings closely parallel those observed in the primary

auditory cortex of the ketamine anesthetized cat, where normalized spike amplitude showed similar low pass behavior and VS and SR showed band-pass responses to repetitive stimuli, with a peak at approximately 8 Hz (Eggermont 1991, 1999). Further, intracellular studies of cat SI have demonstrated that 8-12 Hz periodic subthreshold responses emerge during stimulation of the infraorbital nerve at rates up to 150 Hz (Hellweg et al. 1977). This similarity in activity patterns across species, anesthesia type, and sensory modality, suggests that the band-pass responses we observed emerge from intrinsic dynamics of these sensory systems. Behavioral data showing that rats change their whisking frequencies in the context of different behavioral tasks (Carvell and Simons 1995) and that the frequency power of whisking changes as a rat improves performance of a discrimination task (Harvey et al. 2001) further suggest that whisking frequency is intentionally modulated to optimize the engagement of temporal cortical dynamics, while these dynamics themselves are stable. Interestingly, mice whisk their vibrissae at higher rates than rats, in the range of 10-15 Hz (Woolsey et al. 1981). If the properties we have observed are related to the rate at which rats whisk over the course of life experience, or to evolutionary selection, then we would predict a subtle, parallel shift in the encoding properties of mouse SI neurons towards higher frequencies.

Figure 1. Mean spike responses to repetitive stimuli. Responses of all recording sites were averaged in these post-stimulus time histograms. A. Mean responses to stimulus rates from 1-20 Hz are shown in PSTHs using 1 msec time bins. Stimulus onset occurs at 1000 msec and lasts for 5 seconds, ending at 6000 msec. The *dynamic period* is indicated in gray and the *steady state* period in black. The vertical box indicates the part of the response expanded in panel B. B. The first 200 msec of the mean response is plotted. The PSTHs were convolved with a [1 2 1] filter. Response onset occurs at ~1010 msec, and is followed by suppression of activity for ~ 130 msec followed by a rebound above spontaneous activity levels. Arrows indicate stimulus onset times for all PSTHs. For all figures, the number of sites per frequency is as follows, unless indicated: N = 59 for 1, 3, 20, 30, and 40 Hz. N = 64 for 5, 8, 10, and 5 Hz.

A.

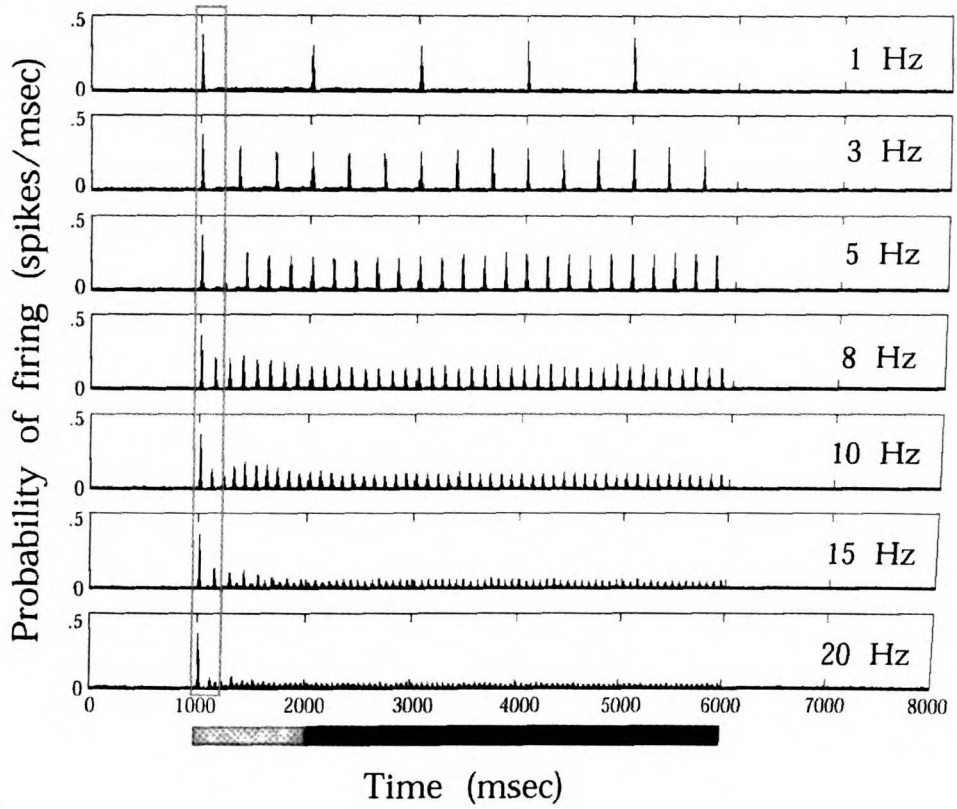
1 Hz
3 Hz
5 Hz
8 Hz
10 Hz
15 Hz
20 Hz
.5
0
0
1000
2000
3000
4000
5000
6000
7000
8000
Probability of firing (spikes/msec)
Time (msec)

B.

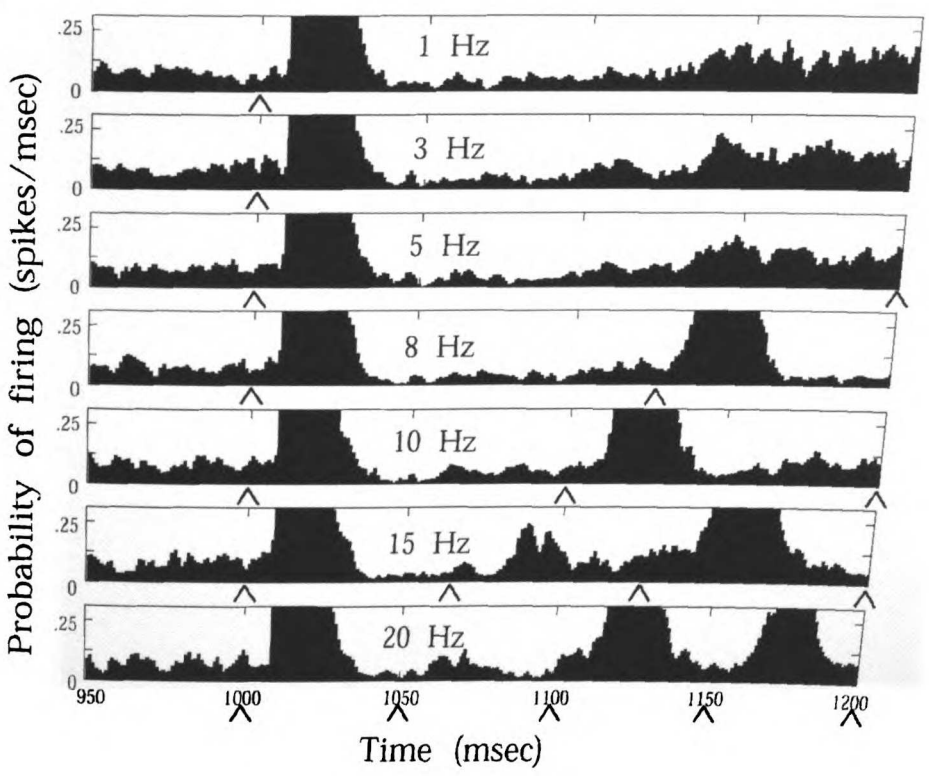
1 Hz
3 Hz
5 Hz
8 Hz
10 Hz
15 Hz
20 Hz
.25
0
950
1000
1050
1100
1150
1200
Probability of firing (spikes/msec)
Time (msec)

Figure 2. Repetition rate transfer functions (RRTF) A. The mean RRTF for all recording sites is plotted. The RRTF was calculated by normalizing the mean responses during the steady state period by the response to the first vibrissa deflection (responses were defined as spikes 0-35 msec post-stimulus). Error bars indicate standard error of the mean for all physiology figures. B. The RRTF functions for each individual recording site.

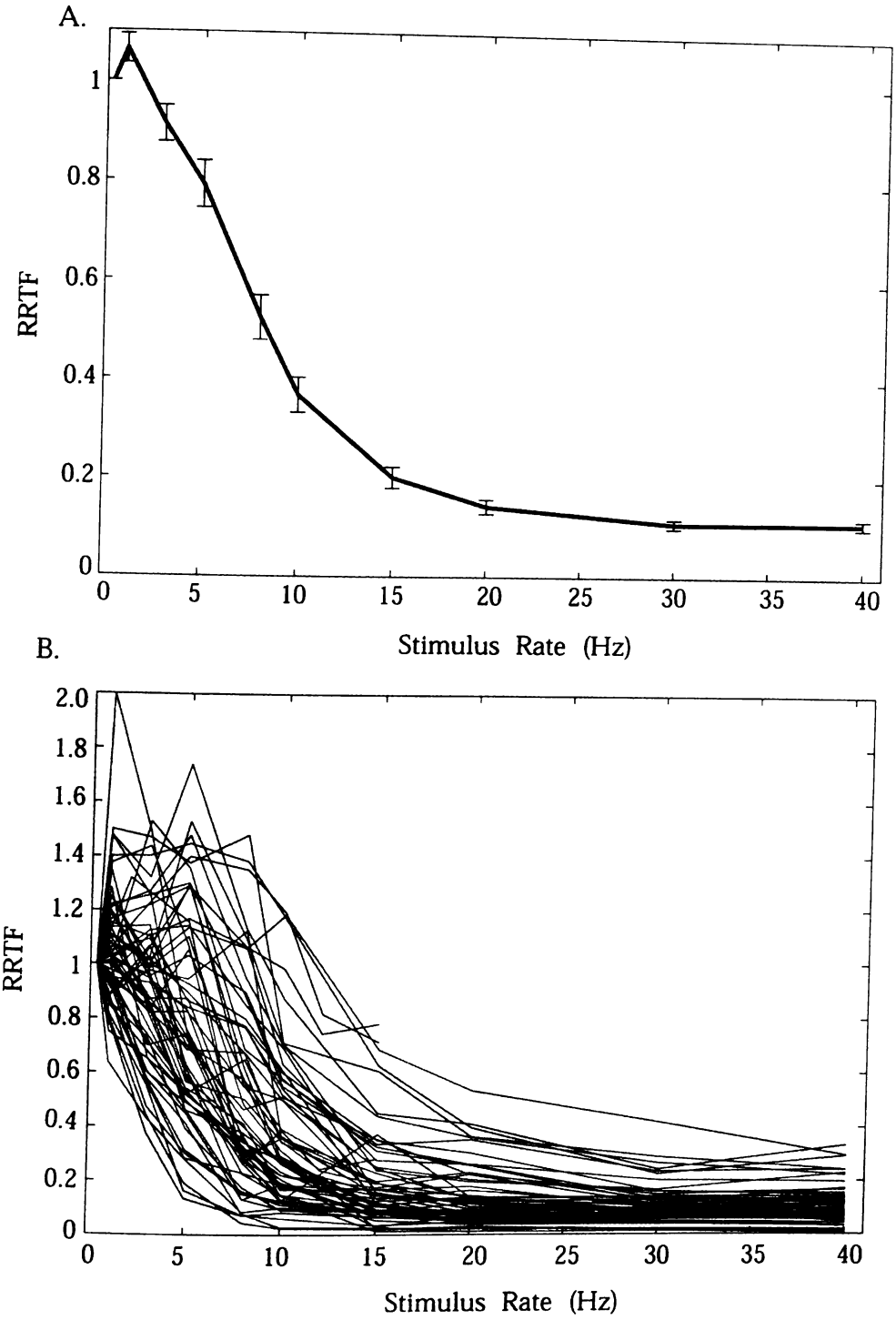
A.
RRTF
Stimulus Rate (Hz)
B.
RRTF
Stimulus Rate (Hz)

Figure 3. Latency of responses as a function of stimulus rate. A. The average steady state cycle histograms for all recording sites are shown for frequencies up to 15 Hz. B. Mean cycle histograms were normalized to the maximal value for each frequency after subtracting baseline activity. C. Mean onset latencies for responses to steady state stimulation from 0.33 (first deflection) to 15 Hz are plotted for 55 recording sites at which VS was $\geq$ 0.3 from 3-15 Hz. Latencies were calculated from mean cycle histograms for each site by taking the time at which the response amplitude was 50% of the maximal amplitude. D. RRTFs were calculated in 5 msec time bins. Each curve is the mean RRTF function for all recording sites, and the time window used to quantify responses is indicated by gray scale.

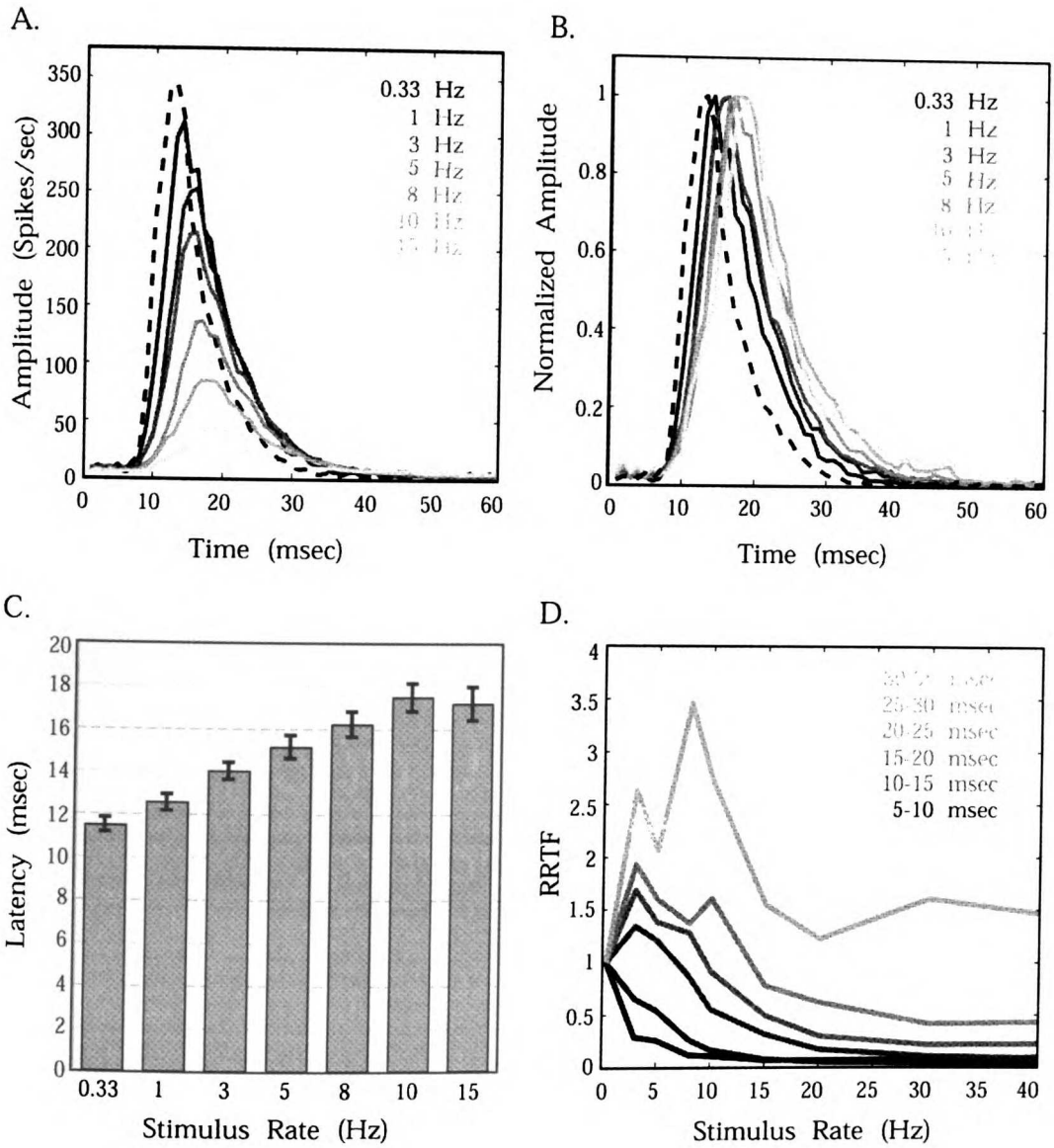
A.
Amplitude (Spikes/sec)
Time (msec)
0.33 Hz
1 Hz
3 Hz
5 Hz
8 Hz
B.
Normalized Amplitude
Time (msec)
0.33 Hz
1 Hz
3 Hz
5 Hz
8 Hz
C.
Latency (msec)
Stimulus Rate (Hz)
D.
RRTF
Stimulus Rate (Hz)
25-30 msec
20-25 msec
15-20 msec
10-15 msec
5-10 msec

Figure 4. Spike rate responses as a function of stimulus rate. A. The mean SR during the steady state period was averaged for all recoding sites and plotted as a function of stimulation rate. B. The SR during the steady state period was plotted as a function of stimulation frequency for each recording site.

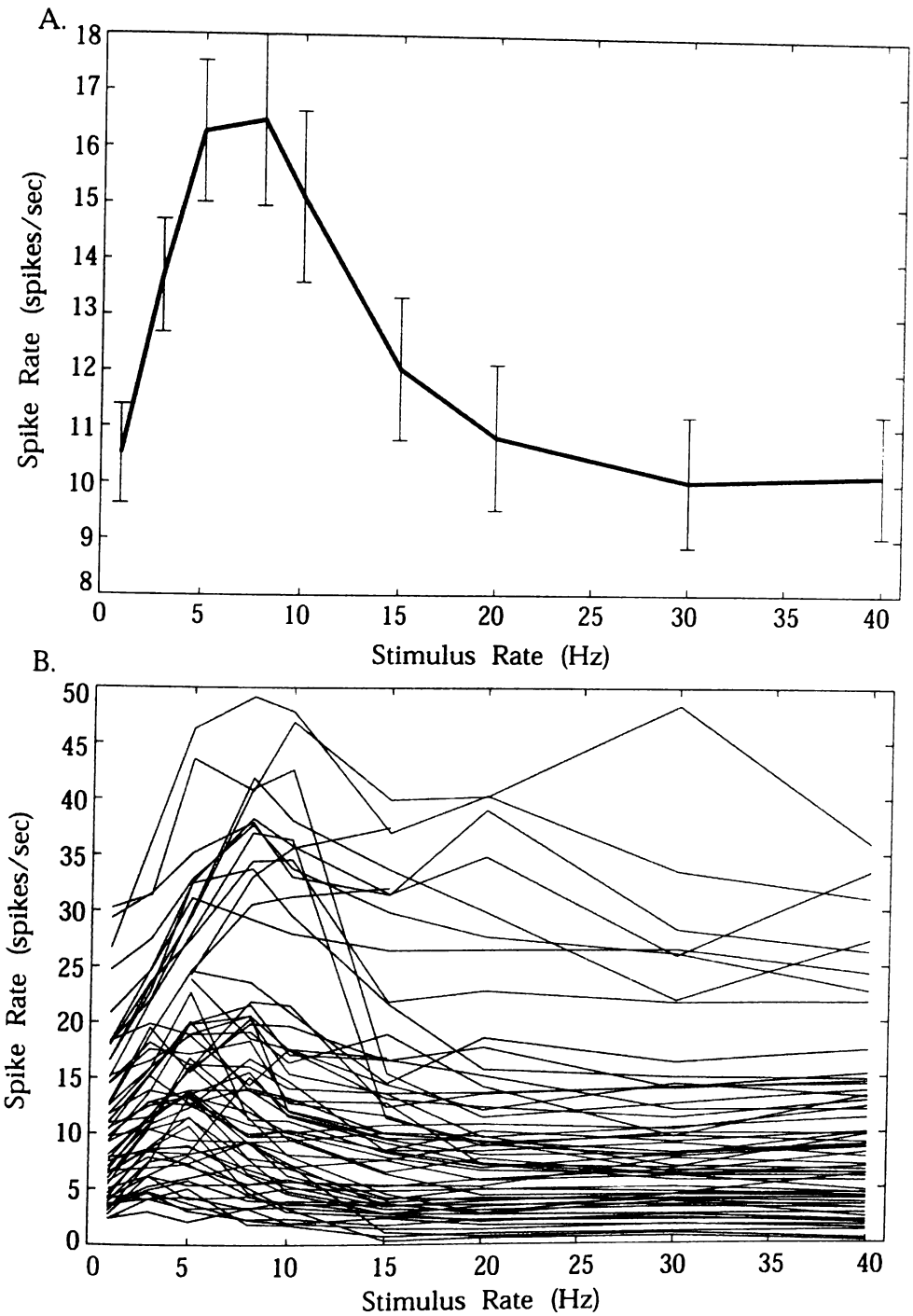
A.
Spike Rate (spikes/sec)
Stimulus Rate (Hz)
B.
Spike Rate (spikes/sec)
Stimulus Rate (Hz)

Figure 5. Temporal precision of spike responses (vector strength) as a function of stimulus rate. A. The VS of the response during the steady state period was calculated for each recording site and stimulus rate. The mean VS across all recordings was plotted as a function of frequency. B. The VS for each recording site was plotted as a function of stimulus rate.

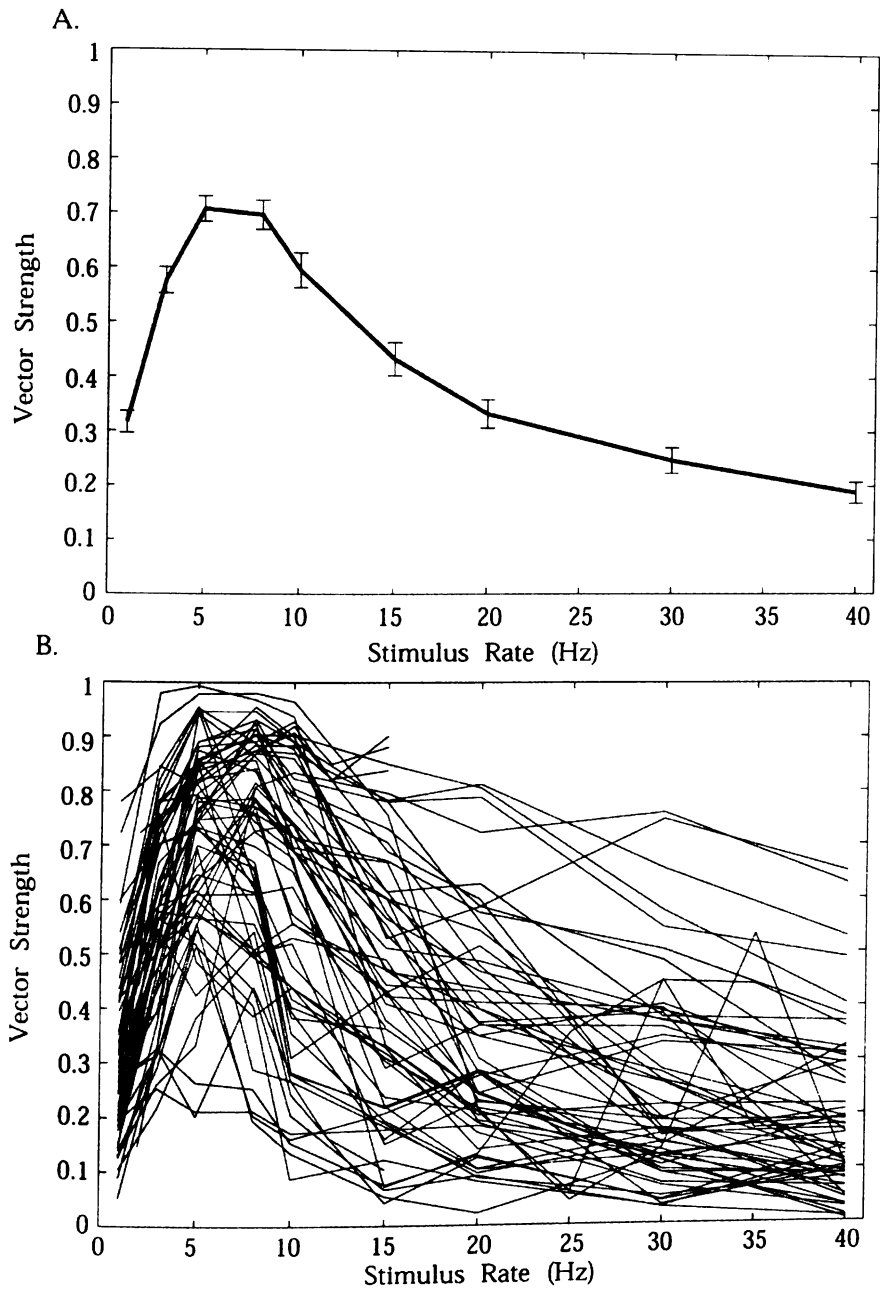
A.
Vector Strength
Stimulus Rate (Hz)
B.
Vector Strength
Stimulus Rate (Hz)

Figure 6. Frequency dependent response properties are constant across cortical depths. Recording sites were divided into five groups based on electrode depth, and average and individual RRTF, onset latency, SR, and VS curves were plotted for each depth (500-550, 551-600, 601-650, 651-700, and 701-750 μms). A. Mean RRTF curves. B. Mean onset latency curves. C. Mean SR curves. D. Mean VS curves. For each measure (RRTF, SR, or VS), a one way ANOVA was conducted across frequencies, and showed no statistical differences between responses as a function of depth (see text).

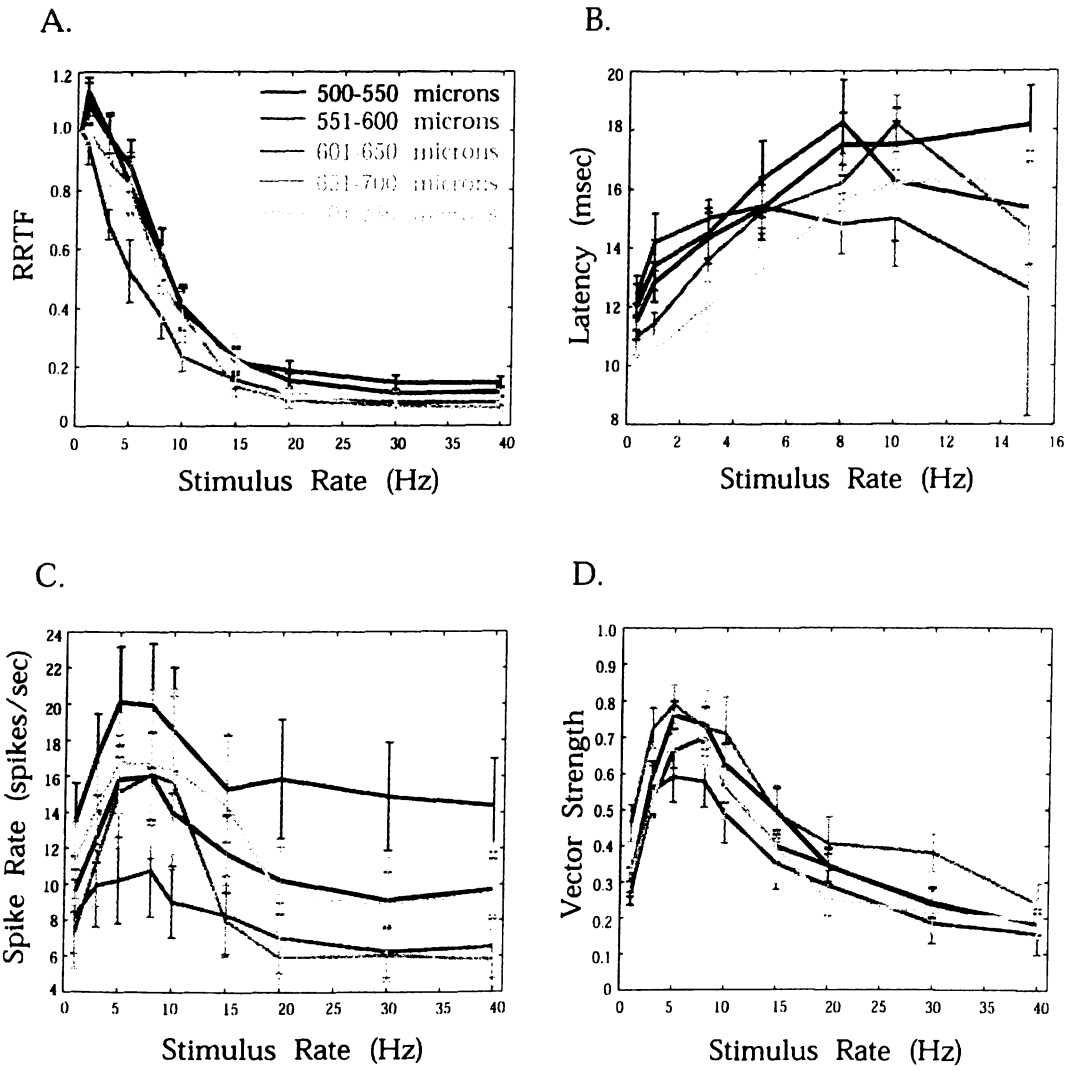
A.
B.
C.
D.
500-550 microns
551-600 microns
601-650 microns
RRTF
Latency (msec)
Spike Rate (spikes/sec)
Vector Strength
Stimulus Rate (Hz)

Figure 7. A minimal network model replicates low pass and band-pass responses. Black curves show data for control conditions, mid-gray curves show data when thalamocortical (TC) adaptation was removed from the model, and light gray curves show responses when slow inhibition was removed from the model. Temporal measures of RRTF, SR, and VS were calculated as described in the experimental procedures. Measures were generated from the spiking activity of the model excitatory cell and were averaged over ten simulations for each frequency of stimulation. Error bars represent standard deviation. A. Schematic diagram showing each element of the computational model consisting of thalamocortical input, one excitatory and one inhibitory unit, and AMPA, $GABA_A$, and $GABA_B$ currents. B. Normalized amplitude of the thalamocortical input function as a function of time for each frequency. The time at which the amplitude reached a steady state for each frequency was: 1Hz: > 5 seconds, 3 Hz: 3030 msec, 5 Hz: 3630 msec, 8 Hz: 2530 msec, 10 Hz: 2330 msec, 15 Hz: 1630 msec, 20 Hz: 1230 msec, 30 Hz: 930 msec. C. PSTHs for simulated data averaging 10 repetitions of stimuli from 1-20 Hz. D. RRTF as a function of stimulus rate. E. SR as a function of stimulus rate. *Inset:* SR as a function of stimulus rate, expanded scale. F. VS as a function of stimulus rate.

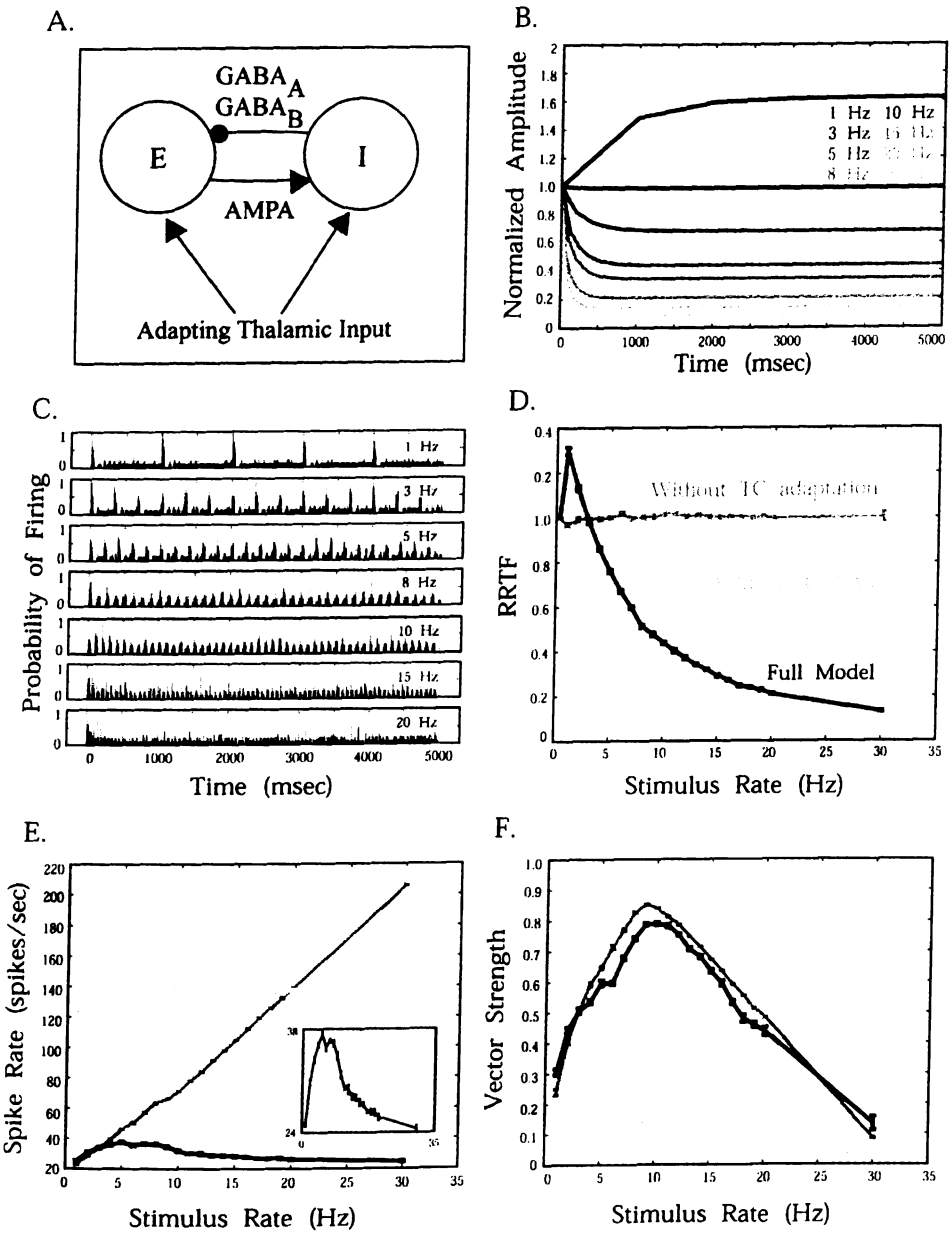
A.
GABA$_A$
GABA$_B$
E
I
AMPA
Adapting Thalamic Input
B.
Normalized Amplitude
1 Hz 10 Hz
3 Hz
5 Hz
8 Hz
Time (msec)
C.
Probability of Firing
1 Hz
3 Hz
5 Hz
8 Hz
10 Hz
15 Hz
20 Hz
Time (msec)
D.
RRTF
Without TC adaptation
Full Model
Stimulus Rate (Hz)
E.
Spike Rate (spikes/sec)
Stimulus Rate (Hz)
F.
Vector Strength
Stimulus Rate (Hz)

REFERENCES

Ahissar, E., and Arieli, A. Figuring space by time. *Neuron* 32: 185-201, 2001a.

Ahissar, E., Haidarliu, S., and Zackenhouse, M. Decoding temporally encoded sensory input by cortical oscillations and thalamic phase comparators. *PNAS* 94: 11633-11638, 1997.

Ahissar, E., Sosnik, R., Bagdasarian, K., and Haidarliu, S. Temporal frequency of whisker movement. II. Laminar organization or cortical representations. *J. Neurophysiol.* 86: 354-367, 2001b.

Ahissar, E., Sosnik, R., and Haidarliu, S. Transformation from temporal to rate coding in a somatosensory thalamocortical pathway. *Nature* 406: 302-306, 2000.

Armstrong-James M., Fox, K., and Das-Gupta, A. Flow of excitation within rat barrel cortex on striking a single vibrissa. *J. Neurophysiol.* 68: 1345-1358, 1992.

Armstrong-James, M. and George, M.J. Influence of anesthesia on spontaneous activity and receptive field size of single units in rat Sm1 neocortex. *Exp. Neurol.* 99: 369-387, 1988.

Berg, R.N. and Kleinfeld, D. Rhythmic whisking by rat: Retraction as well as protraction of the vibrissae is under active muscular control. *J. Neurphysiol. 89: 104-117,* 2003.

Brumberg, J.C., Pinto, D.J., and Simons, D.J. Spatial gradients and inhibitory summation in the rat whisker barrel system. *J. Neurophysiol.* 76: 130-140, 1996.

Brumberg, J.C., Pinto, D.J., and Simons, D.J. Cortical columnar processing in the rat whisker-to-barrel system. *J. Neurophysiol.* 82: 1808-1817, 1999.

Carvell, G.E. and Simons, D.J. Membrane potential changes in rat SmI cortical neurons evoked by controlled stimulation of mystacial vibrissae. *Brain Res.* 448: 186-191, 1988.

Carvell, G.E. and Simons, D.J. Biometric analyses of vibrissal tactile discrimination in the rat. *J. Neurosci.* 10: 2638-2648, 1990.

Carvell, G.E. and Simons, D.J. Task- and subject-related differences in sensorimotor behavior during active touch. *Somatosens. Mot. Res.* 12: 1-9, 1995.

Castro-Alamancos, M.A. Different temporal processing of sensory inputs in the rat thalamus during quiescent and information processing states in vivo. *J. Physiol.* 539: 567-578, 2002a.

Castro-Alamancos, M.A. and Oldford, E. Cortical sensory suppression during arousal is due to the activity-dependent depression of thalamocortical synapses. *J. Physiol.* 541: 319-331, 2002b.

Chung, S., Li, X., and Nelson, S.B. Short-term depression at thalamocortical synapses contributes to rapid adaptation of cortical sensory responses *in vivo*. *Neuron* 34: 437-446, 2002.

Connors, B., Malenka, R., and Silva, L. Two inhibitory postsynaptic potentials, and $GABA_A$ and $GABA_B$ receptor mediated responses in neocortex of rat and cat. *J. Physiol.* 406: 443-468, 1988.

Destexhe, A., Babloyantz, A., and Sejnowski, T.J. Ionic mechanisms for intrinsic slow oscillations in thalamic relay neurons. *Biophys. J.* 65(4): 1538-52, 1993.

Destexhe, A., Contreras, D., and Steriade, M. Mechanisms underlying the synchronizing action or corticothalamic feedback through inhibition of thalamic relay cells. *J.Neurophysiol.* 79: 999-1016, 1998.

Diamond, M.E., Armstrong-James, M., and Ebner, F.F. Somatic sensory responses in the rostral sector of the posterior group (POm) and in the ventral posterior medial nucleus (VPM) of the rat thalamus. *J. Comp. Neurol.* 318: 462-76, 1992.

Diamond, M.E., Huang, W., and Ebner, F.F. Laminar comparison of somatosensory cortical plasticity. *Science* 265: 1885-1888, 1994.

Eggermont, J.J. Rate and synchronization measures of periodicity coding in cat primary auditory cortex. *Hearing Res.* 56: 153-167, 1991.

Eggermont, J.J. and Smith, G.M. Synchrony between single-unit activity and local field potentials in relation to periodicity coding in primary auditory cortex. *J. Neurophysiol.* 73: 227-245, 1995.

Eggermont, J.J. The magnitude and phase of temporal modulation transfer functions in cat auditory cortex. *J. Neurosci.* 19: 2780-2788, 1999.

Fanselow, E.E. and Nicolelis, M.A. Behavioral modulation of tactile responses in the rat somatosensory system. *J. Neurosci.* 19: 7603-7616, 1999.

Fee, M.S., Mitra, P.P., and Kleinfeld, D. Central versus peripheral determinants of patterned spike activity in the rat vibrissa cortex during whisking. *J. Neurophysiol.* 78: 1144-1119, 1997.

Fellous, J.M., Houweling, A.R., Modi, R.H., Rao, R.P.N., Tiesinga, P.H.E., and Sejnowski, T.J. Frequency dependence of spike timing reliability in cortical pyramidal cells and interneurons. *J. Neurophysiol.* 85: 1782-1787, 2001.

Fleidervish, I.A. and Gunick, M.J. Kinetics of slow inactivation of persistent sodium currents in layer V neurons of mouse neocortical slices. *J. Neurophysiol.* 76(3): 2125-2130, 1996.

Foehring, R.C. and Waters, R.S. Contributions of low-threshold calcium current and anomalous rectifier (Ih) to slow depolarizations underlying burst firing in human neocortical neurons *in vitro*. *Neurosci. Lett.* 124(1): 17-21, 1991.

Friedberg, M.H., Lee, S.M., and Ebner, F.F. Modulation of receptive field properties of thalamic somatosensory neurons by the depth of anesthesia. *J. Neurophysiol.* 81: 2243-2252, 1999.

Fuhrmann, G., Markram, H., and Tsodyks, M. Spike frequency adaptation and neocortical rhythms. *J. Neurophysiol.* 88(2): 761-770, 2002.

Gao, P., Bermejo, R., and Zeigler, H.P. Whisker deafferentation and rodent whisking patterns: behavioral evidence for a central pattern generator. *J. Neurosci.* 21(4): 5374-5380, 2001.

Goldberg, J.M. and Brown, P.B. Response of binaural neurons of dog superior olivary complex to dichotic tonal stimuli: some physiological mechanisms of sound localization. *J. Neurophysiol.* 32(4): 613-636, 1969.

Hartings, J.A. and Simons, D.J. Thalamic relay of afferent responses to 1- to 12- Hz whisker stimulation in the rat. *J. Neurophysiol.* 80(2): 1016-1019, 1998.

Harvey, M.A., Bermejo, R., and Zeigler, H.P. Discriminative whisking in the head-fixed rat: optoelectronic monitoring during tactile detection and discrimination tasks. *Somatosensory Mot. Res.* 18(3): 211-222, 2001.

Hellweg, F.C., Schultz, W., and Creutzfeldt, O.D. Extracellular and intracellular recordings from cat's cortical whisker projection area: thalamocortical response transformation. *J. Neurophysiol.* 40(3): 463-479, 1977.

Hernandez, A., Zainos, A., and Romo, R. Neuronal correlates of sensory discrimination in the somatosensory cortex. *PNAS* 97(11): 6191-6196, 2000.

Jones, S.R., Pinto, D.J., Kaper, T.J., and Kopell, N. Alpha-frequency rhythms desynchronize over long cortical distances: A modeling study. *J. Comp. Neurosci.* 9: 271-291, 2000.

Kleinfeld, D., Sachdev, R.N., Merchant, L.M., Jarvis, M.R., and Ebner, F.F. Adaptive filtering of vibrissa input in motor cortex of rat. *Neuron* 34: 1021-1034, 2002.

Koch, C. and Segev, I. *Methods in neuronal modeling: from ions to networks.* Cambridge, MA: The MIT Press 1998.

Kilgard, M.P. and Merzenich, M.M. (1998) Plasticity of temporal information processing in the primary auditory cortex. *Nat. Neurosci.* 1: 727-731, 1998.

Kyriazi, H.T. and Simons, D.J. Thalamocortical response transformations in simulated whisker barrels. *J. Neurosci.* 13: 1601-1615, 1993.

Kyriazi, H.T., Carvell, G.E., Brumberg, J.C., and Simons, D.J. Effects of baclofen and phaclofen on receptive field properties of rat whisker barrel neurons. *Brain Res.* 712: 325-328, 1996.

Monteggia, L.M., Eisch, A.J., Tang, M.D., Kaczmerek, L.K., and Nestler, E.J. Cloning and localization of the hyperpolarization-activated cyclic nucleotide-gated channel family in rat brain. *Mol. Brain Res.* 81(1-2): 129-139, 2000.

Moore, C.I., Nelson, S.B., and Sur, M. Dynamics of neuronal processing in rat somatosensory cortex. *TINS* 22: 513-520, 1999.

Moore, C.I. and Nelson, S.B. Spatio-temporal subthreshold receptive fields in the vibrissa representation of rat primary somatosensory cortex. *J. Neurophysiol.* 80: 2882-2892, 1998.

Mountcastle, V.B., Talbot, W.H., Darian-Smith, I., and Kornhuber, H.H. Neural basis of the sense of flutter-vibration. *Science* 155: 597-600, 1967.

Mountcastle, V.B., Talbot, W.H., Sakata, H., and Hyvarinen, J. Cortical neuronal mechanisms in flutter-vibration studied in unanesthetized monkeys. Neuronal periodicity and frequency discrimination. *J. Neurophysiol.* 32: 453-484, 1969.

Mountcastle, V.B., Steinmetz, M.A., and Romo, R. Frequency discrimination in the sense of fluter: psychophysical measurements correlated with postcentral events in behaving monkeys. *J. Neurosci.* 10: 3032-3044, 1990.

Nicolelis, M.A., Bacala, L.A., Lin, R.C., and Chapin, J.K. Sensorimotor encoding by synchronous neural ensemble activity at multiple levels of the somatosensory system. *Science* 268: 1353-1358, 1995.

Nicolelis, M.A. and Fanselow, E.E. Thalamocortical optimization of tactile processing according to behavioral state. *Nat. Neurosci.* 5: 517-523, 2002.

Pinto, D.J., Brumberg, J.C., Simons, D.J., and Ermentrout, G.B. A quantitative population model of whisker barrels: re-examining the Wilson-Cowen equations. *J.Comp. Neurosci.* 3: 247-264, 1996.

Recanzone, G.H., Merzenich, M.M., and Schreiner, C.E. Changes in the distributed temporal response properties of SI cortical neurons reflect improvements in performance on a temporally based tactile discrimination task. *J. Neurophysiol.* 67: 1071-1091, 1992.

Salinas, E., Hernandez, A., Zainos, A., and Romo, R. Periodicity and firing rate as candidate neural codes for the frequency of vibrotactile stimuli. *J. Neurosci.* 20: 5503-5515, 2000.

Sanchez-Vives, M.V., Nowak, L.G., and McCormick, D.A. Cellular mechanisms of long-lasting adaptation in layer V neurons of mouse neocortical slices. *J. Neurosci.* 20(11): 4286-4299, 2000a.

Sanchez-Vives, M.V., Nowak, L.G., and McCormick, D.A.. Membrane mechanisms underlying contrast adaptation in cat area 17 *in vivo*. *J. Neurosci.* 20(11): 4267-4285, 2000b.

Sheth, B.R., Moore, C.I., and Sur, M. Temporal modulation of spatial borders in rat barrel cortex. *J. Neurophysiol.* 79: 464-470, 1998.

Simons, D.J. Response properties of vibrissa units in rat SI somatosensory neocortex. *J. Neurophysiol.* 41: 798-820, 1978.

Simons, D.J. Temporal and spatial integration in the rat SI vibrissa cortex. *J. Neurophysiol.* 54: 615-635, 1985.

Simons, D.J. and Carvell, G.E. Thalamocortical response transformation in the rat vibrissa/barrel system. *J. Neurophysiol.* 61: 311-330, 1989.

Simons, D.J., Carvell, G.E., Hershey, A.E., and Bryant, D.P. Responses of barrel cortex neurons in awake rats and effects of urethane anesthesia. *Exp. Brain Res.* 91: 259-272, 1992.

Simons, D.J. Neuronal integration in the somatosensory whisker/barrel cortex. In: *Cerebral Cortex*, edited by E.G. Jones and I.T. Diamonds. New York: Plenum Press 1995.

Sosnik, R., Haidarliu, S., and Ahissar, E. Temporal frequency of whisker movement. I. Representations in brainstem and thalamus. *J. Neurophysiol.* 86: 339-353, 2001.

Steriade, M. *The intact and sliced brain.* Cambridge, MA: The MIT Press 2001.

Varela, J.A., Sen, K., Gibson, J., Fost, J., Abbott, L.F., and Nelson, S.B. A quantitative description of short-term plasticity at excitatory synapses in layer 2/3 of rat primary visual cortex. *J. Neurosci.*, 17: 7926-7940, 1997.

Wang, J., McFadden, S.L., Caspary, D., and Salvi, R. Gamma-aminobutyric acid circuits shape response properties of auditory cortex neurons. *Brain Res.* 944: 219-231, 2002.

Welker, W.I. Analysis of sniffing of the albino rat. *Behavior* 12: 223-244, 1964.

Woolsey, T.A. and Van der Loos, H. The structural organization of layer IV in the somatosensory region (SI) of mouse cerebral cortex. The description of a cortical field composed of discrete cytoarchitectonic units. *Brain Res.* 17: 205-242, 1970.

Woolsey, T.A. et al. (1981) Somatosensory development. In: *The development of perception: psychobiological perspectives*, edited by R.N. Aslin and D.B. Pisani, pp. 259-292.

Zhu, J.J. and Connors, B.W. Intrinsic firing patterns and whisker-evoked synaptic responses of neurons in the rat barrel cortex. *J. Neurophysiol.* 81: 1171-1183, 1999.

CHAPTER III:

EFFECTS OF STIMULATION FREQUENCY ON DIRECTION TUNING IN RAT SI NEURONS

ABSTRACT

Neurons tuned to the direction of vibrissa movement are found at each level of the vibrissa processing system. When rats palpate objects with ~8 Hz "whisking" movements of their vibrissae, the shapes and angles of objects in the environment deflect these sensors in new directions, likely activating select direction tuned neurons and providing information that may be used for shape discrimination. Surprisingly, responses of cortical neurons to single vibrissa deflections show broad direction tuning when compared to more peripheral and thalamic sensory tuning. Based on our previous studies (e.g. Chapter 2), we hypothesized that direction tuning of cortical neurons may be modulated at frequencies of stimulation encountered during whisking. In a first experiment, we examined direction tuning of single and multi-unit responses of SI barrel neurons to 4-second long trains of vibrissa deflections at rates from 4-16 Hz. Responses to stimulation > 4 Hz showed adaptation during repetitive stimulation that reached a steady state after ~1 second. Improved tuning resulting from different rates of adaptation in different stimulus directions was observed in multi-unit responses for stimulus rates > 8 Hz. Similarly, a subset of analyses revealed improved tuning in fast-spiking units and regular-spiking units. This increase in direction tuning parallels my previous finding of enhanced temporal fidelity and increased mean firing rate at 8-12 Hz, and suggests that the vibrissa sensory system optimizes processing for discrimination of object shapes at whisking frequency rates. In a second experiment, the direction of vibrissa deflection was changed suddenly after two seconds of repetitive stimulation in a constant direction. Responses to the novel direction were robust, despite significant adaptation in the initial direction. These high amplitude responses in non-stimulated directions may function to

alert animals to novel stimuli encountered during whisking. Results of both the first and second experiments demonstrate the importance of temporal dynamics in coding sensory stimuli in a system that utilizes repetitive sampling during active tactile exploration.

INTRODUCTION

As sensory information is transmitted from peripheral to more central structures, single neurons become increasingly selective for complex features of sensory input. One exception to this pattern is the relatively poor direction tuning of neurons in the primary somatosensory cortex (SI) of rodents compared to that of more peripheral structures. First order sensory neurons in the trigeminal ganglion respond with high selectivity to single deflections of a vibrissa in different directions (Minnery et al. 2003). Direction tuning broadens as it is transmitted through the nucleus principalis of the brainstem and the ventroposterior medial thalamic nucleus (VPm) (Ito 1988; Simons and Carvell 1989; Minnery et al. 2003). Cortical neurons display broad direction tuning that either maintains or degrades direction tuning transmitted from the thalamus (Simons 1989; Bruno and Simons 2002; Swadlow and Gusev 2002; Bruno et al. 2003). This decrease in direction tuning occurs at least in part from the convergence of multiple tuned thalamic inputs onto single layer IV barrel neurons (Swadlow and Gusev 2002; Bruno and Simons. 2002). Regular-spiking units (RSU: putative excitatory neurons) show moderate direction tuning, while fast-spiking units (FSU: putative inhibitory neurons) are more poorly tuned (Simons 1989; Swadlow and Gusev 2002; Bruno and Simons 2002). The broad tuning of cortical neurons suggests that the cortex plays little role in processing information about the direction of vibrissa movement, information thought to be necessary for discriminating shapes of objects contacting the vibrissae during active whisking. The results are particularly puzzling given the emergence of orientation and direction selective responses in the primary visual cortex of mammals (for reviews, see Ferster and Miller 2000; Hirsh 2003).

Behavioral studies show that rats can perform multiple discrimination tasks that may depend on directional cues from their vibrissae. In a recent study rats were trained through fear conditioning to discriminate between arms of a three-arm Y-maze configured with oriented bars (Polley et al. 2004). Using their vibrissae to scan the orientation of bars along the walls of the maze, rats learned to make orientation discriminations of 90° after a single day of training. This study was the first to show that rats can make orientation discriminations using their vibrissae, a task that almost certainly uses the direction of vibrissae movements as a cue. Other studies have demonstrated that rats can learn object discrimination tasks that may also depend on the direction of vibrissa movements. Brecht et al. (1997) trained blind rats to discriminate between small sweet or bitter cookies based on their shapes, and to localize cookies through spatial cues in the environment using their vibrissae. Harvey et al. (2001) trained head-fixed rats to discriminate between a cube and a sphere for a reward by using only their vibrissae to palpate the objects. Although the specific cues used to perform types of tasks are unknown, it is likely that the direction of vibrissae movement provides relevant information. For example, when a vibrissa is whisked against an object, it is deflected in a novel direction away from its normal elliptical path. The direction of this deflection provides information about the shape of object encountered.

Given the presumed importance of direction tuning in the rat vibrissa system, the degradation of direction tuning in the somatosensory pathway raises a question as to what computation is performed by the thalamo-cortical or cortical SI circuit. Previous studies have explored the characteristics of direction tuning by analyzing neuronal responses to single vibrissa deflections in multiple directions. We propose that a complete

understanding of direction processing in SI requires the use of temporally dynamic sensory stimuli to probe the response properties of central SI neurons. There are two main reasons to suggest the use of dynamic stimulus protocols; the first reason is the repetitive "whisking" behavior that is intrinsic to the vibrissa sensory system. A second motivation is that thalamo-cortical networks possess unique temporally dynamic response properties that must be considered when investigating coding strategies for properties of sensory stimuli.

As rats explore the environment, they palpate objects in their path with elliptical "whisking" movements that are typically centered at rates from 4-12 Hz (Welker 1964, Carvell and Simons 1990). Additional whisking behaviors centered at higher frequencies have also been reported, such as whisker "twitching" at 7-12 Hz (Nicolelis et al. 1995; Nicolelis and Fanselow 2002) and "foveal whisking" between 15 and 25 Hz (Berg and Kleinfeld 2003). Some evidence suggests that rats may actively modulate whisking frequencies to optimize perceptual performance in specific contexts (Carvell and Simons 1995; Harvey et al. 2001). For example, when rats where trained to detect the presence of an object with their vibrissae, their whisking patterns peaked at frequencies from 2-5 Hz. However, when the same rats were trained to discriminate between two objects whisking frequencies peaked between 7 and 10 Hz (Harvey et al. 2001). To understand how whisking frequency may alter perception of cues such as the direction of vibrissa movement, it is crucial to know how neural responses are modulated by the rate of sensory inputs.

Transmission of information from the thalamus to SI barrels and between neurons within SI shows dynamic temporal response properties. Synaptic depression at low

frequencies has little effect on responses below the level of the thalamus but dramatically influences cortical responses to repetitive stimuli (Castro-Alamancos 2002a; 2002b; Chung et al. 2002, Garabedian et al. 2003). Though inhibitory neurons may respond robustly to rates up to ~40 Hz, excitatory cortical neurons show low-pass adaptation to vibrissa deflections at rates > 5 Hz (Simons 1978; Chung et al. 2002). Cortico-cortical synapses also exhibit synaptic depression that modulates information transmitted across cortical synapses (Markram and Tsodyks 1998; Abbott et al. 1997). Short-term cortical dynamics could potentially influence the direction tuning of cortical responses to incoming thalamic inputs or recurrent cortical inputs. Inhibitory cortical networks also influence temporal responses, and may modulate direction tuning as a function of frequency (Garabedian 2003; Webber 2004). Inhibition has been shown to sharpen direction tuning to single vibrissa deflections. Brumberg et al. (1996) demonstrated that responses of excitatory barrel neurons showed a decrease in spike rate in conjunction with an increase in direction tuning to primary vibrissa deflections when a neighboring, non-primary vibrissa was simultaneously stimulated to induce recurrent inhibitory activity. Direction tuning was further increased when multiple neighboring vibrissae were stimulated, demonstrating that spatial summation of inhibition increases direction selectivity. Responses to temporally complex stimuli, like these spatially complex stimuli, may modulate direction tuning of cortical neurons.

In this study, we examined response properties of layer IV SI neurons to four-second long trains of single vibrissa deflections at rates up to 16 Hz. In our first experiment, trains were maintained in a given direction for the full stimulus period, and tuning was assessed as a function of stimulus frequency. In this paradigm, responses

showed increased direction tuning in response to single vibrissa deflections that occurred in the context of repetitive stimulation. These results suggest that neurons may sharpen direction selectivity during whisking. In the second experiment the direction of vibrissa stimulation was changed after 2 seconds during the course of repetitive stimulation. Responses to the novel direction were robust despite significant adaptation to the initial direction. This frequency specific effect of direction tuning on thalmo-cortical or cortical networks may function to optimize responses to novel stimuli during active whisking behavior. Both results provide further evidence that temporal dynamics of thalamo-cortical and cortical networks actively modulate basic response properties to repetitive sensory stimuli.

METHODS

Preparation.

Adult Sprague-Dawley rats weighing between 275-325 grams were anesthetized with pentobarbitol (50 mg /kg ip) and the left somatosensory cortex was exposed. A tracheotomy and a cisternum magnum drain were performed. Animals were maintained at a constant level of anesthesia with supplemental doses of pentobarbitol as needed (10% of induction does) so that they remained unresponsive to hindpaw pinch and breathing rate (30-60 breaths/min) remained stable. At the end of each experiment, animals were given a supplemental lethal dose of pentobarbital (150 mg/kg ip) and either a bilateral thoracotomy was performed or animals were perfused transcardially so brains could be used for histology.

Stimulation and Electrophysiology.

We recorded from 91 multi-unit sites and 43 single-units in the primary somatosensory cortex (SI) of 32 rats. Recordings were made with tungsten microelectrodes (FHC # UEWMCJSE2P4G, ~2 Mohm, # UEWLFESX3N4J, 3 Mohm, and A-M Systems # 573400, 5 Mohm) from the middle layers (500-900μm), depths that typically correspond to layer IV in the rat and/or the thalamocortical afferent recipient zones. Data was sampled at 25 kHz and band-pass filtered between 300 Hz and 10 kHz. Spike times and shapes were recorded using a window discriminator that was set above noise levels.

Before each recording, all vibrissae were trimmed to a length of 1 cm and the primary vibrissa corresponding to each recording site was identified by hand mapping. Experiments were limited to the long, caudal vibrissae in columns 1-3 and rows C-E, as well as the gamma and delta vibrissae. Trains of vibrissa deflections at 5-8 Hz were presented in randomly changing directions as search stimuli to identify responsive recording sites. Single units were isolated and waveforms were monitored during the course of the experiment to confirm site stability.

Stimulation.

A custom designed multi-directional stimulator was used to mechanically stimulate vibrissae with trains of deflections. The stimulator was built by securing four piezoelectric wafers (Piezo Systems, #Q215-H4CL-303X) to a plastic frame in the

configuration of a '+' (See Figure 1). The internal diameter of the frame was 5.7 cm, and the ends of opposite piezos were 3.1 cm apart. A circular rubber plate was attached to the end of each wafer with an overlap of 1 cm, and a plastic probe that was 7.5 cm in length and 5 cm in diameter at its base was mounted in the center of the rubber plate.

A small metal loop with a 1.5 mm diameter was attached to the end of the probe. After identification of a primary vibrissa, the probe was manipulated so that the targeted vibrissa passed through the loop at a distance of 5 mm from the rat's face and the sides of the loop did not contact the vibrissa. A small drop of acrylate (OPI Nail lacquer, color: Apple Pie) was used to secure the position of the vibrissa inside the loop for stimulation. The viscosity of the acrylate allowed the vibrissa to recover to its rest position before it hardened, securing the vibrissa in place for the duration of the experiment. At the end of a stimulus set, ethyl acetate (Nail polish remover, Walgreens) was used to remove the vibrissa from the stimulator without damage.

Application of voltage to two of the wafers mounted on opposite sides of the frame resulted in movement of the probe in one direction, while activation of the alternate set of wafers moved the probe in the orthogonal direction. The motion of the stimulator was calibrated by monitoring the movement of the loop mounted to the end of the probe through the use of an infrared slotted optical switch (<10 mm resolution; QVA series; Fairchild) connected to an oscilloscope, and no significant ringing of the stimulator was observed in the frequency range applied to this study.

Two experiments were conducted. In some cases data sets were collected for both experiments from the same neurons. The number of samples collected over both experiments for each type of recording is as follows (MUs, n = 91; RSUs; n = 24; FSUs,

n = 17). In some cases, only a subset of recordings were sampled at each frequency, and number of cells of each type for each analysis are indicated in figure captions.

Stimulus Set #1: Frequency-dependent effects on direction tuning. Four second long trains of deflections were presented to the primary vibrissa in 8 directions. Deflections were designed to have a 5 msec sinusoidal rise time and 50 msec sinusoidal fall time (Figure 1B). The tip of the stimulator attached to each vibrissa at a distance of 5 mm from the face and was deflected 300 μms in each direction during each deflection, for a vibrissa stimulation velocity of 60 mm/sec at the point of attachment. Each stimulus train consisted of deflections in a single direction at a constant rate, with a 3 second recovery period between stimulus trains. Ten repetitions of each train were presented in random order at one frequency; 4, 8, 12, or 16 Hz. If the recording site appeared to be stable at the end of the stimulus set, a new frequency was randomly selected and the entire stimulus set was repeated. For single units, 8 and 12 Hz trains were presented.

Stimulus Set #2: Direction specificity of adaptation effects. The second stimulus set was composed of four second long trains of vibrissa deflections, with a rise/fall structure identical to deflections described in the first stimulus set. For the first two seconds of a train, one of the four cardinal directions (dorsal, ventral, rostral, or caudal) was randomly selected for stimulation. After two seconds, a novel direction was pseudo-randomly selected from the four cardinal directions such that on 25% of trials the direction was constant throughout the four-second train, and on 75% of trials a novel direction was chosen for the last two seconds. The stimulus rate of 8 or 12 Hz remained constant

throughout each train. Each possible dual-direction stimulus (out of a total 16 stimuli) was repeated 10 times, and stimuli were presented in random order.

Analysis

Identification of single units: Spike waveforms were saved and single units were manually selected using Brainware software. Separable clusters of points were chosen from criteria such as maximal and minimal waveform amplitudes, peak to peak amplitude, time to peak, spike width, and total spike area. Autocorrelation functions of each spike trains were constructed and all trains with spike contamination within –1 or +1 msec were rejected as single units.

Stimulus Set #1: Time Epochs Analyzed: Three main types of response were quantified for analysis of the first data set (Figure 1C). Responses to the first deflection (FD) were quantified by counting the number of action potential responses occurring from 0-35 msec after the onset of the stimulus train. Similarly, responses to the "middle deflection" (MD), defined as the deflection occurring two seconds after the onset of the train, were quantified by counting the spikes occurring 2000-2035 msec after onset of the train. For "steady state" responses (SS), responses to vibrissa deflections occurring from 1-4 seconds after the onset of a stimulus train were considered. For analysis during the steady state period, spikes occurring 0-35 msecs after the onset of a vibrissa deflection during this 3 second time period were counted. These responses were averaged for comparison with responses to the first and middle deflections. For the analyses of all deflections shown in Figure 9, spikes occurring 0-35 msec after the onset of each

deflection were considered. Direction tuning was assessed and quantified for each time period during the train using several analysis methods.

Vector Averaging: For each recording site, a vector was defined for each stimulus direction so that the length of the vector was equal to the number of spikes evoked, and the direction of the vector was equal to the direction of vibrissa stimulation. These eight vectors were averaged to define the preferred direction for the recording by the direction of the average vector, and the tuning strength as the length of the average vector.

Tuning Index #1: The preferred ("maxima") direction was chosen as the direction that evoked the maximal number of spikes. In cases where two directions evoked equal maxima, the direction closest to the optimal direction chosen by vector averaging was identified as the preferred direction. Direction tuning for each site was quantified as follows:

$$\textit{Tuning Index \#1} = (Rmax-Rmin)/(Rmax+Rmin)$$

Rmax refers to the maximal response in any of the tested directions, and Rmin refers to the minimum response in any of the tested directions. Thus, a direction tuning index of 0 indicates that a response is not tuned for direction at all, and a direction tuning index of 1 indicates that a response is maximally tuned for direction. This metric has previously been used by Brecht and Sakmann (2002) to quantify direction tuning of barrel neurons.

Tuning Index #2: The preferred direction was chosen as for Tuning Index #1. Direction tuning for each site was quantified as follows:

Tuning Index #2: = Rmax/ Rmean

Rmax refers to the maximal response, while Rmean refers to the mean response averages over all 8 stimulus directions. For responses to 8 stimulus directions, tuning indices range from 0-8, where a value of 0 indicates no tuning and a value of 8 indicates maximal tuning. This metric is commonly employed in studies of direction tuning of rat SI neurons by the Simons laboratory (Lichtenstein et al. 1990; Brumberg et al. 1996; Hartings et al. 2000; Minnery and Simons 2002; Bruno and Simons 2002; Bruno et al. 2003; Lee and Simons 2004).

Stimulus Set #2: Analysis of the second experiment focused on responses to the first and middle deflections of a train, defined as described for stimulus set #1. Direction tuning curves were constructed for responses for each of these response types. Action potentials occurring 0-35 msec after the onset of the first and middle vibrissa deflections were counted to assess response amplitude. The preferred (maximal) and non-preferred (minimal) directions were defined as the directions that resulted in maximum or minimum numbers of evoked action potentials during 0-35 msec period after the first deflection of a vibrissa in the train. In cases where two directions were tied for maximal evoked response, the direction closest to the direction of the vector average was defined as the preferred direction.

Histology

In a subset of recordings, electrolytic lesions were made at the termination of an experiment (5-15 μAmps, 5-15 seconds). Animals were perfused transcardially with phosphate buffered saline followed by 3% formaldehyde. The brain was removed and cryoprotected in a 30% sucrose solution. After a minimum of 3 days, the brain was sliced in 80-100 μm coronal sections and stained for cytochrome oxidase to assess recording depths. Thirteen lesions were identified. All of the lesions were located in layer IV barrels or in deep layer III slightly above a barrel, a zone that receives significant thalamic projections from the VPm (see discussion of M. Deschenes in Minnery 2003). No lesions were identified in layers V or VI.

EXPERIMENT I. RESULTS

Action potential recordings were made from 91 multi-unit (MU) and 41 single-unit recording sites. The widths of the initial and hyperpolarization (AHP) phases of single unit action potential waveforms were quantified and plotted in Figure 2A as previously described by Bruno and Simons (2002). In agreement with this study, we observed two clusters of units. Fast-spiking units (FSUs) had thin, fast action potentials with a shorter AHP, while regular-spiking units (RSUs) showed a longer action potential waveform and longer AHP (Figure 2B). Out of the total sample of single unit recordings, 24 units were classified as RSUs and 17 as FSUs. Interestingly, our sample does not include a subset of those units classified as FSUs by Bruno and Simons (2002), a group with relatively shorter AHPs (Figure 2A,B, see dashed circles). RSUs and FSUs

displayed differences in spike rate responses that confirmed differences observed in other studies (Bruno and Simons 2002). Figure 2 C shows PSTHs of responses to the first and middle deflections (FD and MD) of stimulus trains at 8 Hz. These plots demonstrate that FSU spike rate responses were higher than RSU spike rates in response to both the FD and MD although differences were not statistically significant (Figure 2C).

First Deflection Tuning: Distribution of Tuning Preferences

Action potential activity of MUs, RSUs, and FSUs was assessed in response to the first deflection of stimulus trains in 8 directions. Figure 3 demonstrates the distributions of preferred and non-preferred directions for all recording sites. The preferred direction of each recording was assessed in two ways. First, vector averaging was used to calculate the mean response vector for each recording. Each resulting vector for single recordings is plotted in grey on polar plots in Figure 3 (left column). For each response type (MU, RSU, and FSU) the mean vector for all sites was quantified by averaging mean vectors for individual recording sites. These mean vectors are shown in black overlying the grey vectors (left column). In a second analysis, the mean number of spikes evoked by vibrissa deflections in each direction was quantified. The preferred direction (maxima) was defined as the direction evoking the greatest number or action potentials, while the non-preferred direction (minima), was defined as the direction or directions evoking the smallest number of spikes. Histograms of the position of maxima or minima were plotted for all recordings (Figure 3, middle and right columns). In subsequent analyses, a combination of methods was used to assess direction preferences of recordings because each individual method has specific weaknesses. Vector averaging

fails in circumstances when responses are 'orientation tuned', ie., show relatively large amplitude responses in two opposing (180°) directions. In these cases, responses in opposite directions cancel each other in the vector average, and a weak response in a third direction may dominate the resulting vector. However, the second method, in which the maximal response is defined as the preferred direction, fails to consider the relative amplitude of responses in all 8 directions and may therefore be influenced by noisy data. Comparison of the preferred directions identified using these two metrics showed strong correlation across all recording types ($r^2 = 0.7341$ for MUs, $r^2 = 0.7466$ for RSUs, $r^2 = 0.6562$ for FSUs).

The direction preferences of the MU, RSU, and FSU samples were similar. Over the sample of recordings, a majority of sites showed preferred responses in the dorsal (0°) or ventral (180°) directions (Figure 3). Vector average calculations showed that 68% of MUs, 79% of RSUs, and 65% of FSUs showed preferred directions in the dorsal or ventral quandrants (chance = 50%). Preferences for dorsal deflections were particularly prominent across all samples: 40% of MUs, 37.5% of RSUs, and 41% of FSUs showed preferred directions in the dorsal quadrant, as assessed by vector averaging (chance = 25%). When preferred directions were chosen by maximal spike counts, 46% of MUs, 54% of RSUs, and 59% of FSUs preferred dorsal deflections (chance = 37%).

First Deflection Tuning: Direction vs. Orientation Tuning

Currently, it is an unexamined question whether direction tuning or orientation tuning (or some other type of tuning) is predominant among SI barrel neurons: To the best of our knowledge, no study has even classified the relative predominance of neurons

tuned to an axis of directions (e.g., dorsal-ventral) vs. a direction (e.g., dorsal). Despite this fact, previous studies have solely based their descriptions and discussion on the presumption of direction tuning. To examine the diversity of tuning types across our sample, we plotted the position of minima relative to the position of the maxima for all recordings: Minima located 180° from maxima indicate direction tuning, while minima located at ±90° from the maxima suggest orientation tuning (Figure 4Ai). Pure direction tuned and orientation tuned samples of neurons are easily distinguishable on this plot. Two additional types of tuning curves are depicted in Figure 4Ai and show indistinguishable profiles in Figure 4Aii. Responses without tuning with exhibit multiple minima across all directions excluding that of the maxima. Similarly, sharp tuning curves (i.e., with a response to only one direction) will show minima distributed across all remaining directions. Both of these tuning curves show a flat distribution of responses in the histogram in Figure 4Aii.

Figure 4B demonstrates the relationship between the preferred and non-preferred directions for all recordings in response to the first deflection of stimulus trains. Across all response types, the most common minima position was at 180° (~21% of all responses). In contrast, the lowest probability minima location was at ±45° from the preferred direction (~13 % of all responses). MU responses showed a double-peaked distribution, with the greatest incidence of minima observed at 180° and a second, smaller peak at ±90°. The distribution of single unit responses did not show this peak at 90°, demonstrating a relatively flat function for minima incidence in positions other than 45°. Given other data presented later demonstrating that neural responses were tuned for either direction, orientation or a more complex property, and given the paucity of responses at ±

45°, this minima distribution suggests that a variety of types of tuning were demonstrated by our sample, but that we could not assume that direction tuning was the preferred response mode of SI neurons.

Frequency Dependent Changes in Tuning

Direction/orientation tuning was assessed during three time epochs of responses to vibrissa deflection trains at 4-16 Hz. Tuning was evaluated in response to the first deflection in the train (FD), the middle deflection (MD) occurring 2 seconds after train onset, and the steady state period (SS, 1-4 seconds after stimulus onset, see Methods). Figure 5A shows the average post-stimulus time histogram (PSTH) for all MU recording sites in response to a 12 Hz train of deflections in the preferred (top) and non-preferred (bottom) directions, chosen by the average response amplitude over all deflections. During the first second of the stimulus train, responses showed dynamic adaptation that reached a steady state amplitude after ~1 second. The three time epochs considered for analysis are shown by a black arrow (FD), grey arrow (MD) and grey line (SS). Across all directions, response amplitudes decreased by an average of 39% or 41% at 8 Hz and 70% or 71% at 12 Hz when assessed for the MD and SS respectively.

Figures 5B and 5C show mean tuning curves of all MU responses to the FD, MD, and SS periods of stimulus trains at 8 and 12 Hz. Tuning curves were constructed for each recording site and a preferred direction was defined separately for the FD, MD, and SS responses as the direction evoking the maximum number of spikes. In cases when two directions evoked equal and maximal numbers of spikes the direction closest to the vector average was defined as the preferred direction. Each tuning curve was rotated so

that the preferred direction was oriented upward to 0°, and tuning curves for all recordings were averaged. Inspection of the average tuning curves for both the MD (Figure 5B) and SS (Figure 5C) reveals sharpening of direction tuning at 8 and 12 Hz, in part due to decreased response amplitudes (Figure 5B,C, left-hand plots) but also as a change in tuning curve shapes (Figure 5B, C, right-hand plots).

In Figure 6, direction tuning was assessed using two metrics and plotted as a function of stimulus frequency for MU responses during each time period. The first metric (Rmax-Rmin/Rmax+Rmin) has the advantage of being sensitive either to direction tuning or a more complex tuning property because it considers responses in only two directions. However, it is also a low precision measure. The second metric (Rmax/Rmean) is influenced by responses in every direction, and reveals relatively lower values for neurons that have more complex tuning (e.g., are orientation tuned) than neurons that are direction tuned. Both tuning metrics revealed significant differences between tuning in response to the FD and the MD of trains at rates $\geq$ 8 Hz (Figure 6A, Student's 2-tailed t-test, $p < 0.01$). Tuning assessed during the SS period also showed significantly higher tuning to trains $\geq$ 8 Hz, when assessed with the first metric, while the second metric showed a significant difference between the FD tuning and SS only for 12 Hz trains (T-test, $p < 0.05$).

Figure 7 shows spike rate and normalized tuning curves for single units (RSUs and FSUs) assessed during the FD, MD, and SS periods. Tuning curves were constructed as in Figure 5. Both RSUs and FSUs were more sharply tuned than MUs in response to the FD of the train when assessed with either tuning metric (t-test, $p < 0.01$). There was no significant difference in tuning between RSUs and FSUs in response to the first

deflection, although tuning was slightly sharper for FSUs than RSUs (see Table 1 for tuning values). Spike rates of both RSUs and FSUs adapted to repetitive stimulation at 8 and 12 Hz, showing lower average spike rates for the MD and SS periods than for the FD. Tuning curves were sharper for the MD than for the FD at both 8 and 12 Hz (Figure 7A, 7B). In contrast, tuning assessed during the SS period did not appear significantly different from FD tuning when normalized to responses in the preferred direction.

The tuning values for RSU and FSU responses during the FD, MD, and SS periods are plotted as a function of stimulus frequency in Figure 8. Both RSUs and FSUs showed higher tuning values at 8 and 12 Hz for the MD compared with the FD. This increase in tuning was significant for FSUs at 8 and 12 Hz for both tuning indices (t-test, $p < 0.05$). RSUs showed improved tuning at 8 and 12 Hz when assessed with the second tuning index (Rmax/Rmean, t-test, $p < 0.05$) and at 8 Hz when assessed with the first tuning index (Rmax-Rmin/Rmax+Rmin, t-test, $p = 0.05$). However, no significant differences in tuning were observed at any frequency for the SS period. Table 1 shows tuning values for MUs, RSUs, and FSUs during three time epochs for three different tuning indices.

The development of tuning over time is depicted in Figure 9. For each individual recording site, tuning was assessed using the tuning indices described above for each individual recording site and vibrissa deflection, and tuning values were averaged for each recording type. For each metric, tuning values were lower in response to the first deflection in a stimulus train. In response to 8 Hz stimulus trains, tuning showed dynamic but progressive sharpening throughout the course of stimulus trains. In response

to 12 Hz trains, tuning increased progressively for ~2 seconds after the onset of stimulus trains, and then reached a relatively stable value for the last two seconds of the train.

Because direction tuning did not reach stable amplitude until ~2 seconds after the onset of 12 Hz stimulus trains, we quantified tuning during the last 2 seconds of stimulation (2-4 seconds post-stimulus onset). Calculations were performed as described for the SS period, excluding the onset time difference (SS period = 1-4 seconds post-stimulus adaptation). Tuning values were larger than corresponding values calculated for the SS period for all frequencies and response types. All conditions showing significant improvement in tuning during the SS state also showed significant increases for the 2-4 second time period. In addition a significant difference in tuning from the FD was found for the first tuning index for MU responses at 12 and 16 Hz, and for the second tuning index for RSU responses at 12 Hz (t-test, $p < 0.05$, $p=0.05$ for RSUs). (see Table 1 for a comparison of tuning during the two steady state periods)

Consistency in Tuning Over Time

We analyzed the temporal consistency of direction preference for all recording sites by comparing the preferred direction of the FD with the preferred direction for the MD and SS. Histograms showing the distributions of preferred direction shifts are plotted in Figure 10A-D. The preferred direction for the FD was defined as the direction that evoked the largest number of spikes for each time epoch (see Methods and previous Results). The preferred direction was defined as 0° for the FD, and the preferred directions for the MD and SS were quantified in degrees by their difference from this direction. Tuning direction was largely consistent for all recording types. When all

responses were considered as a combined group, 63% of 8 Hz MD responses and 85% of 8 Hz SS responses maintained tuning within a $\pm 45^{\circ}$ of the FD preferred direction. In response to 12 Hz trains, less consistency of tuning was observed: 56 % of MD responses and 63% of SS responses maintained tuning within $\pm 45^{\circ}$ of the preferred direction for the FD. Despite the decrease in consistency at 12 Hz, the percentage of MD and SS sites showing consistency within $\pm 45^{\circ}$ of the FD preferred direction was higher than the expected chance value of 37.5%. In addition, the breakdown of tuning consistency during the MD period of 12 Hz trains was largely limited to MU responses: 68% of RSUs and 77% of FSUs maintained tuning within $\pm 45^{\circ}$ of the FD responses under this condition. Single units showed higher consistency of direction preferences than MUs for all frequencies and time epochs considered, with consistency was maintained at 62% or above for all single unit conditions.

Tuning Curve Shapes During Stimulus Trains

The distribution of positions of direction tuning minima during 8 and 12 Hz trains was quantified to determine whether there was a shift in the shape of tuning curves with frequency. The histogram of the relative position of minima described in Figure 4B is re-plotted in Figure 11A to facilitate comparisons across frequencies. The positions of non-preferred directions of MD and SS responses were determined as described for the FD response. In contrast to the FD responses, a distinct shift in the distribution of minima was observed during the SS period. The position 180° from the preferred direction was no longer the highest probability category for minima; the total number or minima in this category decreased by a third, from 21% for the FD to ~14% for 8 Hz trains and ~15%

for 12 Hz trains (Figure 11D). A shift in the position of minima towards $\pm 135^{o}$ was observed, with a 6-7% increase in minima probability in those positions for both 8 and 12 Hz conditions. In addition, the + 135 position was now the highest probability category for MUs, RSUs, and FSUs. This change in the relative position of minima suggests a shift in the number of neurons showing direction tuning to orientation or other complex tuning of responses during repetitive trains.

Histograms for MD responses at 8 Hz showed similar results, although an increase in the number of minima across all positions was observed (Figure 11B). This increase in the number of minima resulted from the fact that many recordings displayed no evoked response to the MD in multiple directions because responses were adapted to a null firing rate. Histograms of minima positions for the MD of 12 Hz trains showed a broad distribution, predicting either a lack of tuning or sharply tuned responses with low firing rates that are identical in multiple directions (most likely null firing). The average tuning curves shown in Figure 7A reveal that responses were highly tuned. Therefore, the spread of minima across all positions relative to the preferred direction can be attributed to low firing rates rather than a lack of tuning.

EXPERIMENT I. DISCUSSION

In this study we characterized basic direction and orientation tuning properties of SI barrel neurons and demonstrated a frequency-dependent sharpening of tuning of responses to repetitive vibrissa stimulation in the whisking frequency range. In agreement with previous studies that employed low frequency vibrissa stimulation to sample direction tuning, the first deflection of stimulus trains demonstrated generally

broader tuning for MU, RSU, and FSU recordings, as defined using two common metrics. The MU responses were more broadly tuned than RSU and FSU responses. All recording types showed a greater probability of preferred tuning in the dorsal direction. When the primary vibrissa was stimulated with 4-second trains of deflections at 8 or 12 Hz, each type of response showed considerable adaptation. When tuning for a single deflection in the middle of the train was assessed, MUs, RSUs, and FSUs showed frequency dependent sharpening of tuning at 8 and 12 Hz. Analysis of the entire steady state response revealed sharpening as well, although the magnitude of this change was less robust than when single deflections were considered.

Bias in Direction Tuning Across Sampled Sites

We observed a bias in the direction preferences of sampled neurons towards dorsal and, to a lesser extent, ventral vibrissa deflections. Tuning was quantified using two different methods to identify the preferred direction of sampled recordings (Figure 3), and both analyses demonstrated a dorsal/ventral bias. Similar biases have been reported in the trigeminal ganglion and in cortical neurons. In trigeminal neuron recordings, Shipley (1974) reported a profound bias towards neurons tuned for the dorsal/caudal (-135 °) or ventral/rostral (+45 °) directions. Lichtenstein et al. (1990) also reported a bias in trigeminal neuron direction preferences, although in his study a high percentage of rapidly adapting (RA) neurons responded maximally to dorsal (0°) deflections, and slowly adapting (SA) neurons show no bias in direction preference. Brecht and Sakmann (2002) observed bias in layer IV neurons towards dorsal direction preferences, and Bruno et al. (2003) reported a small but significant bias towards dorsal

and caudal direction preferences. Our findings contribute further evidence for the high incidence of neurons tuned to dorsal vibrissa deflections. The weaker trend towards ventral direction tuning in our data has less precedent in the literature.

The high prevalence of neurons selective for dorsal vibrissa stimulation may reflect the behavioral relevance of upward deflections during sensory sampling by a whisking rat. A typical "whisk" involves the elliptical movement of the vibrissae along a rostral/caudal axis (see Fig. 19 B and Carvell and Simons 1990). An object positioned in the path of the whisking vibrissae would be expected to deflect vibrissae off their typical path in the dorsal or ventral directions. Consideration of the angular protrusion of the vibrissae on the rat's face suggests that dorsal deflections may occur more frequently than ventral deflections. The caudal macro-vibrissae typically protrude from the whisker pad and bend downwards towards the ground. During the course of tactile exploration, small objects on the ground would be expected to deflect these vibrissae upwards, while ventral deflections would be expected to occur only if when an overhanging object contacts the vibrissa from above the rat's head. In agreement with this theory, we observed a higher incidence of neurons tuned to directions within the dorsal quadrant of our stimulus set than the ventral quadrant across sampled MUs, RSUs, and FSUs.

Single Units Tuning Properties: Comparison with Previous Studies

We recorded from two clusters of single units that were identified by previously established methods as regular-spiking (RSU) and fast-spiking (FSU) units. These two types of units were segregated by the AHP length and spike width (Bruno and Simons 2002). As described in several reports, RSUs showed lower evoked spike rates than

FSUs in response to the first deflection of a stimulus train (Figure 2C) and broader direction tuning (Figures 5-8). However, these differences were not statistically significant and were less pronounced than those previously reported. The lack of differentiation between FSU and RSU responses appears to be due to differences between our FSU sample and those previously reported: The RSU values reported here for tuning and for evoked firing probability are both within 10% of those previously reported, while FSU values showed greater than a 50% difference (Bruno and Simons 2002; Lee and Simons 2004). Inspection of the FSU and RSU clusters defined in previous studies also supports the suggestion that our FSU sample was different: Within Bruno and Simons (2002) data, a region of their distribution of FSU spike shapes that we did not observe showed much shorter AHPs, while the RSU distributions for the two studies were largely overlapping. This finding suggests that we selectively identified a sub-population of FSUs. This could result from a variety of factors, including our search strategy (playing high frequency trains of vibrissa stimulation while advancing the electrode) or the tip geometry of our electrode. These findings suggest that the Bruno and Simons data likely included two distinct cell types within their FSU sample, a suggestion consistent with several intracellular studies that have identified a variety of differences in firing properties and cellular anatomy within the neocortical 'FSU' firing type (Kawaguchi 1995; Gupta and Markram 2000).

Frequency Dependent Sharpening of Tuning

Using two previously established metrics, we observed frequency-dependent sharpening of direction/orientation tuning in SI barrel neurons. The first metric (Tuning

Index #1, Rmax-Rmin/Rmax+Rmin) was sensitive to orientation and direction tuning, while a second metric (Tuning index #2, Rmax/Rmean) diminishes tuning values for sites with more than one preferred direction. When assessed with each of these metrics for either a single deflection (MD) or the average response to the train (SS), MU responses showed more selective tuning at 8, 12 and 16 Hz than in response to the FD or 4 Hz trains. Both RSU and FSU responses revealed more selective tuning to 8 and 12 Hz stimuli during the MD than in response to the FD (t-test, $p < 0.05$). However, tuning assessed for the SS period was not significantly different from FD tuning for single units.

The origin of increased direction tuning for MUs, RSUs, and FSUs is due in part to a decrease in the spikes evoked by stimuli in every direction. As shown by the mean tuning curves for each recording type, response amplitudes typically decreased during repetitive stimulation in every direction. As a result of this adaptation, the ratio of the response in the preferred direction to responses in the non-preferred direction typically increased. The change in the preferred/non-preferred response ratio resulted in increased tuning for both tuning indices, each of which is sensitive to the spike rate of evoked responses. However, an average decrease in spike rate cannot account entirely for the increase in tuning at 8 and 12 Hz. If a decrease in spike rate were the only factor contributing to increased tuning, the time course of the tuning change assessed for each deflection, shown in Figure 9, would mimic the time course of spike rate adaptation, demonstrated by the average MU response shown in Figure 5A. The temporal development of tuning selectivity occurred more slowly than the temporal change in spike rate, reaching an approximate "steady state" 2 seconds after the onset of the train.

In contrast, spike rate adaptation typically reached a steady state after only 1 second of stimulation.

We observed different results of frequency-dependent changes in tuning for responses to single deflections during the middle of stimulus trains (the MD) and for the average response to the last three seconds of stimulus trains (the SS). The difference in the results from these two time epochs may result form a variety of factors. The SS period was chosen for analysis based on the temporal characteristics of adaptation, which reaches a steady state after ~1 second. However, because tuning develops over a slower time course, tuning values assessed for the SS are lower than the maximal possible tuning achieved during repetitive stimulation. In support of this argument, tuning assessed for the last two seconds of stimulus trains was higher than tuning for the SS period for all response types at 8 and 12 Hz. In contrast, tuning values for the MD could be falsely amplified because of the low number of spikes evoked in response to single deflections. As shown in Figure 7, less than one spike was typically evoked in any direction in response to a single deflection during the MD period. Consequently, noise could potentially have a large influence on tuning measures. However, if these high tuning values resulted completely from the low probability of spiking, the consistency in the preferred direction of tuning from deflection to deflection would be low. In contrast to this prediction, we observed consistent direction preferences from the FD to the MD. We conclude that the high tuning values reported for the MD period reflect a meaningful increase in tuning with frequency, accompanied by a decrease in the sensitivity of responses to stimulation based on response amplitudes.

Improvement in the direction tuning of MU recordings at 8-16 Hz may reflect interactions between responses of multiple neurons rather than sharpening of a single unit response. Synaptic depression of thalamocortical neurons could potentially cause a subset of neurons to "drop out" of MU responses at high frequencies. Thus, improvements in tuning would reflect a decrease in the number of neural responses rather than sharpening of a single unit response. In support of this hypothesis, nearly complete adaptation of responses to stimulus rates > 5 Hz have been reported (Chung et al. 2002). Although we did not observe complete adaptation of single unit responses to every stimulus direction in our sample of recordings, we may have selected single units with robust temporal responses as a result of searching for recordings sites with 5-8 Hz stimulus trains (see Methods).

Our failure to observe a statistical difference between tuning during the FD and SS periods for single units does not conclusively rule out the possibility that tuning of single units becomes sharper during the SS period. Due to the technical difficultly of isolating single units, we had a lower number of RSU and FSU recordings than MU recordings, lowering the statistical power of our results for tuning of single units. If a larger sample of single unit recordings were examined, significant differences in FD and SS tuning may have been observed. In support of this suggestion, FSU responses showed increased tuning for every measure applied in the SS analyses (for 8 and 12 Hz, Tuning Index 1 and 2).

A Frequency-Dependent Shift to Orientation Tuning?

Several of our observations suggest that during repetitive stimulation at 8 –12 Hz, responses show a shift from direction-tuned to orientation-tuned responses. A decrease in the probability of minima occurring 180° from the preferred direction during 8 and 12 Hz trains was observed, along with an increase in the probability of minima occurring at 135° for SS responses. Inspection of the shapes of RSU and FSU tuning curves in Figure 7 also suggests a change from direction to orientation tuning. The relative loss in response amplitude was greater at 90° than at 180° for these single unit recordings. That said, the probability of minima occurring at 90°, the typical minima position of orientation tuning curves, increased by only 1-2% during the SS period at 8 and 12 Hz; most of the shift away from minima localization to 180° was accounted for by increased minima at 135°. Further analysis is necessary to characterize the kind (or kinds) of shape changes in tuning curves as a function of stimulus frequency.

Putative Mechanisms of Increased Direction Selectivity at 8-12 Hz

Frequency-specific effects on direction tuning may arise from a variety of mechanisms, including the adaptation properties of thalamocortical afferents. Simultaneous recordings from synaptically coupled VPm and barrel neurons have demonstrated that layer IV barrel neurons obtain their direction tuning properties from the tuning characteristics of their thalamic inputs (Bruno and Simons 2002; Swadlow and Gusev 2002; Temereanca et al. 2003). Each cortical neuron typically receives multiple convergent inputs from thalamic afferents with diverse tuning responses. Cortical neurons consequently show broader direction tuning than thalamic neurons in response to

single vibrissa deflections (Simons and Carvell 1989). Differences in the short-term adaptation dynamics of thalamic neurons may influence direction tuning of cortical neurons (see Figure 19). When these thalamic neurons are repetitively stimulated, the temporal dynamics and magnitude of adaptation vary significantly from cell to cell. The resulting tuning characteristics of the target cortical neurons may consequently sharpen as the balance of dominant inputs changes.

Additional mechanisms may contribute to changes in direction tuning with stimulus frequency. Inhibitory influences, either from cortical neurons or from the reticular nucleus, may modulate direction specific responses. Neurons in the reticular nucleus show sharp direction tuning and dynamic changes with frequency that may underlie some of our observed results (Hartings et al. 2000; 2004). Attentional modulation of responses through neuro-modulatory influences may sharpen direction tuning as well, potentially at sub-cortical foci: Local increases in Ach or NE depolarize thalamic neurons, increasing responses to trigemino-thalamic input (Castro-Alamancos 2001).

EXPERIMENT II. RESULTS

Direction Specific Adaptation

The second set of experiments was performed to determine whether adaptation to repetitive stimuli was specific to a single direction. A single primary vibrissa was stimulated with four second-long trains of deflections at a constant stimulus rate of 8 or 12 Hz. During the first two seconds of a train, the direction of stimulation in one of four directions (dorsal, ventral, rostral, or caudal) remained stable. During the last two

seconds of a train, a new direction was randomly selected, such that the direction of stimulation changed on 75% of stimulus trials, and remained stable for all 4 seconds for 25% of stimuli. Responses to the FD and the MD, which represents the first deflection in a new direction on 75% of trials, were assessed in each analysis.

Figure 12A shows the post-stimulus time histogram (PSTH) of a RSU recording in response to two 12 Hz trains of stimuli. For the top plot, the direction of stimulation during the train remained constant in the dorsal direction for the entire 4-second stimulus period. The response to the FD (shown by a black arrow) of the train was robust, and adaptation of the type described in experiment 1 was observed. During the first second of stimulation, responses showed adaptation to repetitive stimulation, reaching a steady state amplitude after ~1 second that was maintained throughout the stimulus period. The bottom plot shows the PSTH for a train in which the stimulus direction was changed. During the first two seconds of the train, the stimulation occurred in the dorsal direction. After two seconds, the direction of stimulation was changed to rostral. As in the top plot, the response to the FD of the train was robust, but adapted to a steady state during the first ~1 seconds of stimulation. However, when the direction of stimulation was changed to the rostral direction, the MD response to the new stimulus direction was robust despite previous vibrissa stimulation in the dorsal direction. Thus, the adaptation to repetitive dorsal deflections was direction-specific; stimulation in the novel rostral direction evoked a robust response, typical of the non-adapted state.

Figure 12B shows the response of the same RSU to the four possible combinations of stimuli. Responses to the FD are plotted in black and responses to the MD are plotted in grey. Each polar plot demonstrates the change in responses after

adaptation in one specific direction, indicated by the black arrow. The resulting grey tuning curves demonstrated direction-specific adaptation for dorsal, ventral, rostral, and caudal adaptation directions.

The average responses to dual-direction stimulus trains are shown in Figure 13. Figure 13A shows the average MU PSTH for all recordings in response to two types of stimulus trains. The top plot shows the average response to a 4-second long train in the rostral direction at 12 Hz. The bottom plot shows the response to a train that switches from the rostral to the dorsal direction after 2 seconds of stimulation. The average response to rostral stimulation showed robust adaptation. However, when the direction of stimulation was changed to dorsal, a robust response to the novel direction was observed.

Figure 13B shows average MU, RSU, and FSU responses to dual-direction stimuli. For each type of stimulus, the direction of adaptation was plotted in the upward direction at 0°. Each type of recording exhibited direction-specific adaptation at both 8 and 12 Hz. Responses to MD stimuli decreased by 49% for MUs, 22% for RSUs, and 51% for FSUs in response to the adapted direction at 8 Hz. On contrast, average decreases in the response amplitudes to MD stimuli to novel directions were much smaller (11% for MUs, 6% for RSUs, and 13% for FSUs). In response to 12 Hz trains, responses to the MD in the adapted direction decreased by 76% for MUs, 51% for RSUs, and 61% for FSUs. Unlike the 8 Hz trains, responses to novel directions largely reduced as well, decreasing by 45% for MUs and by 40% for RSUs and FSUs (see Figure 13 B, bottom row).

Studies of the adaptation properties of visual cortical neurons have demonstrated that adaptation in the preferred and non-preferred directions have differing effects on the

tuning preference of neurons (Marlin et al. 1998; Giaschi et al. 1993; Dragoi et al. 2000; Felson et al. 2002; Kohn and Movshon 2003). To assess potential differences in direction specific adaptation of rat SI neurons, we examined the effects of adaptation in the preferred and non-preferred directions for all MUs, RSUs, and FSUs. Figure 14 shows average responses of these sties before and after preferred and non-preferred adaptation. In Figure 14A, tuning curves were rotated so that the preferred direction was oriented upward at 0^{o}, and average responses were plotted. Black curves show responses to the FD of 8 and 12 Hz stimulus trains, and grey curves show average responses after adaptation in the preferred direction. In Figure 14 B, tuning curves were rotated so that the non-preferred direction was oriented upwards. Black curves show average responses before adaptation (FD), and grey curves show average responses after adaptation in the non-preferred direction (MD). The decrease in response amplitudes to adaptation in the preferred and non-preferred directions was similar to average adaptation effects shown in Figure 13. Average decreases in response amplitudes were greater in the adapted direction than in neighboring directions for all cases. No obvious differences in the magnitude or characteristics of adaptation in preferred and non-preferred directions were observed.

Figure 15 shows the shift in preferred directions of each site in response to adaptation in the preferred and non-preferred directions. Adaptation in the preferred direction resulted in shifts in direction tuning away from the original preferred direction for 75% of recordings at 8 Hz, and 81% of recordings at 12 Hz. In contrast, adaptation in the non-preferred direction changed the preferred direction of neurons much less frequently; only 43% of recordings showed a change in direction preference with 8 Hz

stimuli, and 50% showed a change in direction during at 12 Hz. In both cases, the change in direction tuning after adaptation in the non-preferred direction occurred less frequently than the 75% level expected by chance.

We quantified direction tuning before and after adaptation in preferred and non-preferred directions using Tuning Indices #1 and #2. Figure 16 shows the average change in these tuning values for all recordings types (MU, RSU, FSU) from the FD to the MD of 8 and 12 Hz trains. Adaptation in both the preferred and non-preferred directions caused a significant increase in tuning assessed for the MD of 12 Hz trains for all recording types (t-test, $p < 0.05$). A significant increase in tuning assessed with Tuning Index #1 at 8 Hz was observed for RSUs and FSUs after adaptation in the preferred direction, and for MUs and FSUs after adaptation in the non-preferred direction. In contrast, significance was reached less frequently at 8 Hz with Tuning index #2. This probably results from the fact that the first tuning index (Rmax-Rmin/Rmax+Rmin) is more sensitive than the second tuning index (Rmax/Rmean) to the robust decrease in response amplitudes observed in a single direction.

Population Tuning

Population responses to all conditions of adaptation were plotted for MU, RSU, and FSU recordings, as shown in Figures 17 and 18. For each recording site, the preferred direction was determined as the direction evoking the largest number of spikes in response to the FD of the train. For each plot, average responses to a test stimulus in the 0° direction (defined as the stimulus direction of the MD for each train) are shown for groups of sites with preferred directions at 0°, 90°, -90°, and 180° relative to the test

stimulus direction. Response amplitudes for each recording were normalized to the maximal response of that site.

The left plot of Figure 17A shows the MU population tuning curve for the FD of 8 Hz trains. On the right, the shift in tuning is plotted for MD responses to 0° after adaptation in three different directions (0°, 90°, or 180°, FD tuning is shown by think lines, MD tuning in thick lines). In all cases, the preferred response of the population was maintained despite adaptation. In response to 0° adaptation (the same direction as the test stimulus), average responses decreased significantly over the entire population. After adaptation at 90° at 180°, large responses to the MD were maintained across the population. Figure 17B shows the same plots for responses to 12 Hz trains. In contrast to the responses at 8 Hz, adaptation in all directions tested resulted in near flattening of the population tuning curves. As observed for the 8 Hz population curves, the greatest adaptation occurred when the direction of adaptation was the same as the direction of the MD test stimulus.

Figure 18 shows population tuning curves for RSU and FSU responses to 8 and 12 Hz trains. In agreement with MU data, the preferred tuning of the population was maintained for each condition of adaptation at 8 Hz, and significant decreases in response amplitudes were only observed after 0° adaptation. Adaptation at 12 Hz resulted in more robust adaptation, but in contrast to MU responses, population tuning was not eliminated. Interestingly, RSU responses to neurons tuned to 0° showed a greater loss in spike rate after 12 Hz adaptation at 180° than after 90° adaptation, suggesting complex tuning (ie, orientation tuning) of these responses.

EXPERIMENT II. DISCUSSION

In this experiment, we demonstrated that adaptation of rat SI neurons is direction specific. In response to trains of deflections in a single direction, responses to the MD were dramatically reduced when compared with responses to the FD. However, when adaptation was induced 90° or 180° away from the direction of the MD, average responses showed no significant decrease in amplitude to 8 Hz stimuli. More substantial non-direction-specific adaptation effects were observed when 12 Hz stimuli were applied. One likely perceptual consequence of direction-specific adaptation is that novel directional stimuli evoke a robust neural response, potentially enhancing the detection of novel patterns of vibrissa motion.

Comparison with Adaptation in Visual Cortex

Our investigation of adaptation and direction tuning is similar to prior investigations of adaptation in the visual cortex. In primary visual cortex (V1), adaptation is often specific to the characteristics of the adapting stimulus, including the direction of the stimulus (Hammond et al. 1985; 1988; Marlin et al. 1988; Giaschi et al. 1993). Motion in the preferred direction of the neuron reduces responses to that direction more than to non-preferred direction, often decreasing the direction tuning of the neuron or changing the preferred direction of the cell. Orientation tuning also shows stimulus-specific adaptation (Movshon and Lennie 1979; Muller et al. 1989; Dragoi et al. 2002; Felson et al. 2002). After adaptation, orientation tuning of V1 neurons typically shifts away from the adapting orientation. In contrast to adaptation-induced direction and orientation tuning shifts away from adapting stimuli in V1, it has recently been

demonstrated that motion-sensitive MT neurons show shifts in tuning *towards* to the direction of adaptation (Kohn and Movshon 2004).

Neither direction tuning nor orientation tuning of visual neurons are exactly analogous to the tuning properties of rat SI neurons we refer to as 'direction' and 'orientation' tuning in this study. Different directions of vibrissa stimulation result in activation of separate clusters of mechanoreceptors in the vibrissa follicle (Rice et al. 1986). Direction tuning in the vibrissa sensory system is present throughout the sensory pathway, including the primary sensory afferents (Nord 1968; Lichtenstein et. al. 1990; Minnery and Simons 2003). This contrasts with direction and orientation tuning of V1 neurons, which is constructed at central processing levels (for reviews, see Ferster and Miller 2000; Hirsh 2003). Never the less, the role of adaptation in sensory processing of these signals at the cortical level show similarities that suggest a common role of adaptation in perceptual function across sensory systems.

With these caveats considered, the results of our studies demonstrate a similarity between adaptation effects on rat SI neurons and VI neurons. Adaptation was largely specific to the direction of the adapting stimulus. We observed shifts in direction tuning away from the direction of adaptation when adapting stimuli matched the preferred direction of recording sites (Figure 15). These shifts in preferred direction resulted from a larger decrease in response amplitude in the adapted direction relative to non-adapted directions. Adaptation in non-preferred directions decreased response amplitudes to the adapted direction as well, but typically preserved the same preferred direction of responses. Significant sharpening of direction tuning was observed in response to adaptation in both the preferred and non-preferred directions, which can be attributed to

the dramatic decrease in response amplitude that was limited to one direction only. The results of our experiments demonstrate a basic similarity between adaptation effects on direction and orientation tuning in VI and adaptation effects on rat SI neurons.

Putative Mechanisms of Direction-Specific Adaptation

A model of synapse-specific adaptation/suppression of inputs from the thalamus can explain the findings reported here. As discussed previously, rat SI barrel neurons receive convergent inputs from multiple thalamic afferents with different tuning characteristics (Bruno et al., 2003; Bruno and Simons 2002; Swadlow and Gusev 2002). This convergence provides one explanation for the relatively broader directional tuning curves observed in SI as opposed to thalamic neurons. Vibrissa stimulation in one direction would be expected to maximally activate a subset of VPm neurons with a corresponding tuning preference, causing short-term depression at these thalamocortical synapses, and a consequential decrease in firing rate (adaptation) in their target barrel neurons. A change in the direction of vibrissa stimulation would activate a new subset of VPm neurons tuned to the novel direction whose synaptic connections are separate and not yet significantly depressed. The un-adapted signals from these neurons would excite the same target barrel neurons, resulting in an increase in the magnitude of cortical responses to the novel direction (Figure 19A). Other pre-synaptic mechanisms, such as synaptic depression of cortico-cortical synapses or modulation of recurrent inhibitory feedback, may also contribute to the direction-specific adaptation we observed (Markram and Tsodyks 1996; Abbott et al. 1997; Brumberg et al. 2002).

In addition to direction-specific adaptation of SI responses, we observed smaller amplitude adaptation of non-direction specific responses. These effects can in part be explained by the following model: thalamic neurons are not perfectly tuned (i.e., they have surround inputs also), and these surround inputs should contribute somewhat to the non-preferred direction responses of a neuron. As such, adaptation of those neurons should also result in a decreased response to the surround. This kind of explanation is sufficient to explain the MU, RSU and FSU behavior at 8 Hz. This model would not appear to be able to explain, in isolation, the pattern of surround suppression observed at 12 Hz. For MU responses, adaptation in any given direction resulted in decreased activity in all directions, lowering firing rate to 50% of the peak observed in the preferred direction. Although somewhat more variable, FSU responses also followed this trend. These responses properties suggest the presence of a rate limiting effect that was constant across directions of stimulation. As such, a post-synaptic mechanism is the most probable explanation. One possible post-synaptic mechanism is suggested by investigations of contrast adaptation in the primary visual cortex. Visual stimulation at high contrasts results in long-lasting hyperpolarization of cortical neurons that likely arises from activation of Ca^{++}, N^{++}, or K^{+} conductances (Sanchez-Vives et al. 2000a; 200b). Long hyperpolarizing currents may be responsible for the non-specific adaptation we observed in rat SI cortex. Alternative potential mechanisms involving facilitation of inhibitory neurons are less likely given our observed depression of FSU responses to our stimulus set.

CONCLUSIONS: IMPLICATIONS FOR WHISKING BEHAVIOR

Results of the experiments in this thesis suggest that thalamocortical and cortical temporal dynamics modulate direction selective responses during repetitive stimulation at 8-16 Hz. Whisking behavior may exploit these temporal changes in neural selectivity to optimize sensory processing for specific perceptual goals. When a rodent is in a quiet resting state, their vibrissae are typically immobile. However, during active tactile exploration, rodents whisk their vibrissa against object at rates centered at ~ 8 Hz (Welker 1964; Carvell and Simons 1990). It has been proposed that during quiet states, neural responses may be optimized for *detection* of novel stimuli, while whisking results in optimization of responses for tactile *discrimination* (Moore et al. 1999; Moore 2004).

Our findings support the hypothesis that temporal dynamics of thalamocortical networks modulate direction selective responses to maximize the salience of specific sensory cues. Rats whisk in repetitive elliptical patterns that are centered on a rostral/caudal axis, but include motion in dorsal and ventral directions as well (see Figure 19B). During whisking, responses in each direction may become significantly adapted. Results of our first set of experiments demonstrated that direction tuning of responses to single vibrissa deflections becomes more selective at whisking frequency rates. This result suggests that when a rat is whisking in air and encounters an external stimulus, sensory cortical responses are optimized for direction discrimination (Figure 19C, part 2). While broad direction tuning and high amplitude responses might be ideal for an animal to detect a stimulus, this frequency-specific increase in neural selectivity would be beneficial to an animal during behavioral exploration.

Studies of synaptic depression in cortical networks have predicted that one role of sensory adaptation may be to improve detection of novel stimuli. Recordings between synaptically connected cortical neurons have shown that during steady state adaptation, responses to a changes in the frequency of synaptic input are enhanced (Markram and Tsodyks 1996; Abbott et al. 1997). Based on a recent model of a barrel network, Peterson (2002) predicted that when responses are largely adapted due to synaptic depression, a novel stimulus, such as a change in direction, will result in large increases in neural activity. The results of our second experiment are in agreement with these predictions, demonstrating that adaptation of barrel neurons may enhance detection of changes in the direction of vibrissa deflections.

Results of our second experiment demonstrate that if the vibrissae are stimulated repetitively in a single direction, responses to a change in direction result in increased neural response amplitudes. This type of direction-specific stimulation may result from a variety of factors. Because elliptical whisking patterns are biased towards a rostro-caudal axis, neurons tuned to rostral and caudal stimulus directions may show greater adaptation during active whisking. In this scenario, interruption of stereotyped, elliptical vibrissa motion by a novel stimulus would likely deflect vibrissae in dorsal and ventral directions. This interpretation of our results also suggests a possible explanation of our reported bias towards dorsal tuned neurons in our data sample given the potential behavioral relevance of these directions during whisking. Alternatively, direction-specific sensory input to the vibrissae may occur as a rat whisks continuously against a single object. The high velocity vibrissa deflections that occur during this type of exploration could selectively increase adaptation of neurons tuned to a specific stimulus direction. A change in the

external environment would consequently change the direction of vibrissa stimulation and lead to robust increases in neural activity in select cells. Currently, little is known about the selective adaptation of groups of neurons that may occur during whisking behavior (ie, is adaptation direction specific?). Consequently, we cannot distinguish between these possibilities. However, our results suggest that novel stimuli encountered during whisking cause robust increases in activity, optimizing stimulus *detection*. Interestingly, results of our population tuning analysis show that at least at 8 Hz, direction selectivity is preserved in the population response. Thus, and increase in firing rates to novel stimuli along with preserved direction tuning would provide neural signals that favor detection of change along with discrimination of stimulus direction.

Each of the experiments discussed in this thesis support the hypothesis that neural responses to tactile inputs are modulated by temporal dynamics initiated by whisking behavior. In resting states, when networks are in an un-adapted state, responses to vibrissa stimulation are robust and show weak selectivity for direction. These robust, non-selective responses are ideal for alerting an animal to the detection of a stimulus. During repetitive stimulation at whisking frequencies, response amplitudes decrease, while temporal fidelity increases and direction tuning sharpens. This increase in response selectivity optimizes neural activity for discrimination of tactile objects, which is likely the perceptual goal of an exploring, whisking rat. Relative biases in the direction of adaptation selectively adapt networks to specific stimulus directions, resulting in relative increases in response amplitudes when novel stimuli are encountered. During whisking, this phenomenon may alert an animal to the presence a novel stimulus, shifting sensory responses back towards a mode of detection. Thus, temporal dynamics of

thalamocortical and cortical networks may function to modulate the perceptual salience of tactile sensory responses during specific behavioral states.

Figure 1. The vibrissa stimulation protocol. A. The multi-directional vibrissa stimulator. B. The position of a vibrissa during a single deflection is plotted as a function of time. The grey line indicates the 35 msec window during which spikes were counted for analysis. C. An example of an 8 Hz train of stimuli used for the first experimental paradigm. The black and grey arrows indicate the times of the first and middle deflections (FD and MD), respectively, and the grey line indicates the steady state period (SS). D. Examples of two types of stimuli presented in the second experimental paradigm are shown. The black arrow indicates the time of the FD, and the grey arrow shows the time of the MD. Top plot: the direction of stimulation remains constant during the 4-second train. Bottom plot: After two seconds, the direction of vibrissa stimulation is changed.

A.

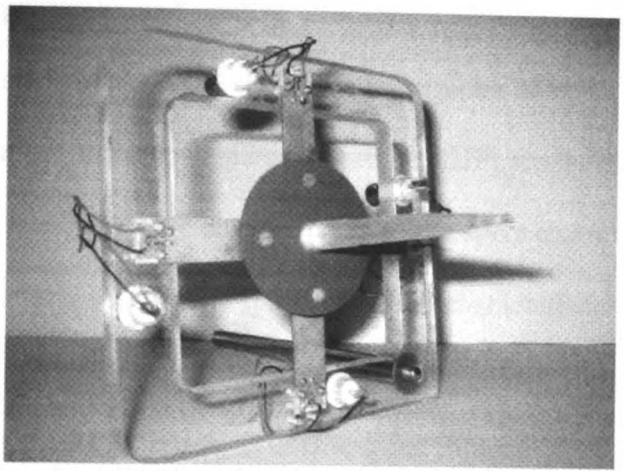

B.

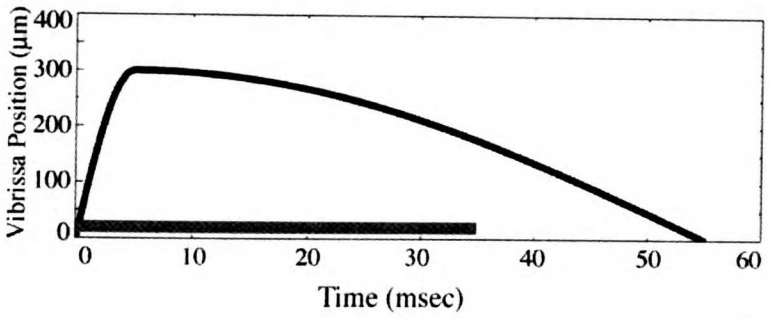
Vibrissa Position (µm)
400
300
200
100
0
0
10
20
30
40
50
60
Time (msec)

C.

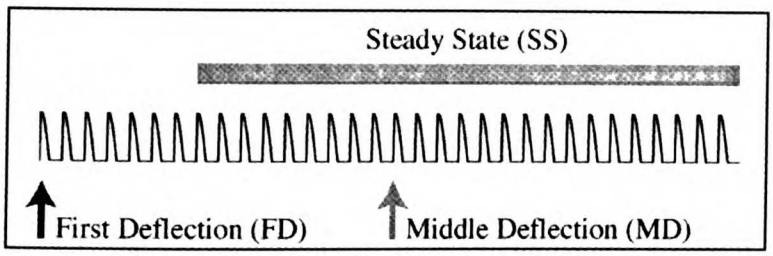
Steady State (SS)
First Deflection (FD)
Middle Deflection (MD)

D.

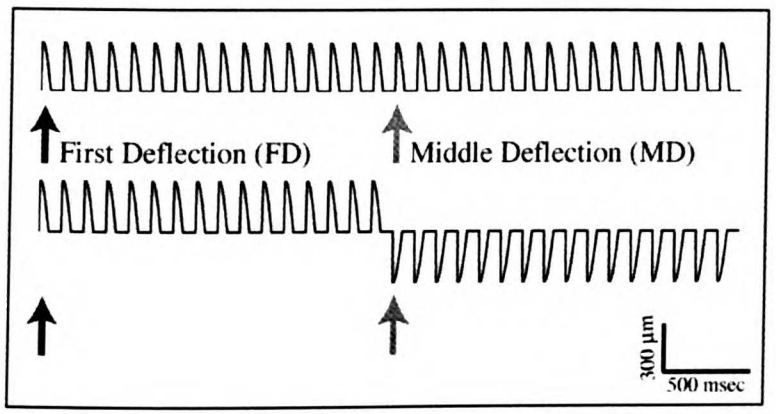
First Deflection (FD)
Middle Deflection (MD)
300 µm
500 msec

Figure 2. Segregation and spiking characteristics of single units. A. A figure taken from Bruno and Simons (2002) shows the segregation of RSUs and FSUs based on the width of the initial and after-hyperpolarization (AHP) phases of the spike waveforms. The dashed circle indicates a cluster of FSUs with spike characteristics that were not captured in our data set. B. The spike waveform characteristics of all single units recorded in this study were characterized by plotting the width of the AHP as a function of the width of the initial phase, as in Bruno and Simons (2002). Two separable clusters of units were observed. RSU data is plotted in grey (24 units), and FSU data is plotted in white (17 units). A dashed line separates the two clusters of units. The dashed circle indicates the absence of a subset of FSU recordings in our data set that were observed in Bruno and Simons' (2002) data. C. Average responses to the FD and MD of 8 Hz trains in the preferred direction for each time epoch for MUs, RSUs, and FSUs. Mean MU responses are shown on the left, and RSU and FSU responses are overlaid on the right in black and grey, respectively. The difference in spike rate for RSU and FSU responses were not significant for the FD or MD.

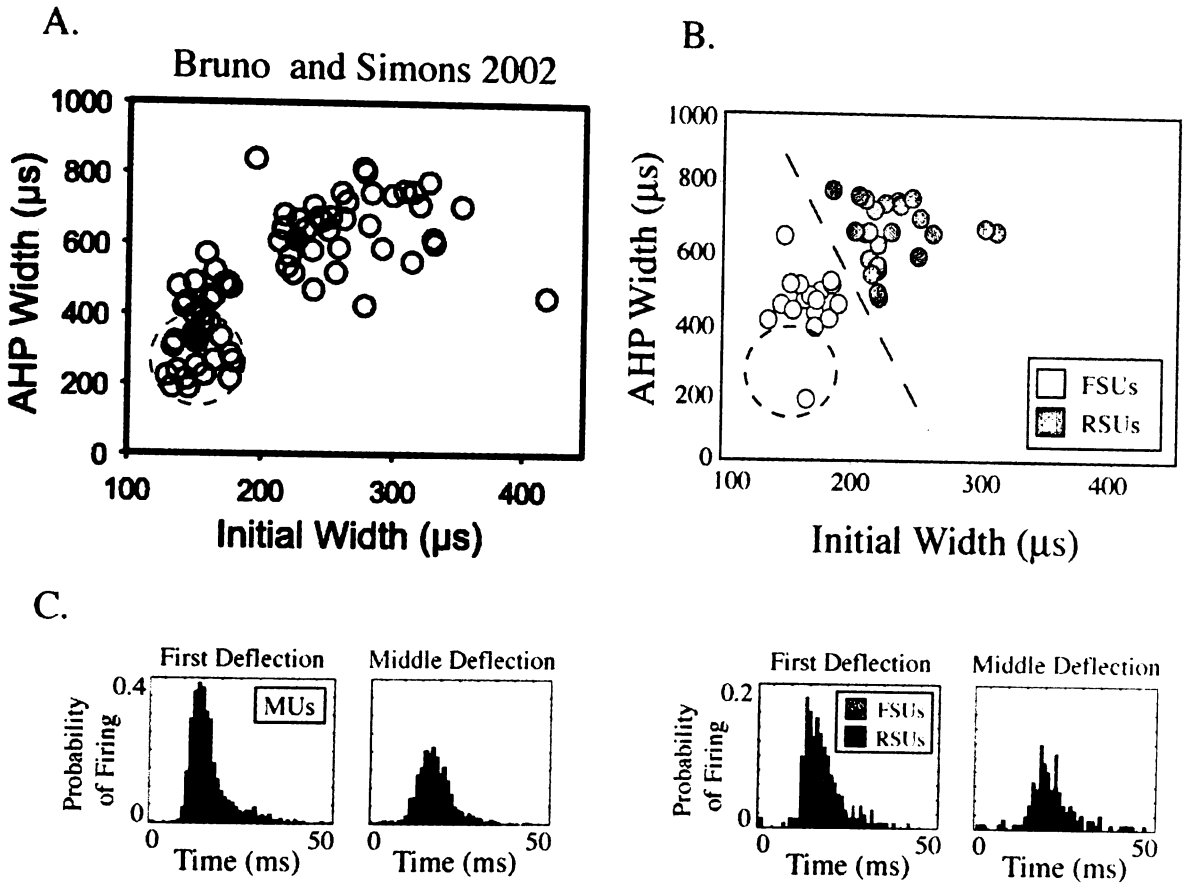
A.
Bruno and Simons 2002
AHP Width (µs)
Initial Width (µs)
B.
AHP Width (µs)
Initial Width (µs)
FSUs
RSUs
C.
First Deflection
Middle Deflection
Probability of Firing
MUs
Time (ms)
First Deflection
Middle Deflection
Probability of Firing
FSUs
RSUs
Time (ms)

Figure 3. Distribution of preferred and non-preferred directions. In the first column, the vector average or responses to all 8 stimulus directions are plotted for each individual MU, RSU, and FSU recording as grey lines. The vector sum for all recordings of each type are shown in black. The second column shows the distribution of preferred directions as chosen by the maximum number of evoked spikes for all MUs, RSUs, and FSUs. The length of each bar shows the number of sites with a corresponding preferred direction. The third column shows a histogram of non-preferred directions. In some cases more than one direction showed minimal response for as single site, and each of these directions was counted on the histogram of non-preferred directions. For all plots, 0° indicates dorsal, 90° indicates rostral, 180° indicates ventral, and –90° indicates caudal. The number of recordings are as follows: MUs, n = 68; n = ;RSUs, n = 24; FSUs, n = 17.

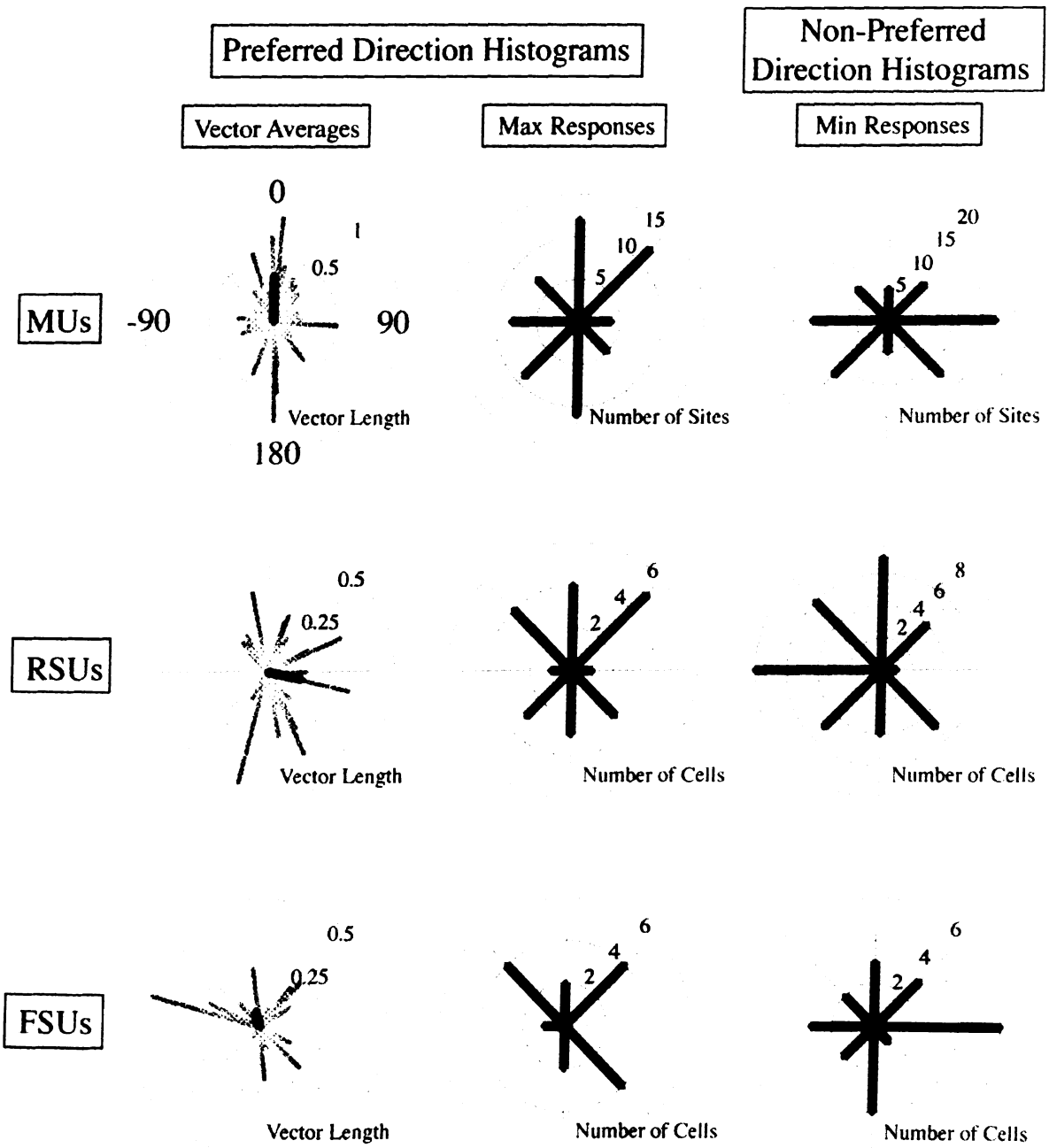
Preferred Direction Histograms
Non-Preferred Direction Histograms
Vector Averages
Max Responses
Min Responses
MUs
RSUs
FSUs
0
90
-90
180
1
0.5
0.25
15
10
5
20
Vector Length
Number of Sites
Number of Cells
6
4
2
8

Figure 4. Relative positions of preferred and non-preferred directions. A. A diagram shows four possible types of tuning curves and the corresponding angular relationship between the preferred and non-preferred directions for each curve. The position of the preferred (maximal) response was defined as 0°, and the position of the non-preferred (minimal) response or responses was defined by their position relative to zero. Ai. Four types of tuning curves are shown with the maximal response oriented upwards at 0°. Black circles on the tuning curves indicate the relative minimal responses. Orientation tuned responses have minima at +90° or –90°, while direction tuned responses have a minimum at 180°. Responses with broad tuning show a spread of minima across all positions around the maximum. Similarly, responses with sharp tuning and a low mean firing rate also have minima in every position around the maximum. ii. A model histogram shows the predicted plot of the position of the minima relative to the preferred direction for samples of neurons with each type of tuning curve. A flat line may predict either an un-tuned response or a sharply tuned response. B. A histogram of the positions of the minima relative to the preferred direction in response to the FD of the stimulus trains for all recordings. MUs are shown in black, RSUs in grey, and FSUs in white. The number of recordings are as follows: N=78 for MUs; N = 40 for RSUs; N=24 for FSUs.

A. i.

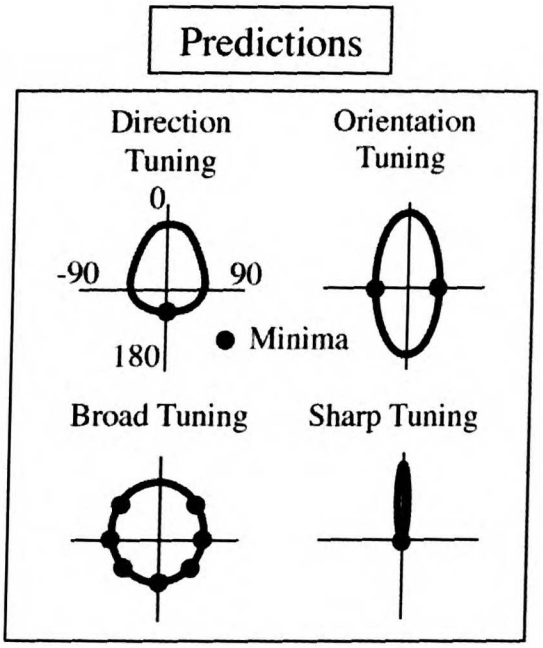
Predictions
Direction Tuning
Orientation Tuning
0
-90
90
180
Minima
Broad Tuning
Sharp Tuning

ii.

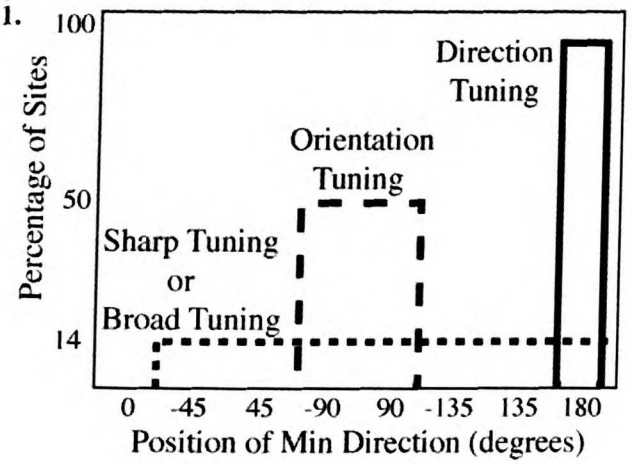
100
50
14
Percentage of Sites
Direction Tuning
Orientation Tuning
Sharp Tuning or Broad Tuning
0 -45 45 -90 90 -135 135 180
Position of Min Direction (degrees)

B.

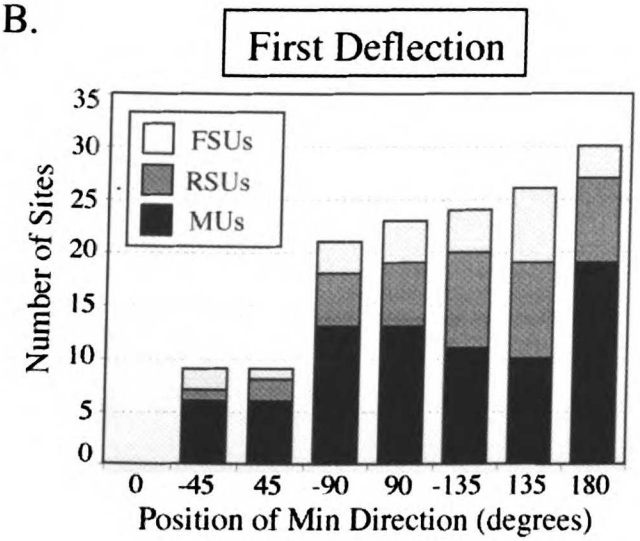
First Deflection
35
30
25
20
15
10
5
0
Number of Sites
FSUs
RSUs
MUs
0 -45 45 -90 90 -135 135 180
Position of Min Direction (degrees)

Figure 5. Mean multi-unit tuning curves. A. Mean responses to 12 Hz trains of deflections are shown in post-stimulus time histograms (PSTHs) with 1-msec time bins. The top plot shows the average response to stimulation in the preferred direction for each site (assessed over all deflections), while the bottom plot show the mean response to the non-preferred direction. The black and grey arrows indicate the time of the FD and MD, while the grey bar signifies the SS. B. Mean tuning curves for the FD and MD responses to 8 and 12 Hz trains. For all recording sites, tuning curves were rotated so that the preferred direction was oriented upward at 0° before averaging. Black curves show responses to the FD and grey curves show MD tuning curves. Left plots for each stimulus rate show relative response amplitudes, while right plots show normalized responses. C. Analysis and plots are the same as B, except that grey curves show tuning assessed during the SS for each stimulus train. The number of recordings per frequency are as follows: N = 70 for 8 Hz; N = 55 for 12 Hz. Error bars indicate SE for all figures.

A.

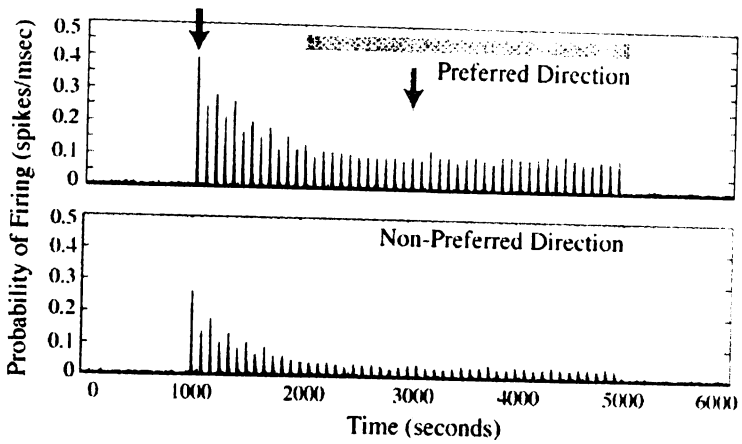
Probability of Firing (spikes/msec)
0.5
0.4
0.3
0.2
0.1
0
Preferred Direction
Non-Preferred Direction
0
1000
2000
3000
4000
5000
6000
Time (seconds)

B.

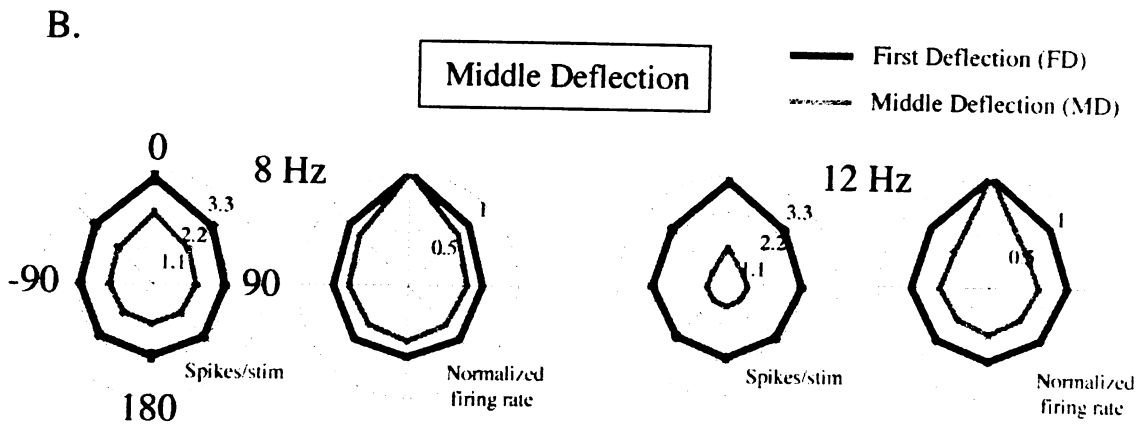
Middle Deflection
First Deflection (FD)
Middle Deflection (MD)
0
8 Hz
3.3
2.2
1.1
-90
90
180
Spikes/stim
1
0.5
Normalized firing rate
12 Hz
3.3
2.2
1.1
Spikes/stim
1
0.5
Normalized firing rate

C.

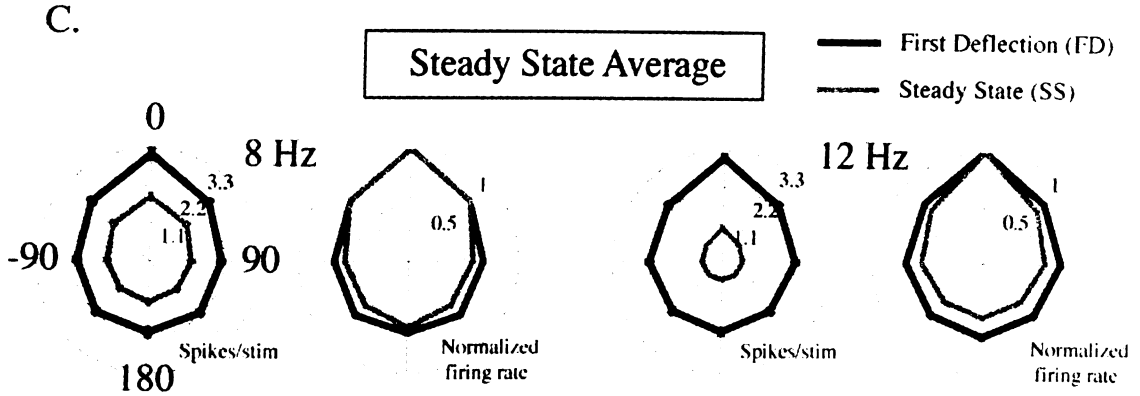
Steady State Average
First Deflection (FD)
Steady State (SS)
0
8 Hz
3.3
2.2
1.1
-90
90
180
Spikes/stim
1
0.5
Normalized firing rate
12 Hz
3.3
2.2
1.1
Spikes/stim
1
0.5
Normalized firing rate

Figure 6. Frequency-dependent changes in direction tuning for MU recordings. A. Direction tuning was assessed for the FD and MD of stimulus trains at 4, 8, 12, and 16 Hz. Mean tuning is plotted as a function of stimulus rate for tuning indices 1 and 2 (see Methods). B. Direction tuning was assessed for the FD and the SS for the same stimulus trains assessed in A. Mean tuning is plotted as a function of stimulus rate for the same direction tuning indices. black stars indicate significant differences in tuning values compared with the FD for all plots (T-test, $p<0.05$). The number of recordings per frequency are as follows: N = 69 for 4 Hz; N = 70 for 8 Hz; N = 55 for 12 Hz; N = 54 for 16 Hz.

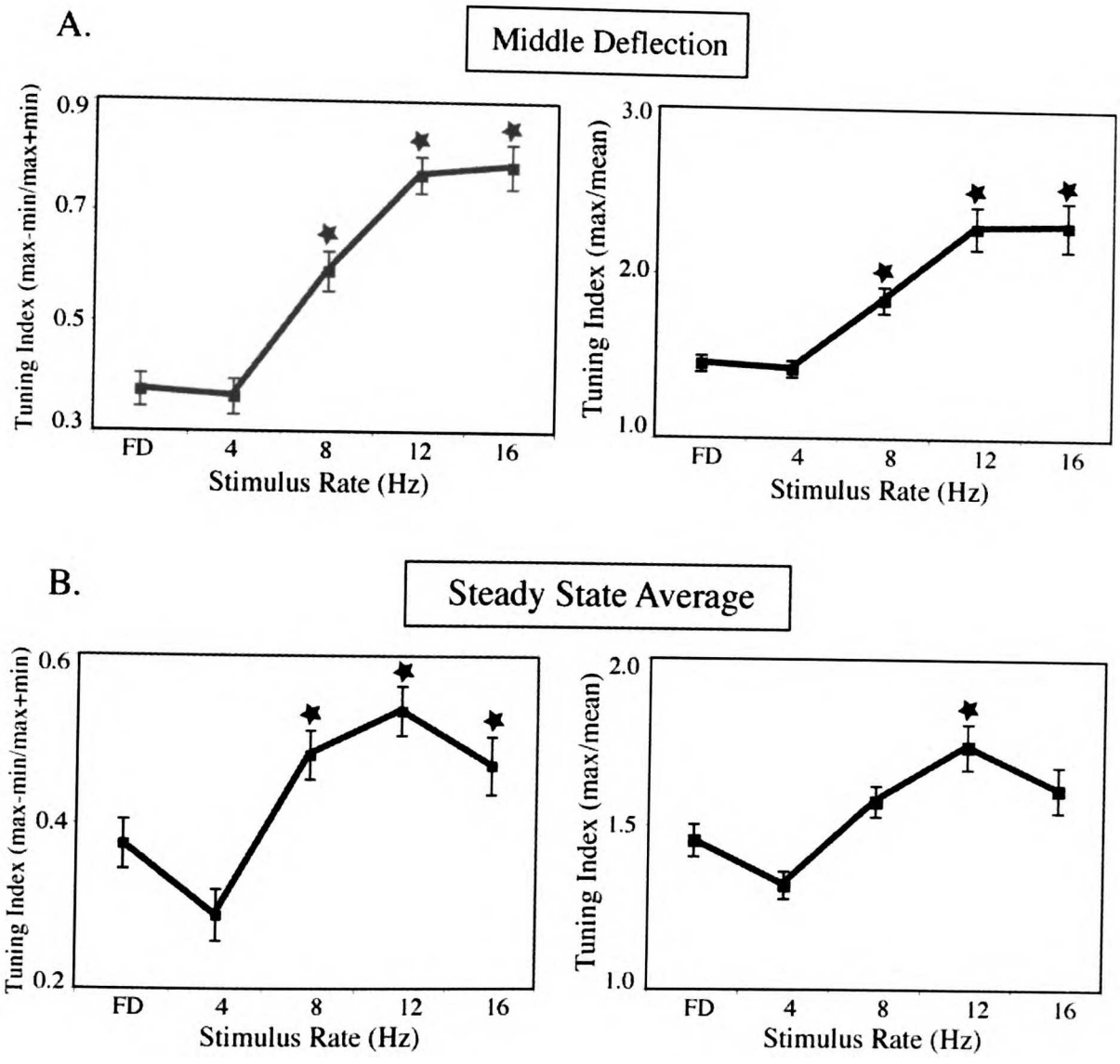
A.
Middle Deflection
Tuning Index (max-min/max+min)
0.9
0.7
0.5
0.3
FD
4
8
12
16
Stimulus Rate (Hz)
Tuning Index (max/mean)
3.0
2.0
1.0
FD
4
8
12
16
Stimulus Rate (Hz)
B.
Steady State Average
Tuning Index (max-min/max+min)
0.6
0.4
0.2
FD
4
8
12
16
Stimulus Rate (Hz)
Tuning Index (max/mean)
2.0
1.5
1.0
FD
4
8
12
16
Stimulus Rate (Hz)

Figure 7. Mean single unit tuning curves. A. Mean direction tuning curves for RSUs and FSUs in response to the FD and MD of 8 and 12 Hz trains. For each recording site, tuning curves were rotated so that the preferred direction was oriented upward before averaging all tuning curves. For each stimulus type, left plots show response amplitudes, and right plots show normalized tuning curves. B. Analysis and plots are the same as B, except that grey curves show tuning assessed during the SS for each stimulus train. Number of recordings sites are as follows: N = 70 for 8 Hz; N = 55 for 12 Hz.

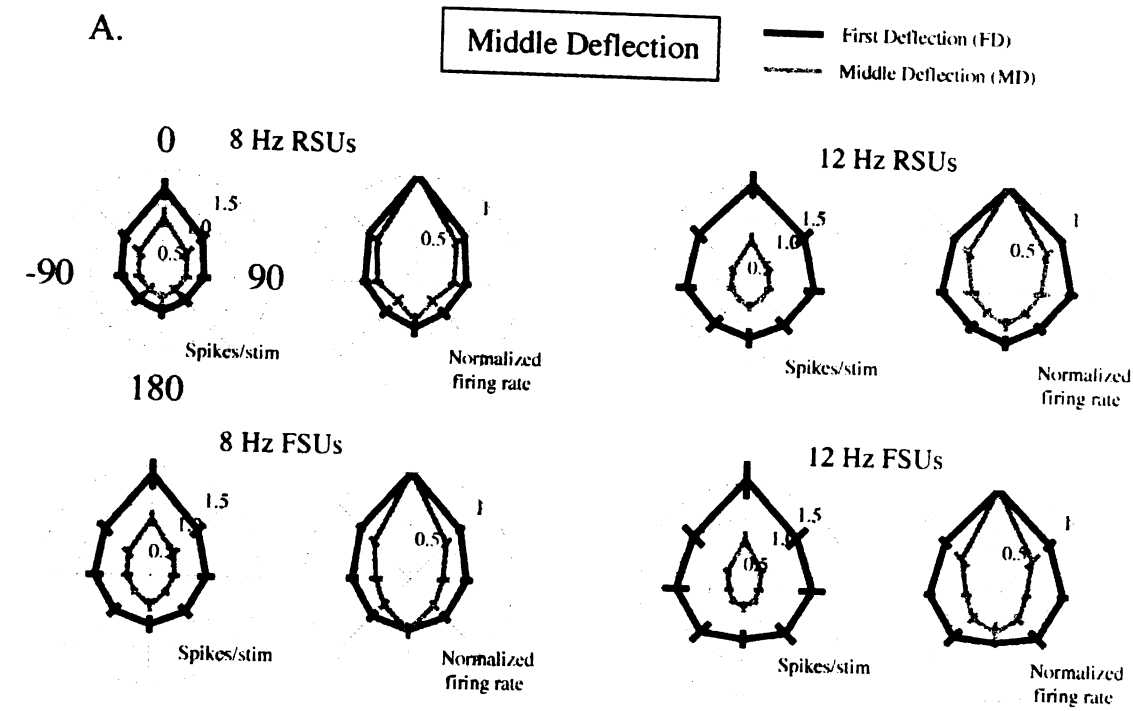
A.
Middle Deflection
First Deflection (FD)
Middle Deflection (MD)
0
8 Hz RSUs
-90
90
180
1.5
1.0
0.5
Spikes/stim
1
0.5
Normalized firing rate
12 Hz RSUs
Spikes/stim
Normalized firing rate
8 Hz FSUs
Spikes/stim
Normalized firing rate
12 Hz FSUs
Spikes/stim
Normalized firing rate

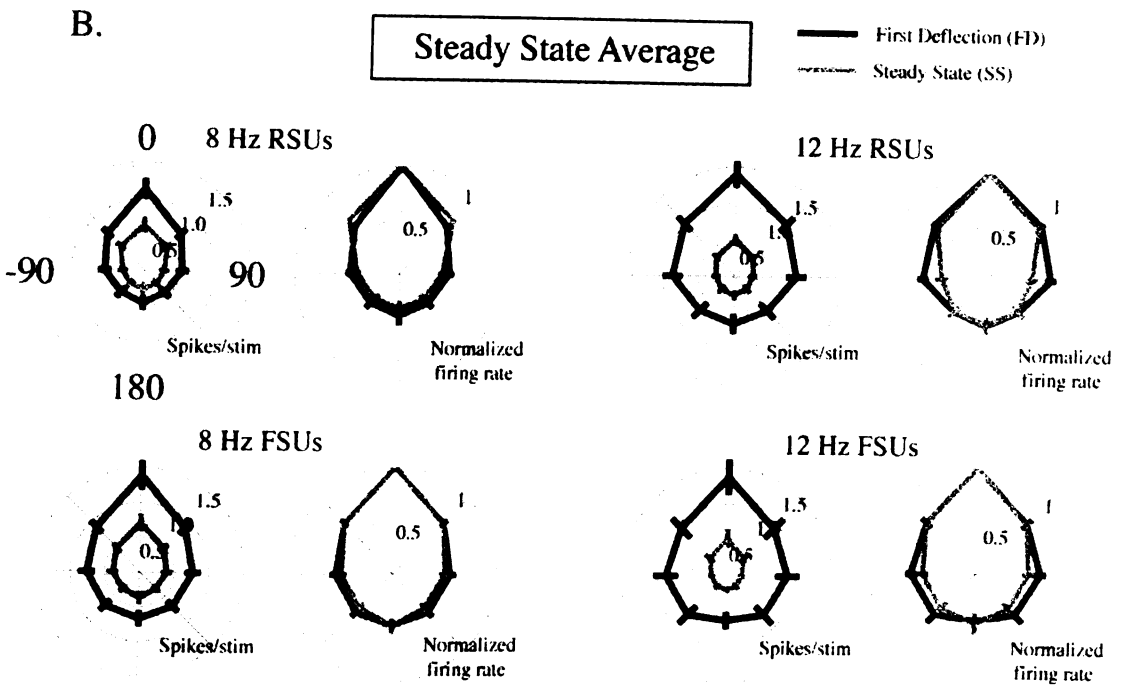
B.
Steady State Average
First Deflection (FD)
Steady State (SS)
0
8 Hz RSUs
-90
90
180
1.5
1.0
0.5
Spikes/stim
1
0.5
Normalized firing rate
12 Hz RSUs
Spikes/stim
Normalized firing rate
8 Hz FSUs
Spikes/stim
Normalized firing rate
12 Hz FSUs
Spikes/stim
Normalized firing rate

Figure 8. Frequency-dependent changes in direction tuning for single units. A. Direction tuning was assessed for the FD and MD of stimulus trains at 8 and 12 Hz. Mean tuning is plotted as a function of stimulus rate for tuning indices 1 and 2 (see Methods). RSU data is shown in black, FSU data in grey. B. Direction tuning was assessed for the FD and the SS for the same stimulus trains assessed in A. The black and grey stars indicate significant differences in tuning values compared with the FD for RSUs and FSUs respectively for all plots (T-test, $p<0.05$). The number of recordings are as follows: RSUs: N= 15 for 8 Hz; N = 16 for 12 Hz; FSUs: N = 16 for 8 Hz; N = 9 for 12 Hz.

A.

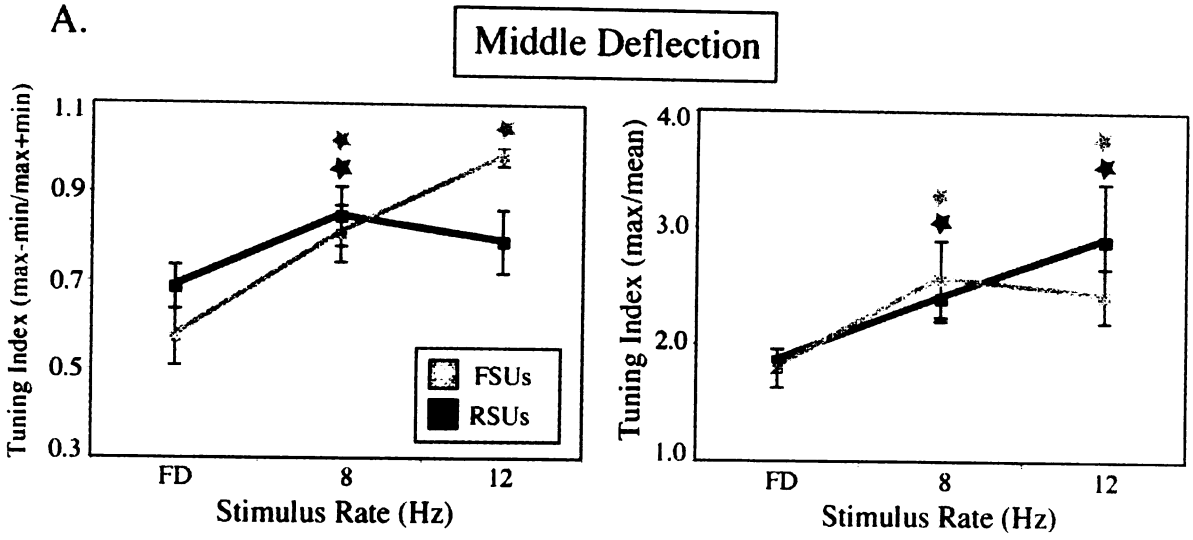
Middle Deflection
Tuning Index (max-min/max+min)
1.1
0.9
0.7
0.5
0.3
FD
8
12
Stimulus Rate (Hz)
FSUs
RSUs
Tuning Index (max/mean)
4.0
3.0
2.0
1.0
FD
8
12
Stimulus Rate (Hz)

B.

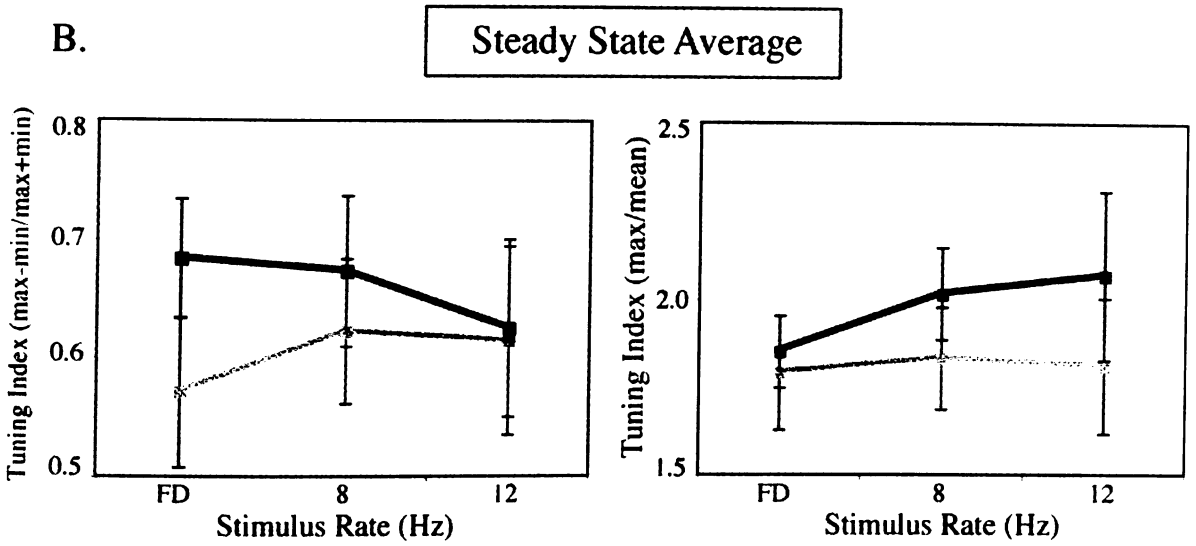
Steady State Average
Tuning Index (max-min/max+min)
0.8
0.7
0.6
0.5
FD
8
12
Stimulus Rate (Hz)
Tuning Index (max/mean)
2.5
2.0
1.5
FD
8
12
Stimulus Rate (Hz)

Table 1. Summary of mean direction-tuning values for all recordings. Two direction-tuning indices were used to evaluate the mean tuning of MUs, RSUs, and FSUs to stimuli in 8 directions (see Methods). Tuning values for the FD, MD, and SS periods (Steady State #1) are shown for each type of recording and tuning metric. In addition, tuning values assessed for a second steady state period (Steady State #2), defined as the time from 2-4 seconds after stimulus onset, are shown (see Results section for Figure 9). Values in bold print indicate a significant difference in tuning from FD values (t-test, $p \leq 0.05$). Numbers of recordings are as follows: MUs: N = 70 for FD; N = 70 for 8 Hz; N = 55 for 12 Hz; RSUs: N = 16 for FD; N= 15 for 8 Hz; N = 16 for 12 Hz; FSUs: N=16 for FD; N = 16 for 8 Hz; N = 9 for 12 Hz.

Table 1.	Recording Type	First Deflection	Middle Deflection		Steady State #1		Steady State #2	
			8 Hz	12 Hz	8 Hz	12 Hz	8 Hz	12 Hz
Tuning Index 1: (Rmax-Rmin) (Rmax+Rmin)	**MUs**	0.374	**0.590**	**0.7669**	**0.481**	**0.534**	**0.51**	**0.58**
	RSUs	0.684	**0.845**	0.7890	0.673	0.625	0.73	0.69
	FSUs	0.571	**0.805**	**0.9808**	0.622	0.614	0.70	0.70
Tuning Index 2: Rmax /Rmean	**MUs**	1.450	**1.840**	**2.2824**	1.570	**1.737**	**1.625**	**1.81**
	RSUs	1.850	**2.394**	**2.8930**	2.015	2.067	2.26	**2.57**
	FSUs	1.790	**2.559**	**2.4202**	1.831	1.809	1.99	2.06

Figure 9. Temporal development of direction tuning. A. Direction tuning was assessed and plotted for each deflection during stimulus trains for MUs, RSUs, and FSUs. A. Tuning assessed by Tuning Index #1. B. Tuning assessed by Tuning Index #2. MUs is shown in black, RSUs in dark grey, and FSUs in light grey. Numbers of recordings are as follows: MUs: N = 70 for 8 Hz; N = 55 for 12 Hz; RSUs: N= 15 for 8 Hz; N = 16 for 12 Hz; FSUs: N = 16 for 8 Hz; N = 9 for 12 Hz.

A.

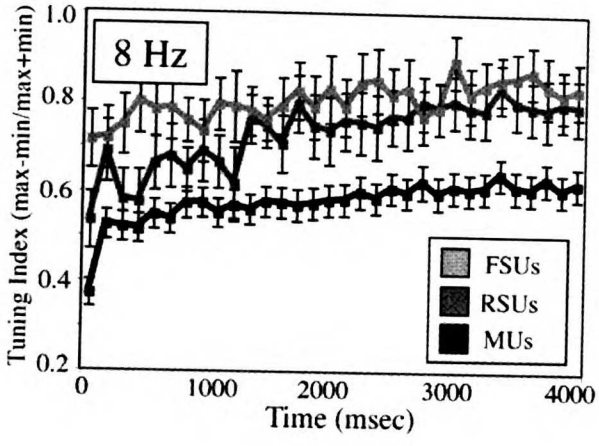
8 Hz
Tuning Index (max-min/max+min)
1.0
0.8
0.6
0.4
0.2
0
1000
2000
3000
4000
Time (msec)
FSUs
RSUs
MUs

B.

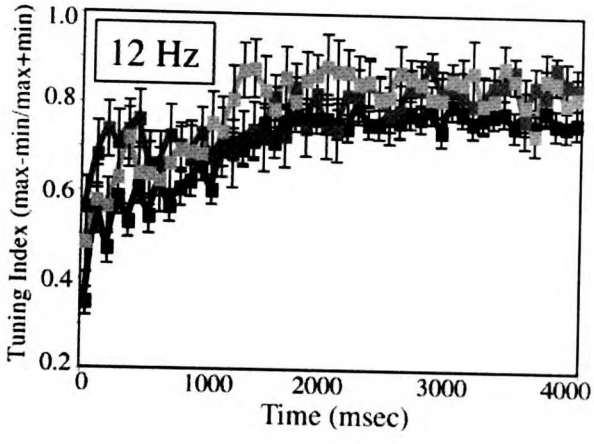
12 Hz
Tuning Index (max-min/max+min)
1.0
0.8
0.6
0.4
0.2
0
1000
2000
3000
4000
Time (msec)

C.

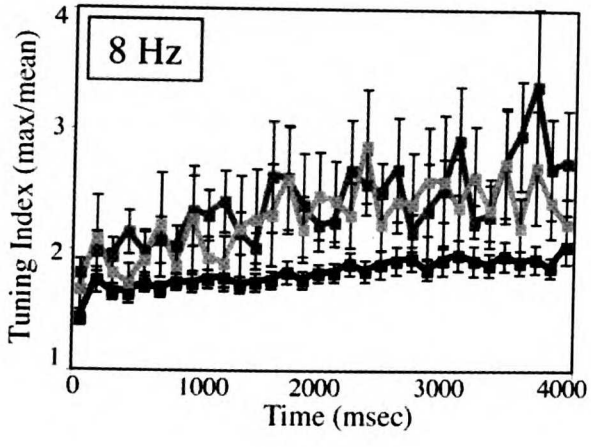
8 Hz
Tuning Index (max/mean)
4
3
2
1
0
1000
2000
3000
4000
Time (msec)

D.

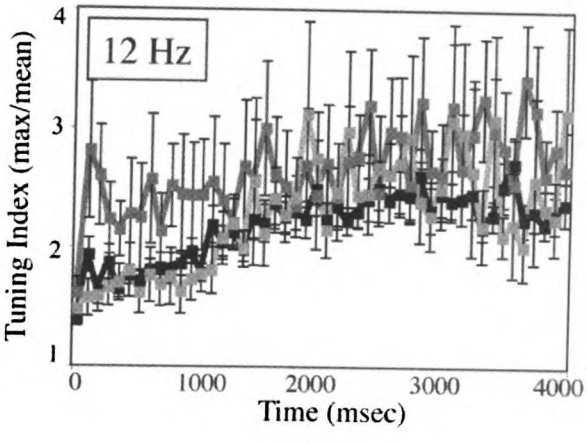
12 Hz
Tuning Index (max/mean)
4
3
2
1
0
1000
2000
3000
4000
Time (msec)

Figure 10. Consistency of direction tuning during stimulus trains. A. The angular position of the preferred direction during the MD relative to the position of the preferred direction for the FD is summarized for all recordings in a histogram. The preferred direction assessed for the FD was defined as 0° for all recordings. Data from 8 Hz trains are shown on the left, and data from 12 Hz trains on the right. MUs are shown in black, RSUs in grey, and FSUs in white. B. Same as in A, but showing the relative position of preferred directions for the SS compared to the FD. Numbers of recordings are as follows: MUs: N = 70 for 8 Hz; N = 55 for 12 Hz; RSUs: N= 15 for 8 Hz; N = 16 for 12 Hz; FSUs: N = 16 for 8 Hz; N = 9 for 12 Hz.

Middle Deflection

A.

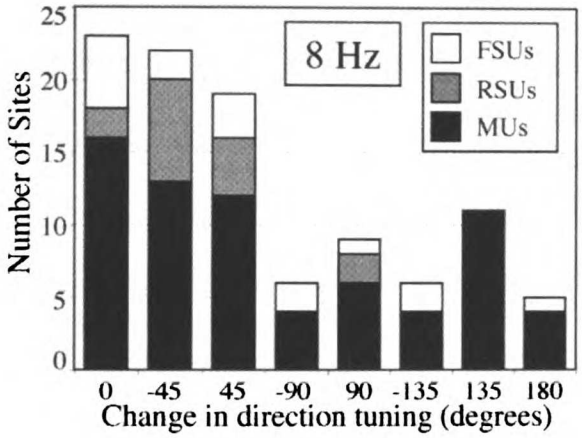

B.

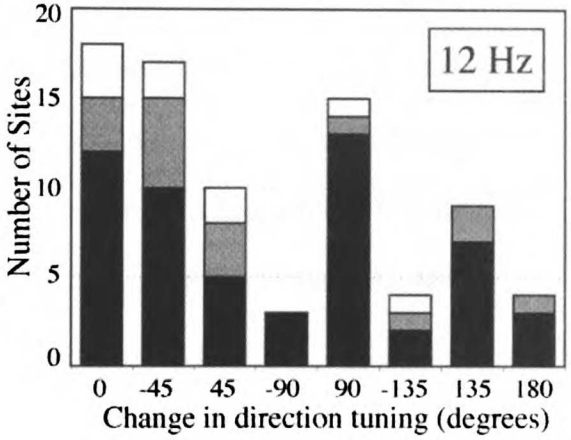

Steady State Average

C.

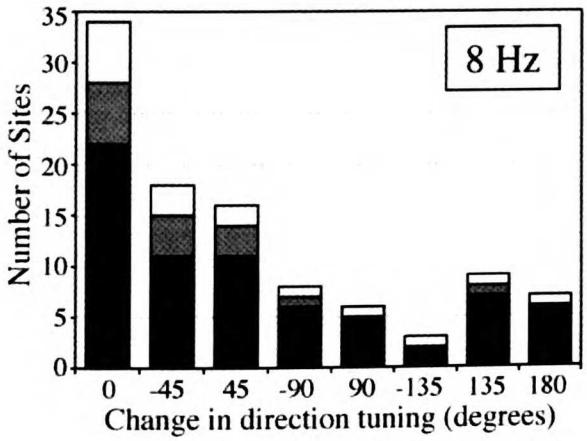

D.

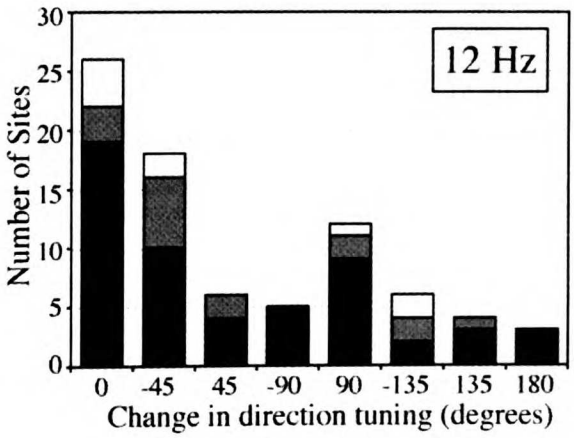

Figure 11. Relative positions of the preferred and non-preferred directions during stimulus trains. A. Figure 4B is re-plotted, showing the relative positions of the preferred and non-preferred directions (minima) for the FD in MU, RSU, and FSU recordings. B. Histograms showing the distribution of relative minima positions for the MD during 8 Hz and 12 Hz stimulus trains. C. The distribution of minima positions for the SS for 8 and 12 Hz trains. The numbers of recordings are as follows: MUs: N = 70 for FD; N = 70 for 8 Hz; N = 55 for 12 Hz; RSUs: N = 16 for FD; N= 15 for 8 Hz; N = 16 for 12 Hz; FSUs: N=16 for FD; N = 16 for 8 Hz; N = 9 for 12 Hz.

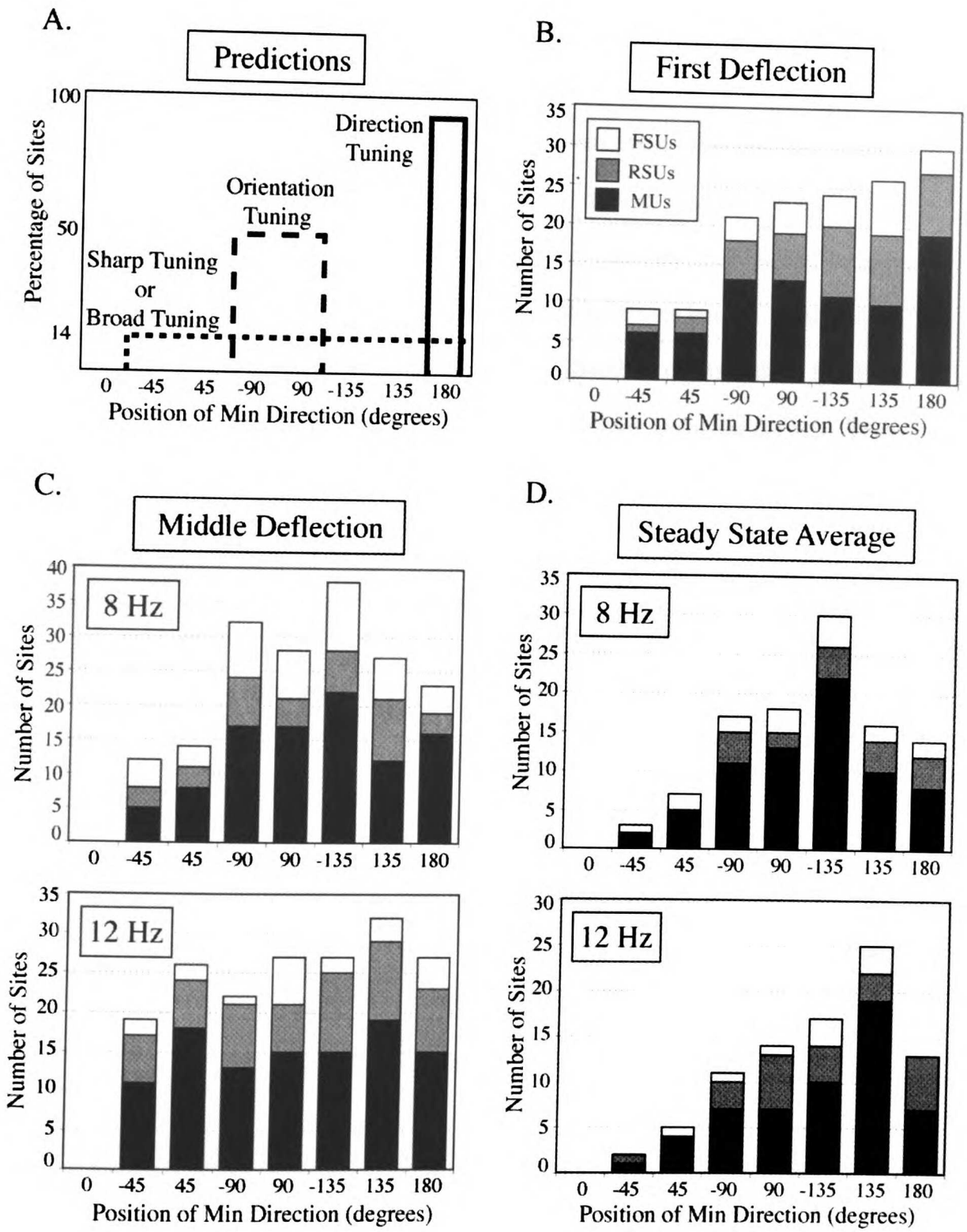
A.
Predictions
100
50
14
Percentage of Sites
Direction Tuning
Orientation Tuning
Sharp Tuning or Broad Tuning
0 -45 45 -90 90 -135 135 180
Position of Min Direction (degrees)
B.
First Deflection
FSUs
RSUs
MUs
Number of Sites
0 -45 45 -90 90 -135 135 180
Position of Min Direction (degrees)
C.
Middle Deflection
8 Hz
12 Hz
Number of Sites
0 -45 45 -90 90 -135 135 180
Position of Min Direction (degrees)
D.
Steady State Average
8 Hz
12 Hz
Number of Sites
0 -45 45 -90 90 -135 135 180
Position of Min Direction (degrees)

Figure 12. An example of an RSU showing direction-specific adaptation. A. The top PSTH shows the response of a single RSU to a 4-second train of vibrissa deflections in the dorsal direction. The bottom PSTH shows the response of the same unit to a train of vibrissa deflections that starts in the dorsal direction and changes to the rostral direction at 3000 msec. Black arrows indicate the onset of the stimulus train (the FD), and the grey arrow shows the time of the MD. PSTHs are based on 2 msec time bins. B. Direction tuning curves for the same neuron shown in A for four directions of adaptation. Black curves show the tuning curves for the FD and grey curves show tuning for the MD. The direction of adaptation for grey curves is indicated and by black arrows on each plot.

A.

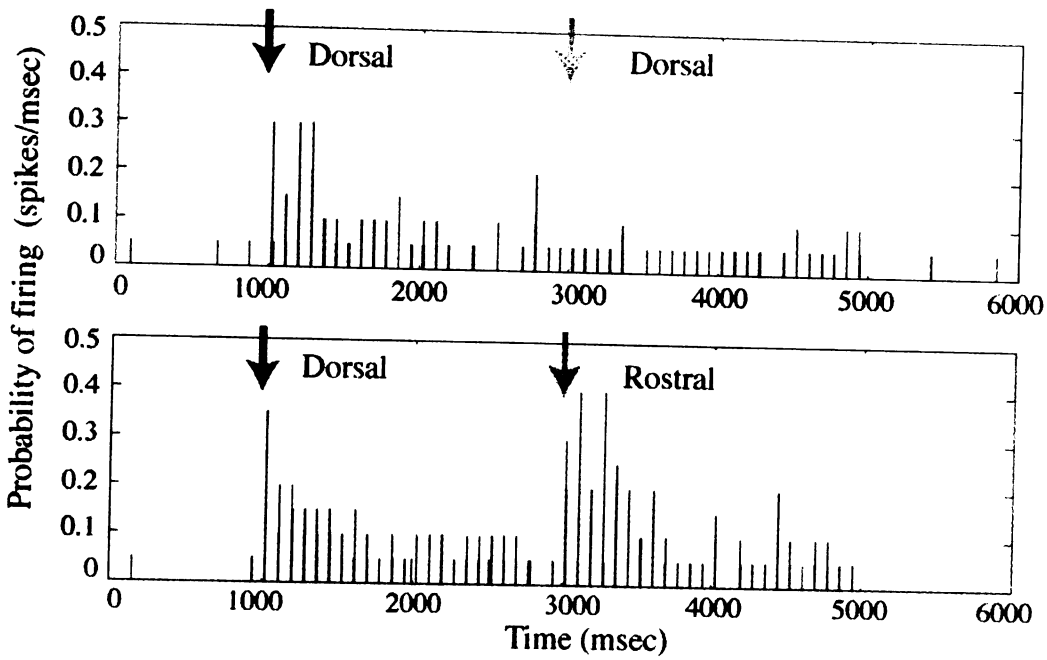
Probability of firing (spikes/msec)
0.5
0.4
0.3
0.2
0.1
0
Dorsal
Dorsal
0
1000
2000
3000
4000
5000
6000
Dorsal
Rostral
Time (msec)

B.

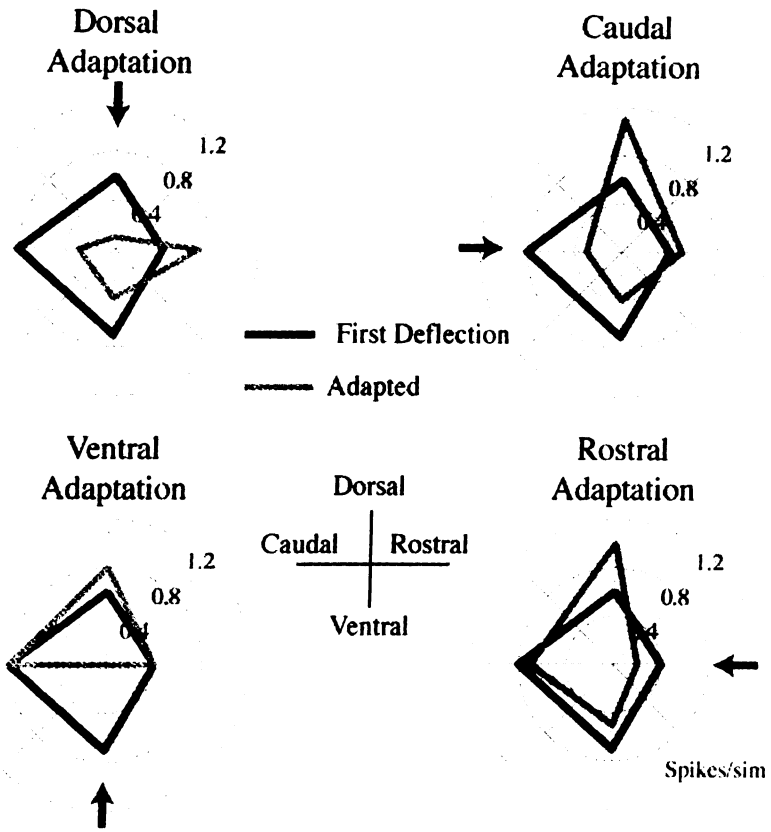
Dorsal Adaptation
Caudal Adaptation
1.2
0.8
First Deflection
Adapted
Ventral Adaptation
Rostral Adaptation
Dorsal
Caudal
Rostral
Ventral
Spikes/sim

Figure 13. Mean tuning curves reveal direction-specific adaptation. A. The top PSTH shows the average response of all multi-unit recordings to a 12 Hz train of vibrissa deflections in the rostral direction. The bottom PSTH shows the average response to a train of vibrissa deflections that starts in the rostral direction and changes to the dorsal direction at the time of the MD. Black arrows indicate the onset of the stimulus train and the grey arrows indicate the time of the MD. PSTHs are based on 5 msec time bins. B. Direction tuning curves show the mean responses of multi-unit and single unit recordings to trains of stimuli at 8 and 12 Hz. For each adaptation condition, tuning curves for single recording sites were rotated so that the direction of adaptation oriented upward at 0^{o} on the plots. Black curves show responses to the FD of stimulus trains and grey curves show responses to the MD. MU responses are plotted in the left column, RSU responses in the middle column, and FSU responses in the right column. Numbers of recordings are as follows: MUs: N = 69 for 8 Hz; N = 48 for 12 Hz; RSUs: N =14 for 8 Hz; N = 17 for 12 Hz; FSUs: N = 16 for 8 Hz; N = 9 for 12 Hz.

A.

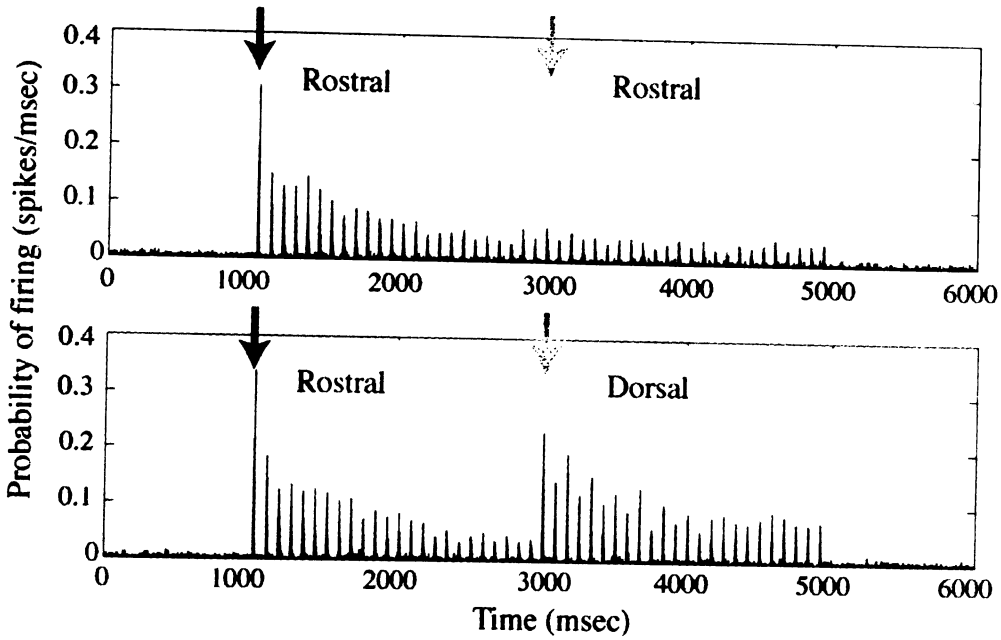
Probability of firing (spikes/msec)
0.4
0.3
0.2
0.1
0
Rostral
Rostral
0
1000
2000
3000
4000
5000
6000
Rostral
Dorsal
Time (msec)

B.

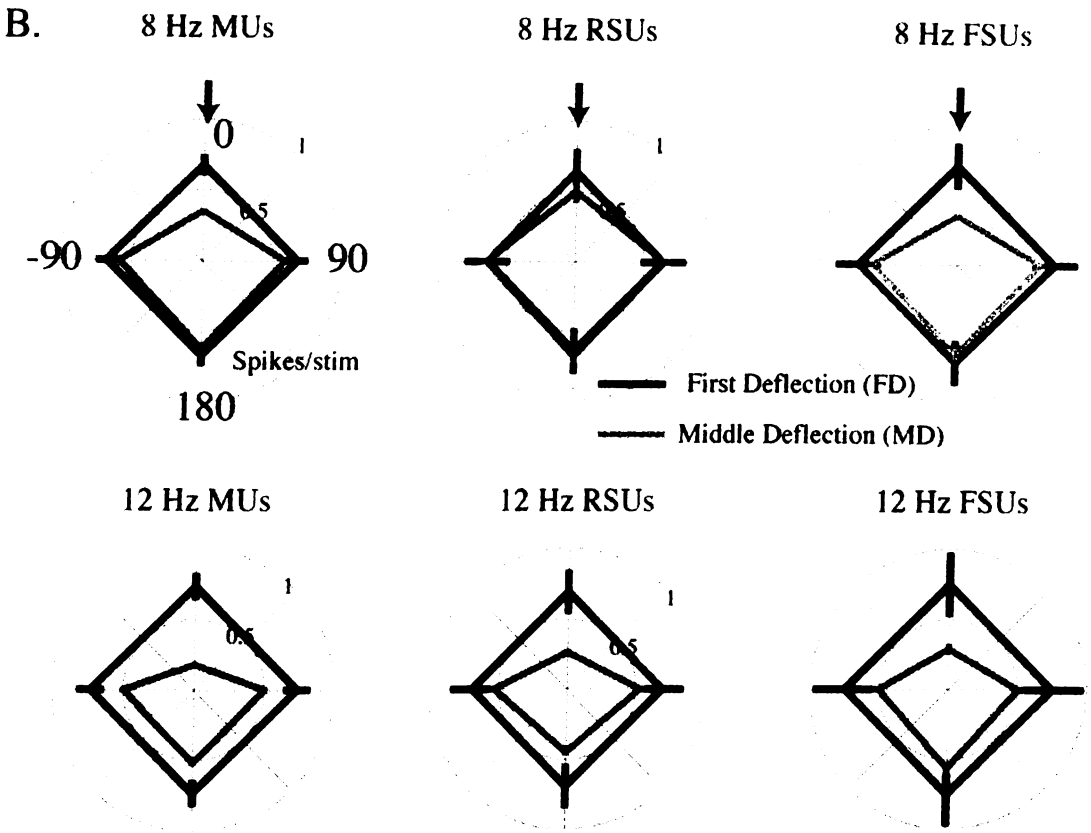
8 Hz MUs
8 Hz RSUs
8 Hz FSUs
0
-90
90
180
Spikes/stim
First Deflection (FD)
Middle Deflection (MD)
12 Hz MUs
12 Hz RSUs
12 Hz FSUs

Figure 14. Adaptation in the preferred and non-preferred directions. A,B. The responses of all multi-unit sites were rotated so that the direction that showed the preferred (A) or non-preferred (B) responses to the FD of trains at 8 or 12 Hz were oriented upward at 0°. Black curves show responses to the FD and grey curves show responses to the MD; In the top panel, tuning curves for the MD after adaptation in the preferred direction are shown, and in the bottom panel tuning curves for the MD after adaptation in the non-preferred direction are shown. MU responses are plotted in the left column, RSU responses in the middle column, and FSU responses in the right column. Numbers of recordings are as follows: MUs: N = 69 for 8 Hz; N = 48 for 12 Hz; RSUs: N =14 for 8 Hz; N = 17 for 12 Hz; FSUs: N = 16 for 8 Hz; N = 9 for 12 Hz.

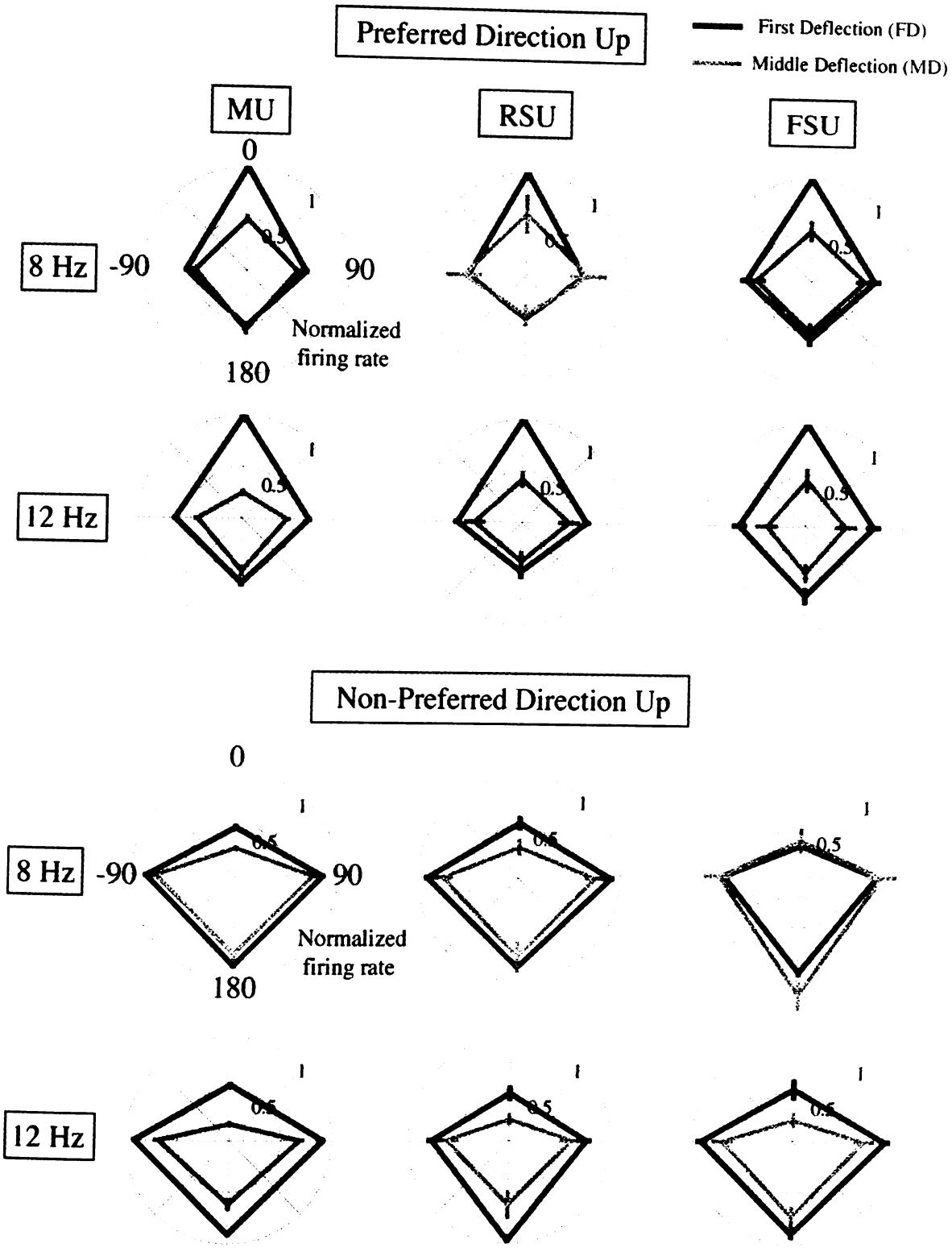
Preferred Direction Up
First Deflection (FD)
Middle Deflection (MD)
MU
RSU
FSU
0
8 Hz
-90
90
180
Normalized
firing rate
12 Hz
1
0.5
Non-Preferred Direction Up
0
8 Hz
-90
90
180
Normalized
firing rate
12 Hz
1
0.5

Figure 15. Shifts in preferred directions after adaptation in preferred and non-preferred directions. For each recording, the angular change in the preferred direction from the FD to the MD was quantified. The preferred direction of the FD response was defined as 0° for each recording, and the preferred direction of MD responses relative to this are shown in histograms. A. Shifts in the preferred direction for MUs, RSUs, and FSUs after adaptation in the preferred direction are shown for 8 and 12 Hz trains. Responses to 8 Hz trains are shown on the left, and responses to 12 Hz trains on the right. MU data is shown in black, RSUs in grey, and FSUs in white. B. Shifts in the preferred direction after adaptation in the *non*-preferred direction. Numbers of recordings are as follows: MUs: N = 69 for 8 Hz; N = 48 for 12 Hz; RSUs: N =14 for 8 Hz; N = 17 for 12 Hz; FSUs: N = 16 for 8 Hz; N = 9 for 12 Hz.

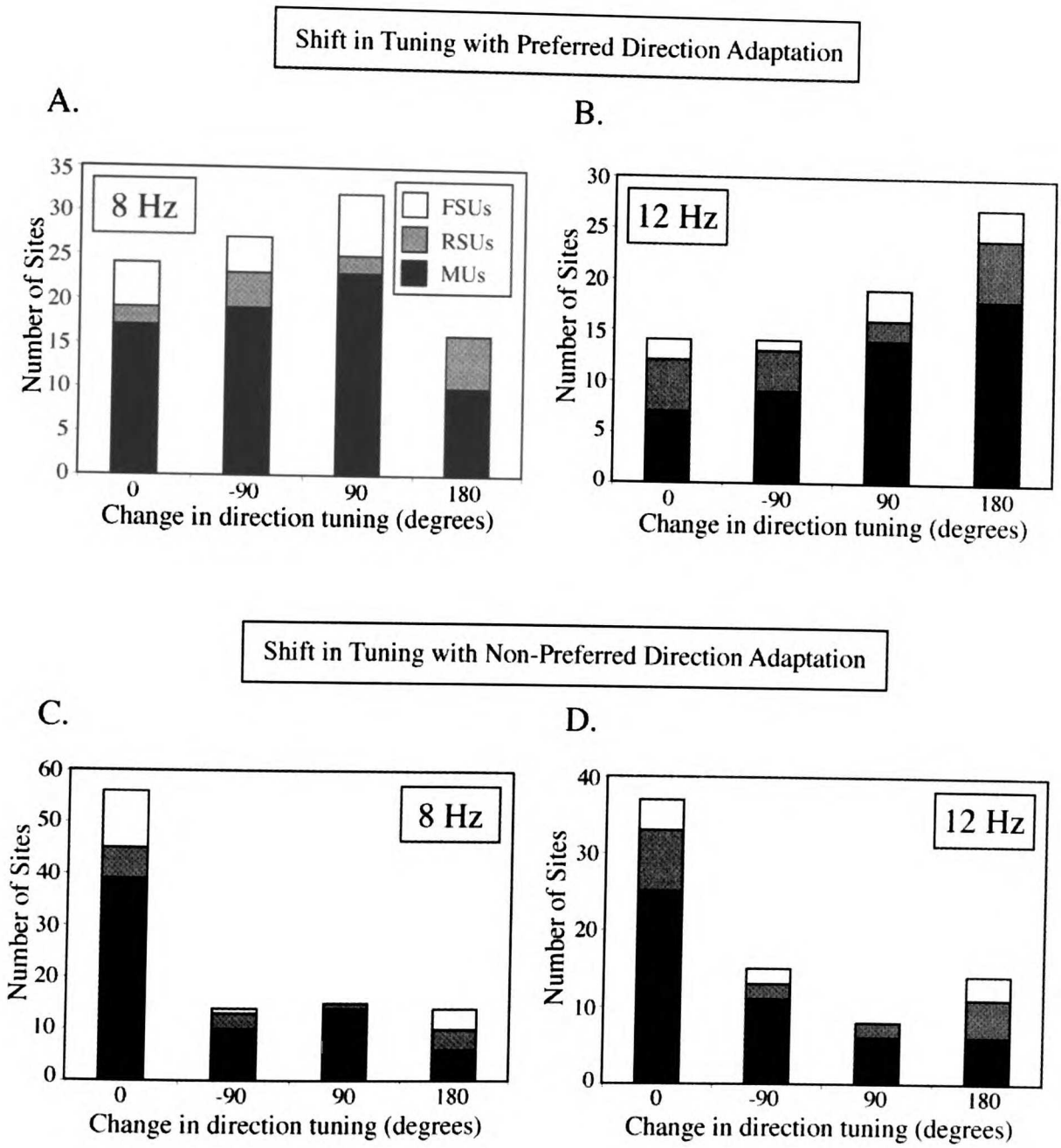
Shift in Tuning with Preferred Direction Adaptation
A.
B.
8 Hz
12 Hz
FSUs
RSUs
MUs
Number of Sites
Change in direction tuning (degrees)
0
-90
90
180
Shift in Tuning with Non-Preferred Direction Adaptation
C.
D.

Figure 16. Changes in mean direction-tuning values after adaptation in the preferred and non-preferred directions. For each recording, tuning was quantified with Tuning Index #1 and Tuning Index #2 for the FD response (before adaptation) and the MD response, after adaptation in preferred or non-preferred directions. A. Average tuning values of MUs, RSUs, and FSUs are plotted for FD, 8 Hz, and 12 Hz responses. MU data is shown in black, RSU in dark grey, and FSUs in light grey. Stars in corresponding colors indicate a significant difference in tuning for the MD compared with FD tuning. B. Same as A, expect that 8 and 12 Hz tuning values were quantified after adaptation in the non-preferred direction. Numbers of recordings are as follows: MUs: N = 69 for 8 Hz; N = 48 for 12 Hz; RSUs: N =14 for 8 Hz; N = 17 for 12 Hz; FSUs: N = 16 for 8 Hz; N = 9 for 12 Hz.

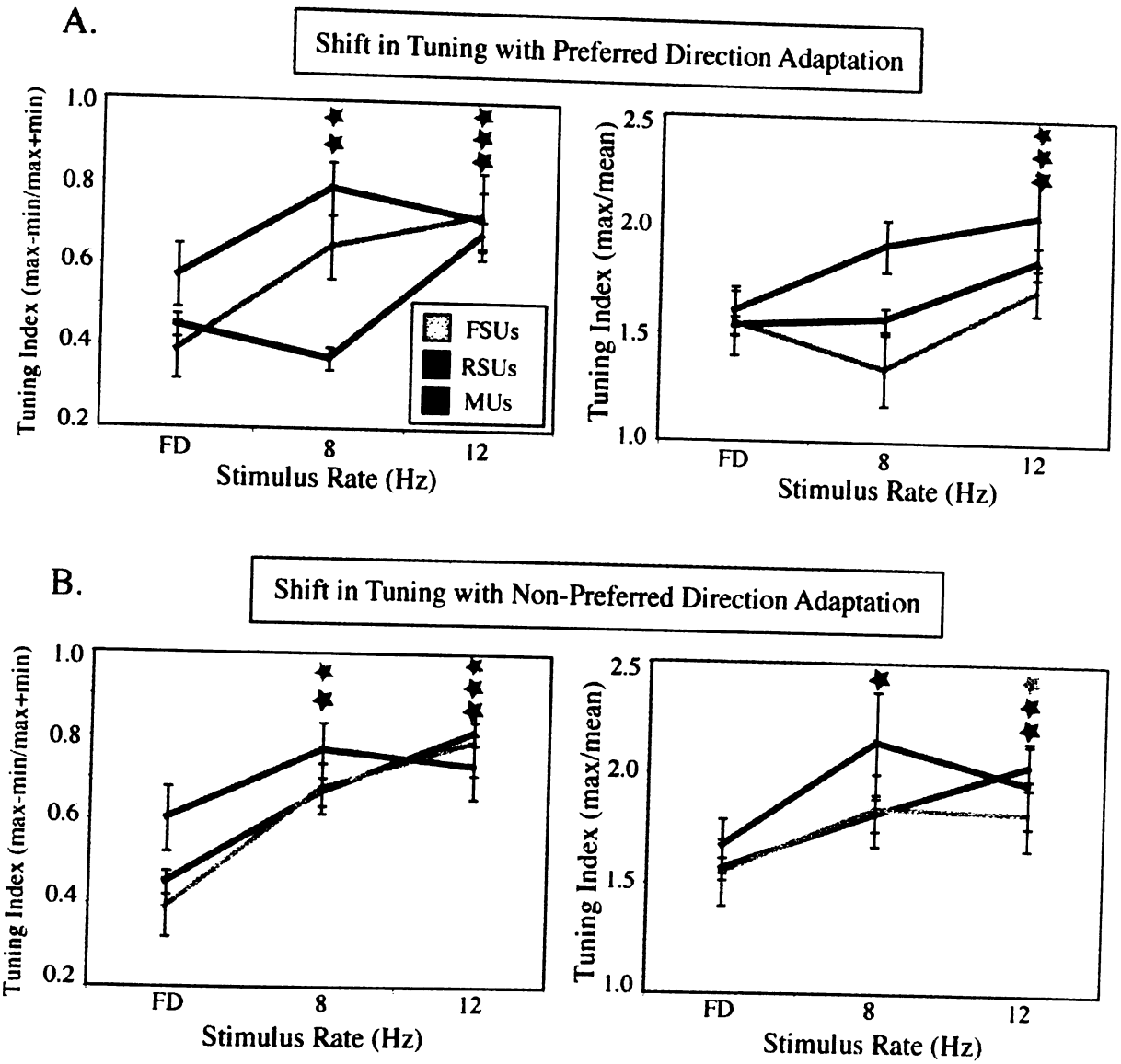
A.
Shift in Tuning with Preferred Direction Adaptation
Tuning Index (max-min/max+min)
1.0
0.8
0.6
0.4
0.2
FD
8
12
Stimulus Rate (Hz)
FSUs
RSUs
MUs
Tuning Index (max/mean)
2.5
2.0
1.5
1.0
FD
8
12
Stimulus Rate (Hz)
B.
Shift in Tuning with Non-Preferred Direction Adaptation
Tuning Index (max-min/max+min)
1.0
0.8
0.6
0.4
0.2
FD
8
12
Stimulus Rate (Hz)
Tuning Index (max/mean)
2.5
2.0
1.5
1.0
FD
8
12
Stimulus Rate (Hz)

Figure 17. Multi-unit population tuning curves. Population tuning curves for MU recordings in response to 8 Hz (A) and 12 Hz (B) stimulus trains. A. The left plots show population responses to the FD of 8 Hz trains. For each recording site, the response to test stimuli at 0° was quantified, and normalized to the maximal firing rate for that site. The preferred tuning of each recording site is indicated on the abscissa, and the normalized response is indicated on the ordinate. Plots on the right show responses to the FD in thin black lines, and responses to the MD in thick black lines. MD responses to a test stimulus at 0° were quantified after adaptation in the 0°, 90°, or 180° directions, indicated by black arrows. B. Each plot shows the same data as in A, calculated for 12 Hz trains. Numbers of recordings are as follows: MUs: N = 69 for 8 Hz; N = 48 for 12 Hz; RSUs: N =14 for 8 Hz; N = 17 for 12 Hz; FSUs: N = 16 for 8 Hz; N = 9 for 12 Hz.

A.

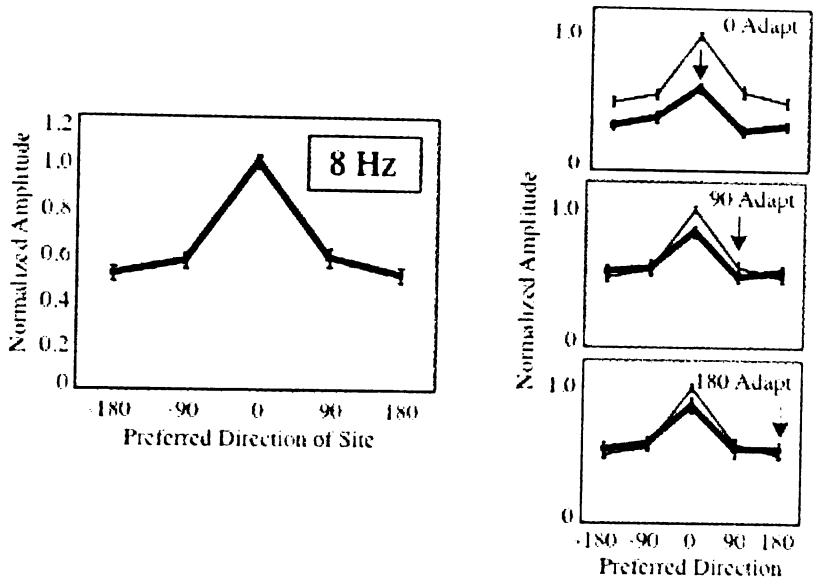
8 Hz
Normalized Amplitude
1.2
1.0
0.8
0.6
0.4
0.2
0
-180
-90
0
90
180
Preferred Direction of Site
0 Adapt
90 Adapt
180 Adapt
Normalized Amplitude
1.0
0
-180 -90 0 90 180
Preferred Direction

B.

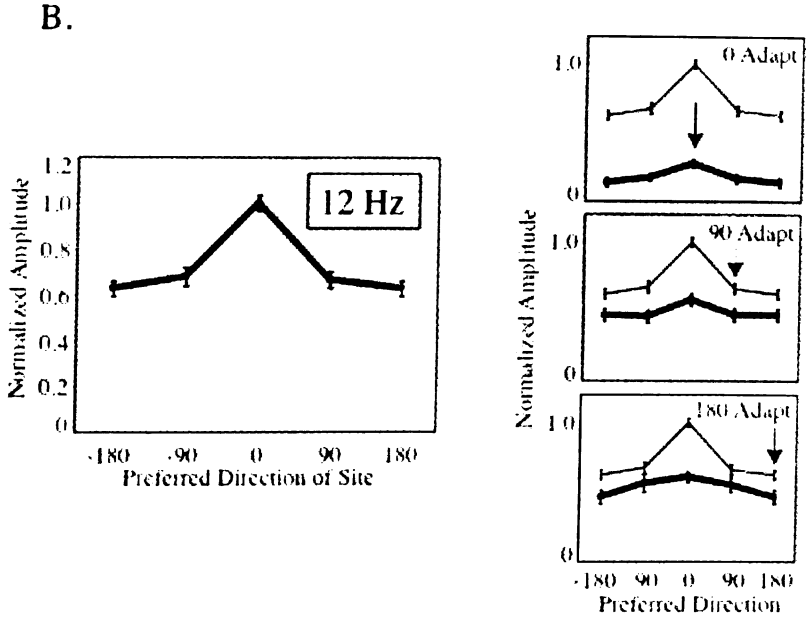
12 Hz
Normalized Amplitude
1.2
1.0
0.8
0.6
0.4
0.2
0
-180
-90
0
90
180
Preferred Direction of Site
0 Adapt
90 Adapt
180 Adapt
Normalized Amplitude
1.0
0
-180 90 0 90 180
Preferred Direction

Figure 18. Single units population tuning curves. Population tuning curves for RSU and FSU recordings in response to 8 Hz (A, C) and 12 Hz (B, D) stimulus trains. A. The left plots show population responses of RSUs to the FD of 8 Hz trains. For each recording site, the response to test stimuli at 0° was quantified, and normalized to the maximal firing rate for that site. The preferred tuning of each recording site is indicated on the abscissa, and the normalized response is indicated on the ordinate. Plots on the right show responses to the FD in thin black lines, and responses to the MD in thick black lines. MD responses to a test stimulus at 0° were quantified after adaptation in the 0°, 90°, or 180° directions, indicated by black arrows. B. Each plot shows the same data as in A, calculated for 12 Hz trains. C, D. Same plots as in A and B for FSU recordings. Numbers of recordings are as follows: MUs: N = 69 for 8 Hz; N = 48 for 12 Hz; RSUs: N =14 for 8 Hz; N = 17 for 12 Hz; FSUs: N = 16 for 8 Hz; N = 9 for 12 Hz.

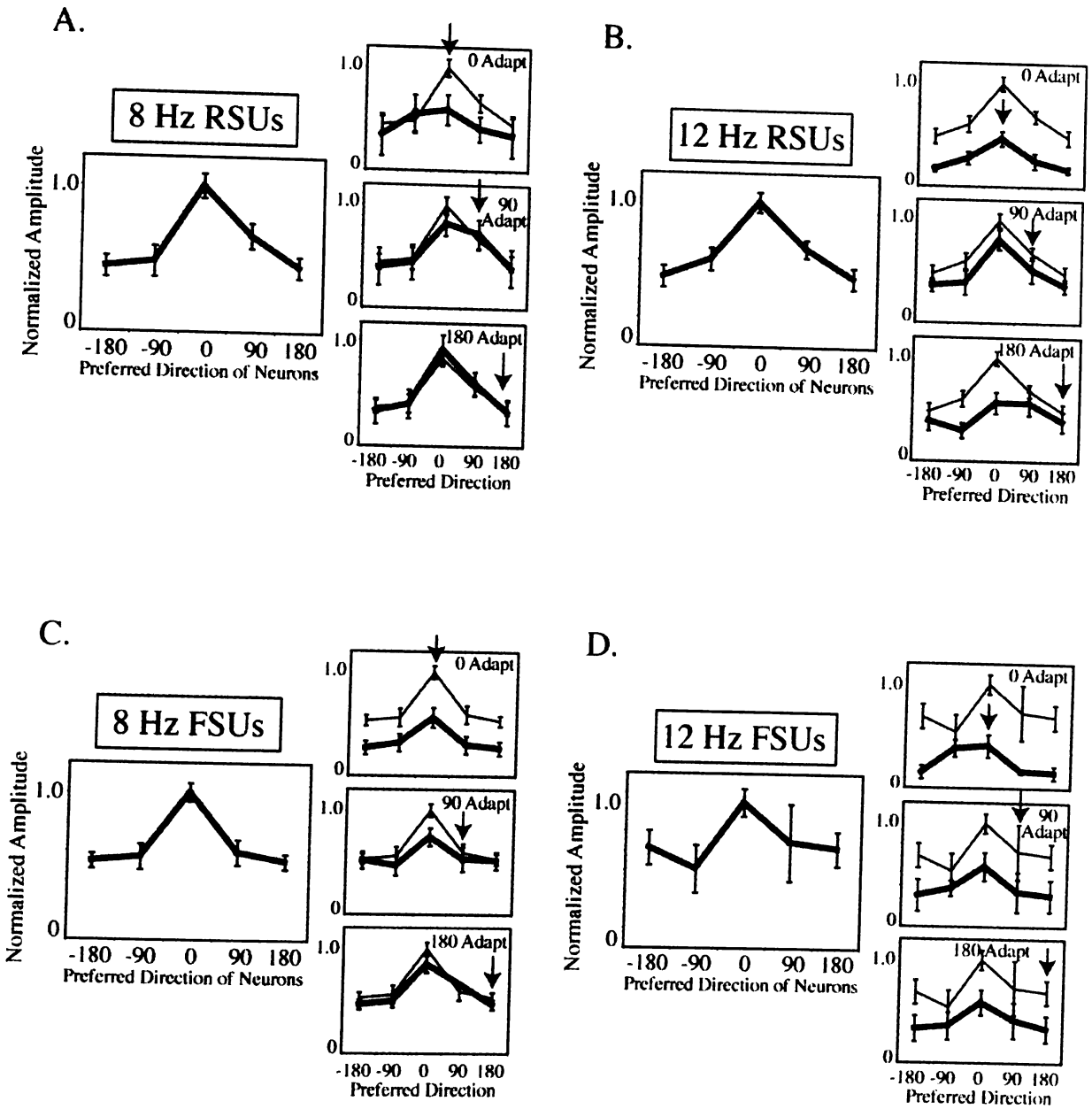
A.
8 Hz RSUs
Normalized Amplitude
1.0
0
-180 -90 0 90 180
Preferred Direction of Neurons
0 Adapt
90 Adapt
180 Adapt
-180 -90 0 90 180
Preferred Direction
B.
12 Hz RSUs
C.
8 Hz FSUs
D.
12 Hz FSUs

Figure 19. A hypothetical model of frequency-dependent changes in tuning evoked by whisking. A. Convergence of well tuned thalamic inputs result in broad tuning in a target cortical neuron. B. Whisking involves elliptical movement of the vibrissa along a rostro-caudal axis. C. A train of vibrissa deflections in two directions evokes three types of responses optimized for different perceptual functions. 1. Responses to the FD are robust, optimizing stimulus detection. 2. Trains of deflections in a single direction evoke low amplitude, sharply tuned responses, optimized for discrimination. 3. Responses to a novel direction in the context of repetitive stimulation are robust, optimizing detection of the novel stimulus.

A.

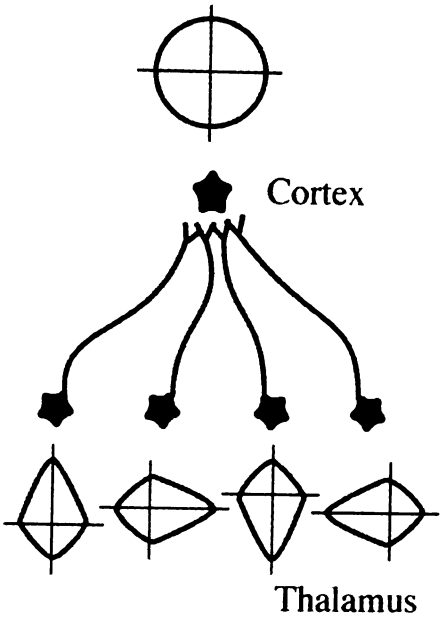
Cortex
Thalamus

B.

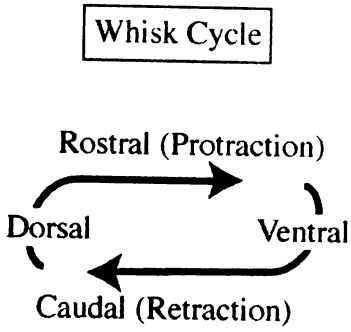
Whisk Cycle
Rostral (Protraction)
Dorsal
Ventral
Caudal (Retraction)

C.

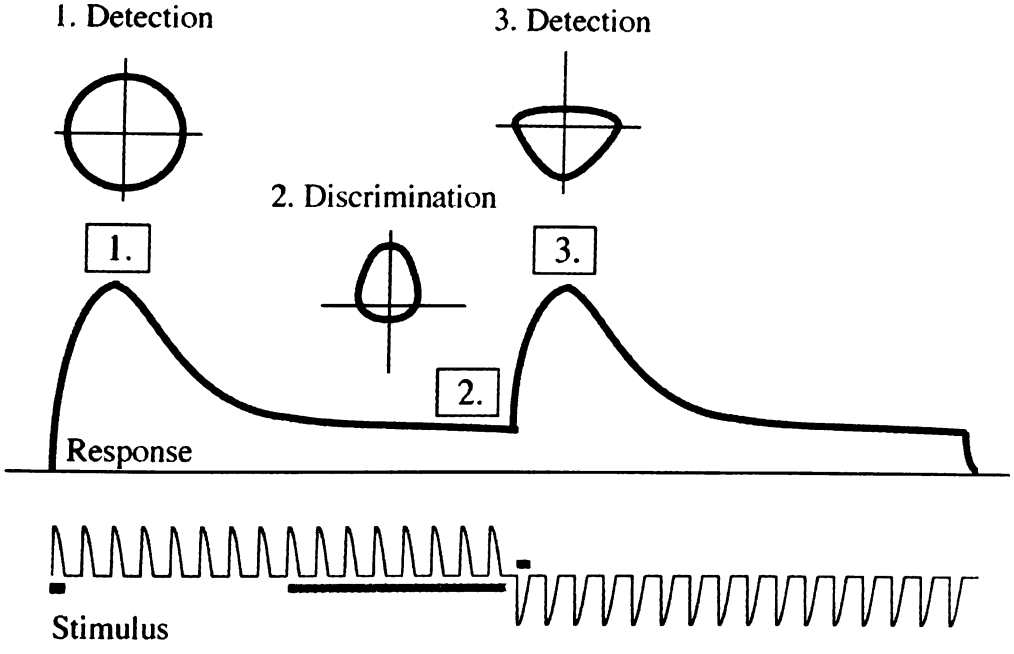
1. Detection
3. Detection
2. Discrimination
1.
2.
3.
Response
Stimulus

REFERENCES

Abbott, L.F., Varela, J.A., Sen, K., and Nelson, S.B. Synaptic depression and cortical gain control. *Science* 275(5297): 220-224, 1997.

Berg, R.N., and Kleinfeld, D. Rhythmic whisking by rat: retraction as well as protraction of the vibrissae is under active muscular control. *J. Neurophysiol.* 89: 104-117, 2003.

Brecht, M., Preilowski, B., and Merzenich M.M. Functional architecture of the mystacial vibrissae. Behav. *Brain Res.* 84: 81-97, 1997.

Brecht, M. and Sakmann, B. Dynamic representation of whisker deflection by synaptic potentials in spiny stellate and pyramidal cells in the barrels and septa of layer 4 rat somatosensory cortex. *J. Physiol.* 543(1): 49-70, 2002.

Brumberg, J.C., Pinto, D.J., and Simons, D.J. Spatial gradients and inhibitory summation in the rat whisker barrel system. *J. Neurophysiol.* 76: 130-140, 1996.

Bruno, R.M. and Simons, D.J. Feedforward mechanisms of excitatory and inhibitory cortical receptive fields. *J. Neurosci.* 22(24): 10966-10975, 2002.

Bruno, R.M., Khatri, V, and Simons, D.J. Thalamocortical angular tuning domains within individual barrels of rat somatosensory cortex. *J. Neurosci.* 23(29): 9565-9574, 2003.

Carvell, G.E. and Simons, D.J. Biometric analyses of vibrissal tactile discrimination in the rat. *J. Neurosci.* 10: 2638-2648, 1990.

Carvell, G.E. and Simons, D.J. Task- and subject-related differences in sensorimotor behavior during active touch. *Somatosens. Mot. Res.* 12: 1-9, 1995.

Castro-Alamancos, M.A. Properties of primary sensory (lemniscal) synapses in the ventrobasal thalamus and the relay of high-frequency sensory inputs. *J. Neurophysiol.* 87: 946-953, 2001.

Castro-Alamancos, M.A. and Oldford, E. Cortical sensory suppression during arousal is due to the activity-dependent depression of thalamocortical synapses. *J. Physiol.* 541: 319-331, 2002.

Chung, S., Li, X., and Nelson, S.B. Short-term depression at thalamocortical synapses contributes to rapid adaptation of cortical sensory responses *in vivo*. *Neuron* 34: 437-446, 2002.

Minnery, B.S. Proceedings of the Barrels II Workshop; Thalamocortical/corticothalamoic loops. *Somatosens. Mot. Res.* 20(3-4): 291-295, 2003.

Dragoi, V., Sharma, J., and Sur, M. Adaptation-induced plasticity of orientation tuning in adult visual cortex. *Neuron* 28: 287-298, 2000.

Felson, G., Shen, Y., Yao, H., Spor, G., Li, C., and Dan, Y. Dynamic modification of cortical orientation tuning mediated by recurrent connections. *Neuron* 36: 945-954, 2002.

Ferster, D. and Miller, K.D. Neural mechanisms of orientation selectivity in the visual cortex. *Annu. Rev. Neurosci.* 23: 441-471, 2000.

Gao, P., Bermejo, R., and Zeigler, H.P. Whisker deafferentation and rodent whisking patterns: behavioral evidence for a central pattern generator. *J. Neurosci.* 21: 5374-5380, 2001

Garabedian, C.E., Jones, S.R., Merzenich, M.M., Dale, A., and Moore, C.I. Band-pass response properties of rat SI neurons. *J. Neurophysiol.* 90:1379-1391, 2003.

Giaschi, D., Douglas, R., Marlin, S., and Cynader, M. The time course of direction selective adaptation in simple and complex cells in cat striate cortex. *J. Neurophysiol.* 70: 2024-2034, 1993.

Gupta, A., Wang, Y., and Markram, H. Organizing principles for a diversity of GABAergic interneurons and synapses in the neocortex. *Science* 287(5451): 273-278, 2000.

Hammond, P., Mouat, G.S., and Smith, A.T. Motion after-effects in cat striate cortex elicited by moving gratings. *Exp. Brain. Res.* 60: 411-416, 1985.

Hartings, J.A., Terereanca, S., and Simons, D.J. High responsiveness and direction sensitivity of neurons in the rat thalamic reticular nucleus to vibrissa deflections. *J. Neurophysiol.* 83: 2791-2801, 2000.

Hartings, J.A., Temereanca, S., and Simons, D.J. Processing of periodic whisker deflections by neurons in the ventroposterior medial and thalamic reticular nuclei. *J. Neurophysiol.* 90(5): 3087-3094, 2003.

Harvey, M.A., Bermejo, R., and Zeigler, H.P. Discriminative whisking in the head-fixed rat: optoelectronic monitoring during tactile detection and discrimination tasks. *Somatosens. Mot. Res.* 18: 211-222, 2001.

Hirsh, J.A. Synaptic physiology and receptive field structure in the early visual pathway of the cat. *Cereb. Cortex.* 13(1): 63-69, 2003.

Ito, M. Response properties and topography of vibrissa-sensitive VPM neurons in the rat. *J. Neurophysiol.* 60(4): 1181-1197, 1988.

Jin, T., Witzemann, V., and Brecht, M. Fiber types of the intrinsic whisker muscle and whisking behavior. *J. Neurosci.* 24(13): 3386-3393.

Kawaguchi, Y. Physiological subgroups of nonpyramidal cells with specific morphological characteristics in layer II/III of rat frontal cortex. *J. Neuroscience* 15(4): 2638-2655, 1995.

Kohn, A. and Movshon, J.A. Adaptation changes the direction tuning of macaque MT neurons. *Nat. Neurosci.* 7(7): 764-772, 2004.

Lee, S.H. and Simons, D.J. Angular tuning and velocity sensititivity in different neuron classes within layer 4 of rat barrel cortex. *J. Neurophysiol.* 91: 223-229, 2004.

Lichtenstein, S.H., Carvell, G.E., and Simons, D.J. Responses of rat trigeminal ganglion neurons to movements of vibrissae in different directions. *Somatosens. Mot. Res.* 7(1): 47-65, 1990.

Markram, H. and Tsodyks, M. Redistribution of synaptic efficacy between neocortical pyramidal neurons. *Nature* 382: 807-810, 1996.

Marlin, S.G., Hasan, S.J., and Cynader, M.S. Direction-selective adaptation to simple and complex cells in cat striate cortex. *J. Neurophysiol.* 39: 1314-1330, 1988.

Minnery, B.S. and Simons, D.J. Response properties of whisker-associated trigeminothalamic neurons in rat nucleus principalis. *J. Neurophysiol.* 89: 40-56, 2003.

Moore, C.I., Nelson, S.B., and Sur, M. Dynamics of neuronal processing in rat somatosensory cortex. *TINS* 22(11): 513-520, 1999.

Movshon, J. A. and Lennie, P. Pattern selective adaptation in cortical neurons. *Nature* 278: 850-852, 1979.

Muller, J.R., Metha, A.B., Krauskopf, J., and Lennie, P. Rapid adaptation in visual cortex to the structure of images. *Science* 285: 1405-1408, 1999.

Nicolelis, M.A., Bacala, L.A., Lin, R.C., and Chapin, J.K. Sensorimotor encoding by synchronous neural ensemble activity at multiple levels of the somatosensory system. *Science* 268: 1352-1358, 1995.

Nicolelis, M.A. and Fanselow, E,E. Thalamocortical optimization of tactile processing according to behavioral state. *Nat. Neurosci.* 5: 517-523, 2002.

Petersen, C.C.H. Short-term dynamics of synaptic transmission within the excitatory neuronal network of rat layer 4 barrel cortex. *J. Neurophysiol.* 87: 2904-2914, 2002.

Polley, D.B., Rickert, J.L., and Frostig, R.D. Whisker-dependent discrimination of object orientation using a one-trial learning paradigm. *Neurobiol. of Memory and Learning*, submitted.

Pubols, B.H., Donovich P.J., and Pubols, L.M. Opossum trigeminal afferents associated with vibrissa and rhinarial mechanoreceptors. *Brain Research* 7: 360-381, 1973.

Rice, F.L., Mance, A., and Munger, B.L. A comparative light microscopic analysis of the sensory innervation of the mystacial pad. I. Innervation of vibrissal follicle-sinus complexes. *J. Comp. Neurol.* 252: 154-174, 1986.

Sanchez-Vives, M.V., Nowak, L.G., and McCormick, D.A. Membrane mechanisms underlying contrast adaptation in cat area 17 in vivo. *J. Neurosci.* 20(11): 4267-4285, 2000a.

Sanchez-Vives, M.V. Nowak, L.G., and McCormick, D.A. Cellular mechanisms of long lasting inhibition in visual cortical neurons in vitro. *J. Neurosci.* 20(11): 4286-4299, 2000b.

Shipley, M.T. Response characteristics of single units in the rat's trigeminal nuclei to vibrissa displacements. *J. Neurophysiol.* 37(1): 73-90, 1974.

Simons, D.J. and Carvell, G.E. Thalamocortical response transformation in the rat vibrissa/barrel system. *J. Neurophysiol.* 61(2): 311-330, 1989.

Swadlow, H.A. Efferent neurons and suspected interneurons in S-1 vibrissa cortex of the awake rabbit: receptive fields and axonal properties. *J. Neurophysiol.* 62(1): 288-307, 1989.

Swadlow, H.A. and Gusev, A.G. Receptive-field construction in cortical inhibitory interneurons. *Nat. Neurosci.* 5(5): 403-404, 2002.

Webber, R.M. and Stanley, G.B. Nonlinear encoding of tactile patterns in the barrel cortex. J. *Neurophysiol.* 91(5): 2010-22, 2003.

Welker, W.I. Analysis of sniffing in the albino rat. *Behavior* 12: 223-244, 2964.

CHAPTER IV:

FUTURE DIRECTIONS

The experiments discussed in this thesis represent one of the first careful studies of responses of SI barrel neurons in anesthetized rats to trains of vibrissa deflections at whisking frequencies. In this section I outline some future directions of research in the barrel system that would expand the findings from my studies.

Synaptic Mechanisms of Temporal Processing

Each of the results presented in this thesis relates to the temporal response properties of barrel cortex neurons. However, the mechanisms that underlie these response properties are uncertain. One of the advantages of performing experiments on the vibrissa processing system is that questions relating to cortical processing *in vivo* may easily be translated to the cortical slice preparation in order to investigate the cellular or synaptic mechanisms that underlie these phenomena. In contrast to other cortical areas, spatial topography of the barrel cortex can easily be visualized in cortical slices based on the anatomical prominence of the layer IV barrels. In addition, thalamocortical slices can be made that preserve the sensory inputs to barrel cortex (Agmon and Connors 1991).

The cortical slice preparation is an ideal system with which to investigate questions about temporal response properties relating to my thesis. For example, the mechanisms that underlie band-pass responses discussed in Chapter II of this thesis are unknown. The model discussed in this chapter suggests that slow inhibition with a time course similar to synaptic $GABA_B$ currents cause the band-pass peak in vector strength. However, other ionic currents may also be responsible for this result. Using specific pharmacological agents to block $GABA_B$ or other currents, some of these possibilities

may be picked apart. Similarly, in Chapter III, I suggested that thalamocortical adaptation is a possible cause of frequency-specific sharpening of direction tuning. However, post-synaptic fatigue or inhibition may also contribute to these effects. Using thalamocortical slices, cortical responses to dynamic temporal stimuli from subsets of VPm neurons could be further investigated and the relative contribution of these frequency-sensitive mechanisms to my results could be dissected.

Multi-Vibrissa Integration

In this thesis I explored the how complex temporal inputs to individual vibrissae are encoded by rat SI neurons. In order to fully understand sensory coding in the vibrissa system, studies of complex spatial inputs must be investigated as well. The vibrissae move largely as a unified array of sensors, protracting and retracting in an elliptical cycle (Welker 1964; Carvell and Simons 1990). However, when they encounter an external object, individual vibrissae are deflected from the whisking trajectory at slightly different times. In addition, the directions of these deflections are likely to vary. Thus, in order to fully understand how vibrissa sensory system encodes information about complex stimuli, we must not only understand how neurons respond to temporally modulated input to individual vibrissa, but also how they integrate complex *spatio*-temporal stimuli.

Many of the experiments described in this thesis could be expanded to include the spatial location of multiple inputs as a variable. In Chapter II, I demonstrated band-pass characteristics of the spike rate and temporal fidelity of responses to stimuli at rates of 5-8 Hz. How does stimulation of multiple vibrissae change this result? For example, are response properties optimized when the temporal movement of the vibrissae is

synchronized as opposed to when movement of multiple vibrissae is out of phase? Does the fidelity of responses to non-primary vibrissa deflections increase when a primary vibrissa is moving at whisking frequencies? In Chapter III, direction tuning was characterized in response to different temporal histories of individual vibrissa deflections. How does the *spatio*-temporal history of vibrissa deflections change direction tuning? Brumberg et al (1996) demonstrated that direction tuning increases as a function of the number of neighboring vibrissae stimulated. Does the direction of movement of these neighboring vibrissae modulate tuning of responses to primary vibrissa deflections? Does the timing of directional movements of neighboring vibrissae change tuning responses to primary vibrissa deflections?

The most interesting multi-vibrissa integration may occur outside of layer IV barrels. Although barrel neurons do respond to multiple vibrissae (Moore et al. 1998; Zhu and Connors 1999), neurons in the septa and in supra- and infra-granular layers are less selective for single vibrissae (Simons 1978; Armstrong-James et al. 1992). SII neurons also have broad spatial receptive fields, suggesting that they play a role in integrating information across vibrissae (Kwegyir-Afful and Keller 2004). The contribution of non-barrel somatosensory cortex to sensory processing is often ignored because of the appeal of barrel anatomy for physiological studies, but investigations of cortical responses in these areas are crucial for a complete understanding of the sensory system.

Neural Coding in Alert Animals

Due to the deleterious effects of anesthesia on cortical response properties, an obvious future direction of my studies would be to perform similar experiments in awake, behaving animals. Although the use of anesthesia has the advantage of allowing precise and tractable stimulation of the vibrissae, it is difficult to replicate the complex patterns of stimulation encountered during whisking behavior. In this thesis, vibrissae were stimulated at whisking frequency rates to address questions regarding temporal modulation of tuning properties in barrel neurons. However, the cyclical movements of vibrissa during whisking are more complex than the stimuli we presented, and involve synchronized movement of all vibrissae. In addition, responses in awake rats are modulated by attention and behavioral state, influences that are impossible to account for in anesthetized animals.

The studies I have presented may be replicated with some variation in awake animals. Recently, physiological recordings have been performed successfully in head-posted, awake rats (Brecht, M., personal communication). Using this preparation, responses to simple externally applied stimuli, such as an air puff to the vibrissa array, could be recorded while a rat is naturally whisking or immobile. Although the precise movements of the vibrissae would be difficult to monitor, the temporal properties and direction specific responses under these conditions could be assessed to determine how whisking modulates tuning of responses to simple stimuli. This type of experiment would address some questions that were left unanswered in my thesis experiments. For example, does elliptical whisking adapt responses to some directions more than others?

Do the increases in temporal fidelity, spike rate, and direction tuning that we observed reflect optimization of tuning that occurs in an awake, whisking animal?

Behavioral Experiments

The behavioral significance of sensory stimuli employed in this thesis and the perceptual correlates of response properties we observed require further investigation. Behavioral studies have demonstrated that rodents use their vibrissae for a variety of tasks (see Introduction), but the specific sensory cues utilized by rodents to accomplish these tasks are unclear. In addition, correlations between the tuned responses of barrel neurons and sensory perception of rodents have only recently been reported (Fanselow et al. 2001; Swadlow et al. 2002; Swadlow and Gusev 2002; Castro-Alamancos et al. 2004; Krupa et al. 2004).

Although numerous groups have studied direction tuning in rat SI, the behavioral relevance of vibrissa direction cues for rats is unclear. To date, only one study has directly demonstrated that rats use the direction of vibrissa movements to perform discriminations (Polley et al. 2004). This study determined that rats are capable of discriminating between orthogonally oriented bars in a maze. However, the relevance of vibrissa direction for broader perceptual goals has not been shown. What other kinds of tasks require direction as a sensory cue for signal processing? In a different experimental paradigm, would rats show more selective direction discrimination abilities? Are there cues other than direction of vibrissa movement that could underlie the ability to discriminate orientation as they did in Polley's experiment? Can rats perceive the

direction of single vibrissa movements, or do they use multi-vibrissa interactions to obtain information about direction?

An additional goal of future experiments should be to demonstrate the relevance of direction tuning of SI neurons for direction perception. For example, the discrimination threshold for direction could be correlated with direction tuning of neurons at different levels of the vibrissa processing system to show a link between perception and neural coding. The influence of neural activity of specific cell groups on perception could also be shown. Although organized maps of direction have not been documented in SI, neurons with similar direction tuning are clustered in SI cortical columns (Bruno et al. 2003). It would be interesting to train rodents to perform direction discriminations, and then to determine whether stimulation of specific clusters of tuned neurons could influence direction perception in these animals. Experiments of this type might demonstrate differences between barrels and setpa, between cortical layers, or between SI and SII in the relative contribution of direction tuning to sensory perception.

REFERENCES

Agmon, A. and Connnors, B.W. Thalamocortical responses of mouse somatosensory (barrel) cortex *in vitro*. *Neuroscience* 1(2-3): 365-79, 1991.

Armstrong-James M., Fox, K., and Das-Gupta, A. Flow of excitation within rat barrel cortex on striking a single vibrissa. *J. Neurophysiol.* 68: 1345-1358, 1992.

Brumberg, J.C., Pinto, D.J., and Simons, D.J. (1996) Spatial gradients and inhibitory summation in the rat whisker barrel system. *J. Neurophysiol.* 76(1): 130-140.

Bruno, R.M., Khatri, V., Land, P.W., and Simons, D.J. Thalamocortical angular tuning domains within individual barrels of rat somatosensory cortex. *J. Neurosci.* 23(29): 9565-9574, 2003.

Castro-Alamancos, M.A. Absence of rapid sensory adaptation in neocortex during information processing states. *Neuron* 41(3): 455-464, 2004.

Carvell, G.E. and Simons, D.J. Biometric analyses of vibrissal tactile discrimination in the rat. *J. Neurosci.* 10: 2638-2648, 1990.

Fanselow, E.E., Sameshima, K., Baccala, L.A., and Nicolelis, M.A. Thalamic bursting in rats during different awake behavioral states. *PNAS* 98(26): 15330-15335, 2001.

Kwegyir-Afful, E.E. and Keller, A. (2004) Response properties of whiker related neurons in rat second somatosensory cortex. *J. Neurophysiol.* (in press)

Krupa, D.J., Wiest, M.C., Shuler, M.G., Laubach, M., and Nicolelis, M.A. Layer-specific somatosensory cortical activation during active tactile discrimination. *Science* 304(5679): 1989-1992, 2004.

Moore, C.I. and Nelson, S.B. Spatio-temporal subthreshold receptive fields in the vibrissa representation of rat primary somatosensory cortex. *J. Neurophysiol.* 80: 2882-2892, 1998.

Polley, D., Rickert, J.L., and Frostig, R.D. Whisker-based discrimination of object orientation determined with a rapid training paradigm. *Neurobiol. of Learning and Memory,* submitted.

Simons, D.J. Response properties of vibrissa units in rat SI somatosensory neocortex. *J. Neurophysiol.* 41: 798-820, 1978.

Swadlow, H.A., Gusev, A.G., and Bezduudnaya, T. Activation of a cortical column by a thalamocortical impulse. *J. Neurosci.* 22(17): 7766-7773, 2002.

Swadlow, H.A. and Gusev, A.G. Receptive-field construction in cortical inhibitory interneurons. *Nat. Neurosci.* 5(5): 403-404, 2002.

Welker, W.I. Analysis of sniffing of the albino rat. *Behavior* 12: 223-244, 1964.

Zhu, J.J. and Connors, B.W. Intrinsic firing patterns and whisker-evoked synaptic responses of neurons in the rat barrel cortex. *J. Neurophysiol.* 81: 1171-1183, 1999.